Gülhane Medical Journal

ISSN: 1302-0471
E-ISSN: 2146-8052

Gulhane Med J June 2026 Volume 68 Issue 2

www.gulhanemedj.org

68/2

Gülhane
Medical Journal
Gülhane Tıp Dergisi

Editorial Board

GÜLHANE MEDICAL JOURNAL
Gülhane Tıp Dergisi

GÜLHANE MEDICAL JOURNAL
Gülhane Tıp Dergisi

Gülhane Medical Journal

Gülhane Tıp Dergisi

Editorial Board

Gülhane
Medical Journal
Gülhane Tıp Dergisi

GÜLHANE MEDICAL JOURNAL
Gülhane Tıp Dergisi

Please refer to the journal's webpage **(https://gulhanemedj.org/)** for "Aims and Scope", "Ethical Policy", "Instructions to Authors" and "Peer Review Process".

The editorial and publication process of Gülhane Medical Journal are shaped in accordance with the guidelines of the ICMJE, WAME, CSE, COPE, EASE, and NISO. The journal is in conformity with the Principles of Transparency and Best Practice in Scholarly Publishing. Gülhane Medical Journal is indexed in **Scopus, British Library, DOAJ, Ulakbim TR Index, CABI, Ebsco HOST, OCLC Worldcat, Embase, Türk Medline, Türkiye Atıf Dizini, J-Gate** and **Gale**.

The journal is published online.

Owner: Gülhane Faculty of Medicine, University of Health Sciences Türkiye

Responsible Manager: Mehmet Ali Gülçelik

galenos yayınevi

Publisher Contact
Address: Molla Gürani Mah. Kaçamak Sk.
No: 21/1 34093 İstanbul, Türkiye
Phone: +90 (530) 177 30 97 / +90 (539) 307 32 03
E-mail: info@galenos.com.tr • yayin@galenos.com.tr
Web: www.galenos.com.tr

Publisher Certificate Number: 14521
Publication Date: June 2026
E-ISSN: 2146-8052
International scientific journal published quarterly.

GÜLHANE MEDICAL JOURNAL
Gülhane Tıp Dergisi

Gülhane Medical Journal

Gülhane Tıp Dergisi

Contents

ORIGINAL ARTICLES

72 **Evaluation of the relationship between gastrointestinal symptoms, ultra-processed food consumption, acute stress, and reward-related eating behavior among shift-working healthcare professionals**
Fatma Elif Eroğlu, Büşra Göktürk Açıkalın, Özge Mengi Çelik; Ankara, Türkiye

81 **Investigation of factors associated with the diagnosis process and delayed diagnosis in Familial Mediterranean fever patients: a single-center experience**
Merve Öztürk, Yusuf Çetin Doğaner, Ümit Aydoğan, Sedat Yılmaz; Yozgat, Ankara, Türkiye

87 **Age-related effects of smartphone and tablet reading on ocular surface parameters**
Selcan Ekicier Acar, Zennure Özdemir Yıldız; Ankara, Türkiye

94 **Comparison of positron emission tomography, computed tomography, magnetic resonance imaging and surgical staging in para-aortic lymph node sampling in cervical cancer**
Tolga Çiftpınar, Faruk Köse, Mufit Cemal Yenen; İstanbul, Türkiye; Kyrenia, Cyprus

102 **The predictive role of hemoglobin-albumin-lymphocyte-platelet (HALP) score and serum inflammatory markers in intrahepatic cholestasis of pregnancy**
Özge Öztürk, Seval Yılmaz Ergani, Recep Taha Ağaoğlu, Figen Günday, Aysu Yeşim Tezcan, Kadriye Yakut Yücel, Zehra Vural Yılmaz; Ankara, Türkiye

109 **Hematological indices in children with *Helicobacter pylori* infection: a retrospective analysis**
Yasin Maruf Ergen, Selçuk Teke; Ankara, Türkiye

118 **Short-term effects of +Gz exposure on respiratory functions: results from human centrifuge training**
Abdurrahman Engin Demir, Memduh Savaş İlbasmış, Nuran Küçük, Şükrü Hakan Gündüz, Cantürk Taşçı; Ankara, Kayseri, Eskişehir, Türkiye

127 **Evaluation of the incidence and clinical outcomes of permanent pacemaker implantation after the Ozaki procedure: a retrospective cohort study**
Salim Yaşar, Özkan Eravcı, Serdar Fırtına, Mehmet Sadık Karpat, Erkan Yıldırım, Tayfun Özdem, Emre Kubat, Kubilay Karabacak, Hasan Kutsi Kabul; Ankara, Türkiye

132 **Assessment of stress level, sleep quality and heart rate variability among the individuals with symptoms of depression**
Monisha Ravi, Dhamodhini K S, Maheshkumar Kuppusamy, Suvarna Kantipudi, Santhi Silambanan, Padmavathi Ramaswamy; Chennai, India

138 **Influence of age and cerebrospinal fluid diversion techniques on infection risk in pediatric hydrocephalus: a 10-year single-center experience**
Sait Kayhan, Adem Doğan, Şahin Kırmızıgöz, Mehmet Can Ezgü, Mehmet Ozan Durmaz, Demet Evleksiz Karımzada, Ecma Yılmaz, Cafer Ak, Sezen Yılmaz Sarıaltın, Yusuf İzci; Ankara, Gaziantep, Çorum, Türkiye

CASE REPORT

147 **Alström syndrome presenting with life-threatening variceal bleeding in an adolescent: the youngest reported case in Türkiye**
Birce İzgi Akçay, Selçuk Teke, Yasin Maruf Ergen, İsmihan Merve Tekin, Necati Balamtekin; Ankara, Türkiye

Gülhane
Medical Journal
Gülhane Tıp Dergisi

Editor in Chief

Dear Readers and Esteemed Authors,

As spring gradually gives way to summer, the renewal seen in nature reminds us of the importance of continued growth and productivity in academic life as well. With the completion of another busy academic term, the approaching summer break offers a valuable opportunity for rest and renewal. The recent celebration of Eid al-Adha also provided a meaningful occasion to reflect on the values of solidarity, generosity, and togetherness.

On this occasion, I would like to express my sincere appreciation to all members of our editorial team—particularly the Managing Editors, Editorial Board members, Statistics Editor, and all contributing editors—for their dedicated efforts and valuable contributions to the preparation of each issue of our journal.

We also extend our heartfelt thanks to our reviewers for their careful and timely evaluations, which play a crucial role in maintaining the scientific quality of our journal and ensuring the efficient progress of the publication process.

On behalf of our journal, we sincerely thank all authors who submitted their valuable work, our reviewers, and our readers for their continued support.

The second issue of 2026 includes ten original research articles and one case report.

We wish you health, peace, and success in the coming months and look forward to welcoming you again in the third issue of 2026.

Sincerely,

M. Ali Gülçelik, M.D., Prof.
Editor-in-Chief

GÜLHANE MEDICAL JOURNAL
Gülhane Tıp Dergisi

DOI: 10.4274/gulhane.galenos.2025.23600
Gulhane Med J 2026;68(2):72-80

Evaluation of the relationship between gastrointestinal symptoms, ultra-processed food consumption, acute stress, and reward-related eating behavior among shift-working healthcare professionals

Fatma Elif Eroğlu[1], Büşra Göktürk Açıkalın[2], Özge Mengi Çelik[1]

[1]University of Health Sciences, Türkiye, Faculty of Gülhane Health Sciences, Clinic of Nutrition and Dietetics, Ankara, Türkiye
[2]Ankara Medipol University School of Fine Arts, Design and Architecture, Department of Gastronomy and Culinary Arts, Ankara, Türkiye

Cite this article as: Eroğlu FE, Göktürk Açıkalın B, Mengi Çelik Ö. Evaluation of the relationship between gastrointestinal symptoms, ultra-processed food consumption, acute stress, and reward-related eating behavior among shift-working healthcare professionals. *Gulhane Med J.* 2026;68(2):72-80.

Date submitted:
05.08.2025
Date accepted:
21.11.2025
Epub:
05.06.2026
Publication Date:
16.06.2026

Corresponding Author:
Fatma Elif Eroğlu, PhD., University of Health Sciences, Türkiye, Faculty of Gülhane Health Sciences, Clinic of Nutrition and Dietetics, Ankara, Türkiye
uzman.dyteliferoglu@gmail.com

ORCID:
orcid.org/0000-0003-0394-4640

Keywords: Gastrointestinal symptoms, ultra-processed food consumption, acute stress, reward-related eating, shift-working healthcare professionals

ABSTRACT

Aims: Shift-working healthcare professionals (SWHPs) are prone to gastrointestinal symptoms (GSs) due to irregular work schedules, unhealthy eating behavior, and psychological stress. This study examined the interrelationships among GSs, consumption of ultra-processed foods (UPF), acute stress, and reward-related eating (RRE) behavior in SWHPs.

Methods: This cross-sectional study included SWHPs. Socio-demographic data, body mass index (BMI), and eating habits were recorded. The Gastrointestinal Symptom Rating Scale (GSRS), Screening Questionnaire of Highly Processed Food Consumption (sQ-HPF), Self-applied Acute Stress Scale for Healthcare Providers (EASE), and RRE Scale were used to assess relationships among the variables.

Results: A total of 301 participants (mean age =32.9±8.1 years; 55.1% female) were included in the study. The mean BMI was 24.1±3.3 kg/m². GSRS total scores correlated positively with sQ-HPF (ρ=0.208, p<0.001), EASE (ρ=0.353, p<0.001), and RRE (ρ=0.313, p<0.001). The EASE score was also positively correlated with all GSRS subdimensions (ρ=0.202-0.370, all p<0.001). In multivariable regression analyses, sQ-HPF scores were predicted by age (β=-0.145, p=0.011) and EASE (β=0.136, p=0.017) (R^2=0.202). RRE scores were predicted by EASE (β=0.340, p<0.001) and BMI (β=0.227, p<0.001) (R^2=0.408). GSRS total score was predicted by gender (β=-0.210, p<0.001), sQ-HPF (β=0.137, p=0.008), RRE (β=0.233, p<0.001), and EASE (β=0.201, p<0.001) (R^2=0.485).

Conclusions: The findings indicate that GSs are significantly associated with UPF consumption, acute stress, and RRE among SWHPs. These results emphasize the importance of acute stress management in reducing unhealthy eating behaviors and related GSs in this population.

Introduction

Shift or on-call systems are implemented in healthcare units to ensure the smooth flow of services (1). Working in shift or on-call systems can cause physical and psychological health problems because it disrupts an individual's normal circadian rhythm. This is because the human organism is designed to be awake during the day and asleep at night (2). A study of shift and on-call workers demonstrated that shift work negatively affects their physiological and psychological health and social lives (1). In shift work systems, changes in circadian rhythms can lead to eating disorders, reduced sleep duration and quality, and reduced physical activity (3). In shift workers, sleep irregularities can lead to changes in energy intake and dietary patterns, which in turn can increase the risk of various chronic diseases, primarily obesity (2). Shift work causes both increased stress and decreased stress-coping skills among workers (4). A study showed that, as stress levels increased, individuals tended to consume foods that rapidly raise blood glucose levels, particularly ultra-processed foods (UPFs) that are high in saturated fats, salt, and sugar, and high-calorie snacks, rather than main meals. This leads to the development of unhealthy eating habits (5). Another study of shift workers revealed that a significant proportion experienced unbalanced dietary habits, physical and mental fatigue, and sleep disturbances. Furthermore, most participants reported that their working hours negatively affected their physical health (6). It has been suggested that changes in eating habits associated with shift work may be linked to gastrointestinal symptoms (GSs). It has been found that the amount of food consumed during night shifts is lower than that consumed at other meals, and this can lead to various stomach disorders (7). Additionally, it has been noted that the number of snacks consumed during night shifts is greater than the number of main meals consumed, leading to an increased preference for foods high in carbohydrates, sugars, and fats (8). Shift workers who feel the need for quick consumption to obtain rapid energy tend to consume foods low in protein and high in refined sugars and processed carbohydrates. In this context, an association between an unhealthy diet and obesity has been demonstrated among shift workers. It has been recommended that foods high in carbohydrates, sugars, and fats be limited and that individuals be encouraged to consume protein-rich foods (9). Protein-rich foods increase alertness, whereas fatty foods decrease it (8). UPFs are low in micronutrients and fiber, while being high in fat and sodium. The consumption of UPFs, along with increased intake of simple sugars and fats and decreased fiber intake, can increase intestinal permeability and lead to systemic inflammation. As a result, negative changes in the composition and function of the gut microbiota may occur (10). Recently, eating behavior has been conceptualized as a coping or reward mechanism in response to negative situations or emotions. Among these, positive emotions (happiness, joy, celebratory feelings) and negative emotions (stress, anxiety) can trigger reward-related food cravings (11). In hedonic hunger, defined as the desire to consume food for pleasure in the absence of physiological hunger, individuals often prefer UPFs that contain high amounts of fat, sugar, or salt, or combinations thereof (12). These foods are often low in nutritional value due to their inadequate nutrient profiles (high salt, added sugars, saturated fatty acids, and low dietary fiber) and processing that alters their physical and textural properties, removes water, and uses flavor enhancers, colorings, and other additives. Furthermore, the additives in these foods may be addictive in some individuals (13).

As no studies to date have examined the relationships among UPF consumption, GSs, acute stress, and reward-related eating (RRE) among Shift-working healthcare professionals (SWHPs) in Türkiye, this study aims to investigate these relationships.

Methods

Study design and participants

This cross-sectional study was conducted face-to-face between December 2024 and May 2025 among volunteer SWHPs residing in Ankara. Inclusion criteria: adults aged 18-65 years who signed the informed consent section at the beginning of the questionnaire, completed the survey in full, and were SWHPs. Exclusion criteria: individuals who did not agree to participate, had incomplete questionnaire data, were younger than 18 or older than 65 years, or were not SWHPs. The study was approved by the Gülhane Scientific Research Ethics Committee (approval number: 2024-531, dated 05.11.2024).

Data collection

The general characteristics of the individuals (gender, age, education level, marital status, and income level) and anthropometric measurements (body weight and height) were assessed using a questionnaire. SWHPs' consumption of UPFs was assessed via a dedicated questionnaire, GSs were evaluated using the GSRS, acute stress was assessed using the EASE scale for healthcare professionals, and eating behaviors were evaluated using the RRE scale.

The high-processed food consumption short screening questionnaire (sQ-HPF)

Martinez-Perez et al. (14) originally developed this brief screening instrument in 2024, and Erdoğan Gövez et al. (15) subsequently adapted it into Turkish. The instrument uses an 11-point scoring system to evaluate the frequency of UPF consumption, with scores ≥6 indicating high consumption levels.

The Gastrointestinal Symptom Rating Scale (GSRS)

The GSRS was developed by Revicki et al. (16) to evaluate the severity of GSs based on clinical insights and symptom

patterns. Its Turkish adaptation was validated by Turan et al. (17). The scale consists of 15 items scored on a 7-point Likert scale. The scale is composed of five subdimensions: reflux, indigestion, diarrhea, constipation, and abdominal pain. Conversely, higher total scores are indicative of more pronounced symptom severity.

The Self-administered Acute Stress Scale (EASE)

The EASE scale, developed by Mira et al. (18) in 2021, is a 10-item instrument designed to assess acute emotional stress in healthcare providers. These items are rated on a 4-point Likert scale, with higher scores indicating greater stress. The Turkish version was adapted by Şimşek et al. (19). The total score ranges from 0 to 30, with cut-off values denoting varying levels of emotional burden: scores ranging from 0 to 9 indicate adequate regulation, while scores between 10 and 14 suggest distress, 15 to 24 indicate an excessive emotional load, and scores of 25 and above signify acute stress

The Reward-related Eating Scale (RRE)

The RRE scale, a 13-item instrument developed by Mason et al. (20) in 2017, utilizes a 5-point Likert scale to evaluate reward-driven eating behaviors. Saruhan and Konuşkan (21) conducted their Turkish adaptation. The scale is composed of three subscales: satiety impairment, food-related cognitive preoccupation, and loss of control in eating. The attainment of elevated scores indicates increased craving, particularly for sweet or palatable foods.

Anthropometric measurements

Participants self-reported their body weight and height following standardized guidance. Anthropometric indices were calculated based on self-reported height and weight. BMI was determined and categorized according to World Health Organization criteria (22).

Statistical Analysis

An a priori power analysis for sQ-HPF and GSRS was conducted using G*Power. At a two-tailed α=0.05 level, assuming an expected correlation of r=0.25, the required sample size to achieve 95% power was calculated to be 210. All analyses were conducted using the Statistical Package for the Social Sciences software, version 22.0 (IBM Corp., Armonk, NY, USA). Descriptive statistics, including medians, frequencies, and percentages, were used to summarize the data. Data distribution was assessed using histograms, descriptive statistics (coefficient of variation, skewness, and kurtosis), and the Kolmogorov–Smirnov test. Multiple linear regression analyses were performed to identify predictors of sQ-HPF, RRE, and GSRS scores. For the multiple regression analyses, we employed a backward elimination method. All potential predictor variables were initially included in the model, and non-significant variables were sequentially removed based on their p-values. The final models presented in Tables 3 and 4 include only the statistically significant predictors. Statistical significance was set at $p<0.05$, and results were interpreted at the 95% confidence level.

Results

Descriptive characteristics of the participants

A total of 301 participants (mean age 32.9±8.1 years; 55.1% female) were included. The mean body mass index (BMI) was 24.1±3.3 kg/m². Most participants held a university degree (78.4%), master's or doctoral degrees, and 5.6% had completed high school. By BMI category, 1.7% were underweight, 65.1% were normal weight, 28.6% were overweight, and 4.7% were obese. Regarding income, 23.3% reported income above expenses, 45.8% reported income equal to expenses, and 30.9% reported income below expenses. High UPF consumption was observed in 68.1% of participants, compared with low consumption in 31.9%. Acute stress classification showed that 68.4% had good emotional adjustment, 24.9% had emotional distress, 6.3% had emotional overload, and 0.3% had extreme acute stress (Table 1).

Correlations among GSRS, sQ-HPF, EASE, and RRE scores

There were significant positive correlations between GSRS total score and sQ-HPF ($\rho=0.208$, $p<0.001$), EASE ($\rho=0.353$, $p<0.001$), and RRE ($\rho=0.313$, $p<0.001$) (Table 2). The EASE scale correlated positively with all GSRS subdimensions ($\rho=0.202$-0.370, all $p<0.001$).

Predictors of sQ-HPF and RRE scores

In multivariable linear regression (Table 3), the model predicting sQ-HPF scores was statistically significant ($R^2=0.202$, $p<0.001$); within this model, age emerged as a significant negative predictor ($\beta=-0.145$, $p=0.011$), whereas the EASE score was a significant positive predictor ($\beta=0.136$, $p=0.017$). Likewise, the regression model for RRE total scores was significant ($R^2=0.408$, $p<0.001$), with both EASE score ($\beta=0.340$, $p<0.001$) and BMI ($\beta=0.227$, $p<0.001$) acting as significant positive predictors.

Predictors of Gastrointestinal Symptoms (GSRS)

The regression model predicting GSRS total score (Table 4) was statistically significant ($R^2=0.485$, $p<0.001$), with gender emerging as a negative predictor ($\beta=-0.210$, $p<0.001$) and sQ-HPF ($\beta=0.137$, $p=0.008$), RRE ($\beta=0.233$, $p<0.001$), and EASE ($\beta=0.201$, $p<0.001$) emerging as positive predictors.

Table 1. Distribution according to the general characteristics of individuals

Characteristics	Value
Gender, n (%)	
Female	166 (55.1)
Male	135 (44.9)
Education level, n (%)	
High school	17 (5.6)
University	236 (78.4)
Master's degree/doctorate	48 (15.9)
BMI classification, n (%)	
Underweight (<18.50 kg/m^2)	5 (1.7)
Normal (18.50-24.99 kg/m^2)	196 (65.1)
Overweight (25.00-29.99 kg/m^2)	86 (28.6)
Obese (≥30.0 kg/m^2)	14 (4.7)
Marital status, n (%)	
Married	141 (46.8)
Unmarried	160 (53.2)
Income status, n (%)	
Income exceeds expenses	70 (23.3)
Income equals expenses	138 (45.8)
Income is less than expenses	93 (30.9)
Highly processed food consumption, n (%)	
High consumption	205 (68.1)
Low consumption	96 (31.9)
Acute stress classification, n (%)	
Good emotional adjustment	206 (68.4)
Emotional distress	75 (24.9)
Emotional overload	19 (6.3)
Extreme acute stress	1 (0.3)
Age (years), mean ± SD	32.9±8.1
BMI (kg/m^2), mean ± SD	24.1±3.3
GSRS total score, mean ± SD	33.8±15.0
GSRS score subdimensions, mean ± SD	
Abdominal pain	7.0±3.7
Reflux	4.6±3.0
Diarrhea	5.1±3.0
Indigestion	10.8±5.6
Constipation	6.2±3.7
sQ-HPF score	6.7±2.5
EASE scale score	7.4±4.5
RRE scale total score, mean ± SD	31.8±10.6
RRE scale score subdimesions, mean ± SD	
Loss of control over eating	17.0±5.5
Lack of satiety	7.9±3.9
Preoccupation with food	6.8±2.8

BMI: Body mass index, SD: Standard deviation, GSRS: Gastrointestinal Symptom Rating Scale, sQ-HPF: Screening Questionnaire of Highly Processed Food Consumption, EASE: Self-applied Acute Stress, RRE: Reward-related Eating

Table 2. Correlation coefficients between scale scores

		1	2	3	4	5	6	7	8	9	10	11	12
1. GSRS-total score	ρ	-											
	p												
2. Abdominal pain	ρ	0.846***	-										
	p	<0.001											
3. Reflux	ρ	0.739***	0.718***	-									
	p	<0.001	<0.001										
4. Diarrhea	ρ	0.542***	0.347***	0.297***	-								
	p	<0.001	<0.001	<0.001									
5. Indigestion	ρ	0.879***	0.723***	0.549***	0.327***	-							
	p	<0.001	<0.001	<0.001	<0.001								
6. Constipation	ρ	0.688***	0.390***	0.372***	0.539***	0.481***	-						
	p	<0.001	<0.001	<0.001	<0.001	<0.001							
7. sQ-HPF score	ρ	0.208***	0.244***	0.142*	0.072	0.202***	0.050	-					
	p	<0.001	<0.001	0.014	0.212	<0.001	0.391						
8. EASE scale score	ρ	0.353***	0.302***	0.202***	0.325***	0.231***	0.370***	0.140*	-				
	p	<0.001	<0.001	<0.001	<0.001	<0.001	<0.001	0.015					
9. RRE scale total score	ρ	0.313***	0.265***	0.176***	0.156**	0.342***	0.233***	0.110	0.335**	-			
	p	<0.001	<0.001	0.004	0.007	<0.001	<0.001	0.056	<0.001				
10. Loss of control over	ρ	0.324***	0.283***	0.188***	0.077	0.374***	0.196***	0.196***	0.258***	0.881***	-		
	p	<0.001	<0.001	0.001	0.185	<0.001	0.001	0.001	<0.001	<0.001			
11. Lack of satiety eating	ρ	0.232***	0.170**	0.119*	0.237***	0.206***	0.254***	0.011	0.354***	0.799***	0.480***	-	
	p	<0.001	0.003	0.039	<0.001	<0.001	<0.001	0.851	<0.001*	<0.001	<0.001		
12. Preoccupation with food	ρ	0.188*	0.177**	0.097	0.115*	0.208***	0.150**	0.009	0.251***	0.841***	0.592***	0.747***	-
	p	0.001	0.002	0.092	0.047	<0.001	0.009	0.882	<0.001	<0.001	<0.001	<0.001	

*p<0.05, **p<0.01, ***p<0.001, Spearman's correlation analysis was used to calculate the p-value
GSRS: Gastrointestinal Symptom Rating Scale, sQ-HPF: Screening Questionnaire of Highly Processed Food Consumption, EASE: Self-Applied Acute Stress, RRE: Reward-Related Eating

Table 3. Linear regression model for screening questionnaire of highly processed food consumption and reward-related eating prediction

Screening Questionnaire of Highly Processed Food Consumption Score					
Model	**Standardized beta**	**t**	**p-value**	**95% confidence interval**	
				Lower	**Upper**
Age (years)	-0.145	-2.553	**0.011**	-0.081	-0.011
EASE scale score	0.136	2.402	**0.017**	0.014	0.140
R^2=0.202; **p<0.001***					
Reward-related Eating Scale Total Score					
Model	**Standardized beta**	**t**	**p-value**		
EASE scale score	0.340	6.424	**<0.001**	0.550	1.036
BMI (kg/m^2)	0.227	4.284	**<0.001**	0.395	1.066
R^2=0.408; **p<0.001***					

*Significant at p-value <0.05
EASE: Self-applied Acute Stress, BMI: Body mass index

Table 4. Linear regression model for gastrointestinal symptoms prediction

Gastrointestinal Symptom Rating Scale Total score					
Model	**Standardized beta**	**t**	**p-value**	**95% confidence interval**	
				Lower	**Upper**
Gender	-0.210	-4.005	**<0.001**	-9.451	-3.223
sQ-HPF	0.137	2.654	**0.008**	0.206	1.388
RRE scale score	0.233	4.297	**<0.001**	0.178	0.480
EASE scale score	0.201	3.607	**<0.001**	0.302	1.026
R^2=0.485; **p<0.001***					

*Significant at p-value <0.05, Variables: Gender (0: female, 1: male)
sQ-HPF: Screening Questionnaire of Highly Processed Food Consumption, RRE: Reward-Related Eating, EASE: Self-Applied Acute Stress

Discussion

This study investigated the associations between UPF consumption, GSs, acute stress, and eating behaviors among SWHPs. The findings indicated that participants exhibited high UPF consumption. Moreover, greater UPF intake was associated with increased GSs, increased acute stress levels, and increased RRE. Shift work disrupts an individual's normal biological rhythms, leading to sleep disorders, increased stress, changes in eating habits, and physical or psychological disorders (23,24).

When examining the relationship between UPF consumption and gastrointestinal findings, evidence indicates that the types and amounts of food consumed, especially during night shifts, may cause stomach discomfort, and that increased consumption of simple sugars and fats, along with decreased fiber intake associated with UPF consumption, may increase intestinal permeability. Consequently, increased inflammation affects the gut microbiota and leads to gastrointestinal disorders (GDs) (25). A study examining the relationship between UPF consumption and GDs found that high UPF consumption increases the risk of irritable bowel syndrome (IBS) and, consequently, of dyspepsia (26).

In this study, consistent with the findings reported by Haghighatdoost et al. (27), a positive correlation was observed between UPF consumption and the total GSRS score. Furthermore, increased UPF consumption was associated with greater GSs such as indigestion, abdominal pain, constipation, diarrhea, and reflux. A substantial body of evidence has emerged linking diets rich in UPFs to the development of various intestinal diseases, including inflammatory bowel disease (IBD), IBS, diarrhea, and constipation. A diet rich in saturated or trans fats, meat proteins, reduced sugars, and salt but deficient in fiber has been shown to trigger dysbiosis by altering the microbiota. Microbial dysbiosis is thought to play a role in the development and exacerbation of GDs.

Another study showed that UPF consumption was positively associated with higher total energy intake and that inflammatory gastrointestinal diseases and low fruit and vegetable consumption were positively associated with specific fecal microbiota taxa (28). A study found that increased UPF intake was positively correlated with IBD onset. The study found that consumption of processed foods (e.g., carbonated beverages, refined sugar, and other sugary foods) was associated with an increased risk of adverse health outcomes. The study found

a correlation between IBD and higher risk ratios associated with various UPF subtypes, including processed meat and poultry (29). In this study, a significant and positive correlation was found between the GSRS and sQ-HPF total scores. The SQ-HPF score correlated significantly with abdominal pain, gastroesophageal reflux, and indigestion.

Examination of the relationship between UPF consumption and health problems reveals that obesity is also a significant issue. One study examined the relationship between UPF consumption and weight gain over nine years. The study found that individuals with the highest UPF consumption were 26% more likely to become overweight or obese than those in the lowest quartile of consumption (30). In another study, individuals in the top fifth of UPF consumption had a 32% higher likelihood of obesity than those in the bottom fifth. Furthermore, shift workers may be more prone to obesity due to imbalances in the secretion of hormones, such as leptin and ghrelin, which are associated with sleep irregularities, dietary changes, and altered meal timing (31). Although previous studies have linked UPF consumption to weight gain and obesity, participants in this study had BMI values within the normal range. This likely reflects the relatively young and health-conscious profiles of healthcare workers rather than an absence of risks associated with UPF consumption.

Increased UPF consumption may cause functional abnormalities in the intestinal microbiota that affect neurological development and contribute to adverse mental health outcomes, such as stress and depression (32). A meta-analysis has revealed a positive correlation between excessive UPF consumption and an increase in stress and anxiety symptoms. Furthermore, studies have shown that individuals who work rotating shifts experience a decline in sleep quality and symptoms of psychological distress, including stress and anxiety (33). In this study, consistent with findings in the literature, participants experienced emotional distress, emotional overload, and excessive acute stress. Studies have shown that the main mechanisms linking UPF consumption to mental health include inflammation, oxidative stress, and alterations in the gut microbiota. However, mental illness prevalence is associated with increased consumption of UPFs (34).

It is also emphasized that stressed individuals may turn to unhealthy eating as a coping mechanism. One study found that individuals with higher UPF intake were significantly more likely to report mentally unhealthy and anxious days. It has been suggested that UPFs may affect cognitive function and mental health by altering the gut-brain axis (35). In this study, the linear regression model predicting sQ-HPF scores was statistically significant, and the EASE score was identified as a significant positive predictor.

RRE tendency is defined as an individual's desire to overconsume palatable foods and to derive intense pleasure from eating these foods. Positive emotions, such as happiness and celebration (positive reinforcement), and negative emotions, such as stress or anxiety (negative reinforcement), can trigger RRE, thereby enhancing or reducing an individual's emotional state (36). Furthermore, it has been suggested that the activation of the hypothalamic-pituitary-adrenal axis in chronic stress and the resulting excessive glucocorticoid exposure may play a role in the development of excessive food intake. It has been proposed that cortisol levels associated with stress and reward circuits may promote the intake of calorie-dense foods (37).

This study found that high scores on the RRE scale were associated with increased appetite and cravings for sweets. It was emphasized that consumption of UPFs, which are energy-dense and typically contain simple sugars, was positively correlated with RRE scale scores (20). Additionally, another study highlighted that stress-related RRE behavior increases the consumption of highly processed foods, and this situation increases susceptibility to infections by disrupting the gut microbiota (38). Furthermore, another study suggested that psychological stress and reward-seeking eating behavior affect gastrointestinal motility in acute or short-term stress responses by inhibiting gastric emptying and stimulating colonic transit (39). In this study, the linear regression model predicting total RRE scores was also statistically significant. In this model, the EASE scale score and BMI were significantly positively associated with RRE.

Consequently, the changes mentioned above may be associated with an increased frequency of dyspepsia and other GSs in patients with stress-related functional GDs, potentially due to underlying pathophysiological processes (40). In this study, consistent with these findings, significant positive correlations were observed between GSs and the subdimensions of the RRE scale. Additionally, the total RRE score was significantly associated with all gastrointestinal subdimensions; the strongest correlations were observed for indigestion, constipation, abdominal pain, reflux, and diarrhea. Furthermore, the EASE score showed positive correlations with all gastrointestinal subdimensions. The sQ-HPF score, RRE score, and EASE score were identified as positive predictors of the GSRS.

Study Limitations

A number of limitations should be acknowledged in the context of this study. Moreover, the cross-sectional nature of this study limits the possibility of drawing definitive conclusions regarding causality. The study's findings reveal a homogeneous distribution, with a predominance of individuals with a high level of education. This phenomenon has been linked to the adoption of healthier eating habits, although the findings are not widely generalizable.

Additionally, the present study has several strengths. As far as we are aware, this is the first investigation to explore

the association between UPF consumption and stress, RRE behavior, and GSs among healthcare workers. The data obtained from this study will underscore the impact of stress and eating habits on gastrointestinal well-being in SWHPs and their ramifications for the individual. The current findings are likely to guide further inquiry in this area.

In future research, the implementation of dietary guidelines, including food processing, should be supported by long-term and clinical studies, which will facilitate examination of causal relationships. Furthermore, the execution of analogous studies across diverse age groups will be possible. In addition, structural equation modeling or path analysis could be employed to examine the potential mediating role of acute stress in the associations among UPF consumption, stress, and BMI outcomes.

In clinical nutrition practice, screening of healthcare professionals' eating behaviors could also include the evaluation of factors such as UPF consumption, acute stress, and RRE patterns.

Conclusion

This study found significant positive associations among UPF consumption, GSs, acute stress, and RRE in SWHPs. This study demonstrates that SWHPs can lead to disruptions in physiological balance, hormonal changes, unhealthy eating behaviors, and stress. These changes can lead to increased consumption of UPFs and the development of RRE behaviors as a coping mechanism. Higher UPF consumption increases intake of refined sugar, salt, and saturated fat and decreases intake of protein, fiber, vitamins, and minerals. This can lead to various negative health outcomes, particularly GDs.

In response to the growing food industry, countries need to develop national policies that promote healthy eating, facilitate access to unprocessed foods, and encourage balanced eating habits. Furthermore, screening for UPF consumption, acute stress, and GDs during clinical dietitian assessments of groups with high stress levels, such as healthcare workers, can facilitate early risk detection.

Developing effective intervention programs targeting UPF consumption, acute stress, and GSs can help improve both health outcomes and quality of life. Strategies developed for shift workers should include practices that both enhance work performance and support quality of life. Addressing issues such as UPF consumption, acute stress, GSs, and RRE behaviors is expected to enhance work performance, improve quality of life, and reduce chronic disease risks.

Ethics

Ethics Committee Approval: The study received approval from the Gülhane Scientific Research Ethics Committee of the University of Health Sciences, Türkiye (approval number: 2024-531, dated: 05.11.2024).

Informed Consent: Informed consent was obtained from all participants prior to data collection.

Acknowledgements

The authors thank all individuals who participated in the study. Additionally, the authors would like to thank Begüm Pala, Öykü Çakıroğlu, and Ceren Yağabasan for their valuable support in the study. The authors express their gratitude to the Scientific and Technological Research Council of Türkiye (TÜBİTAK). The National Undergraduate Student Research Projects Support Program (TÜBİTAK 2209-A) supported this project.

Footnotes

Authorship Contributions

Concept: F.E.E., B.G.A, Ö.M.Ç., Design: F.E.E., B.G.A, Ö.M.Ç., Data Collection or Processing: F.E.E., Analysis or Interpretation: Ö.M.Ç., Literature Search: F.E.E., B.G.A, Writing: F.E.E., B.G.A, Ö.M.Ç.

Conflict of Interest: The authors declare that they have no conflict of interest.

Financial Disclosure: This research did not receive any specific grant from funding agencies in the public, commercial, or not-for-profit sectors.

References

1. Silva I, Costa D. Consequences of shift work and night work: a literature review. *Healthc.* 2023;11:512.
2. James SM, Honn KA, Gaddameedhi S, Van Dongen HPA. Shift work: disrupted circadian rhythms and sleep-implications for health and well-being. *Curr Sleep Med Rep.* 2017;3(2):104-112.
3. Park JH, Park H, Bae S, Kang J. Associations between the timing and nutritional characteristics of bedtime meals and sleep quality for nurses after a rotating night shift: a cross-sectional analysis. *Int J Environ Res Public Health.* 2023;20(2):1489.
4. Peplonska B, Bukowska A, Sobala W. Association of rotating night shift work with BMI and abdominal obesity among nurses and midwives. *PLoS One.* 2015;10:e0133761.
5. Buz EH. Yetişkin bireylerin iş stres düzeylerinin beslenme durumu ve diyet kalitesi üzerine etkisi. *Bes Diy Derg.* 2022;50(2):145-154.
6. Vural S, Vural S, Coskun F. The impact of shift work on the lifestyle and well-being of emergency physicians: a comprehensive examination of eating habits and health behaviors. *Eurasian J Emerg Med.* 2024;23(2):112-120.
7. Güneşer R, Atalay E. Evaluation of sleep quality, work stress, and nutritional behavior of ambulance service employees. *Journal of Pre-Hospital.* 2020;5(3):143-156.
8. Çalık KY, Aktaş S, Bulut HK, Anahar EÖ. Vardiyalı ve nöbet sistemi şeklindeki çalışma düzeninin hemşireler üzerine etkisi. *Sag Bil Mesl Derg.* 2015;2(1):33–45. Turkish.

9. Çakmak DG. Vardiyalı çalışan işçilerde beslenme durumu, uyku kalitesi ve bazı biyokimyasal bulgular arasındaki ilişki. *Yüksek Lisans Tezi.* Ankara: Hacettepe Üniversitesi; 2019.
10. Doğanay D, Bakkal LZ, Görey CN, Büyükbektaş T. Ultra-processed food consumption: effects on the gut microbiota. *Bes Diy Derg.* 2023;51(2):109-116. Turkish.
11. Ha OR, Lim SL. The role of emotion in eating behavior and decisions. *Front Psychol.* 2023;14:1265074.
12. Mengi Çelik Ö, Güler Ü, Ekici EM. Factors affecting ultra-processed food consumption: hedonic hunger, food addiction, and mood. *Food Sci Nutr.* 2025;13(5):e70248.
13. Martini D, Godos J, Bonaccio M, Vitaglione P, Grosso G. Ultra-processed foods and nutritional dietary profile: a meta-analysis of nationally representative samples. *Nutrients.* 2021;13(10):3390.
14. Martinez-Perez C, Daimiel L, Climent-Mainar C, Martínez-González MÁ, Salas-Salvadó J, Corella D, et al. Integrative development of a short screening questionnaire of highly processed food consumption (sQ-HPF). *Int J Behav Nutr Phys Act.* 2022;19(1):6.
15. Erdoğan Gövez N, Köksal E, Martinez-Perez C, Daimiel L. Validity and reliability of the Turkish version of the screening questionnaire of highly processed food consumption (sQ-HPF). *Nutrients.* 2024;16(15):2552.
16. Revicki DA, Wood M, Wiklund I, Crawley J. Reliability and validity of the Gastrointestinal Symptom Rating Scale in patients with gastroesophageal reflux disease. *Qual Life Res.* 1998;7(1):75-83.
17. Turan N, Aşt TA, Kaya N. Reliability and validity of the Turkish version of the gastrointestinal symptom rating scale. *Gastroenterol Nurs.* 2017;40(1):47-55.
18. Mira JJ, Cobos A, Martínez García O, Bueno Domínguez MJ, Astier-Peña MP, Pérez Pérez P, et al. An acute stress scale for health care professionals caring for patients with COVID-19: validation study. *JMIR Form Res.* 2021;5:e27107.
19. Şimşek Ç, Mercan Baspinar M. Turkish validity and reliability of the Self-Applied Acute Stress Scale (EASE) for healthcare providers. *Psychiatry J.* 2024;2024:7673595.
20. Mason AE, Vainik U, Acree M, Tomiyama AJ, Dagher A, Epel ES, et al. Improving assessment of the spectrum of reward-related eating: the RED-13. *Front Psychol.* 2017;8:795.
21. Saruhan N, Konuşkan ZG. A validity and reliability study of reward-related eating scale RED-13 into Turkish. *Karya J Health Sci.* 2023;4(2):132-138.
22. Madden AM, Smith S. Body composition and morphological assessment of nutritional status in adults: a review of anthropometric variables. *J Hum Nutr Diet.* 2016;29(1):7-25.
23. Elizabeth L, Machado P, Zinöcker M, Baker P, Lawrence M. Ultra-processed foods and health outcomes: a narrative review. *Nutrients.* 2020;12(7):1955.
24. Calixto Andrade G, Julia C, Deschamps V, Srour B, Hercberg S, Kesse-Guyot E, et al. Consumption of ultra-processed food and its association with sociodemographic characteristics and diet quality in a representative sample of French adults. *Nutrients.* 2021;13(2):682.
25. Steele EM, Ponce JM, Cediel G, Louzada M, Khandpur N, Machado P, et al. Potential reductions in ultra-processed food consumption substantially improve population cardiometabolic-related dietary nutrient profiles in eight countries. *Nutr Metab Cardiovasc Dis.* 2022;32(11):2739–2750.
26. Monda A, de Stefano MI, Villano I, Allocca S, Casillo M, Messina A, et al. Ultra-processed food intake and increased risk of obesity: a narrative review. *Foods.* 2024;13(16):2627.
27. Haghighatdoost F, Feizi A, Hajihashemi P, Ani A, Roohafza H, Adibi P. The association between ultra-processed foods consumption and disorders of gut-brain interaction: The Isfahan Functional Disorders (ISFUN) Study. *Neurogastroenterol Motil.* 2025;37(11):e70071.
28. Reuzé A, Delvert R, Perrin L, Benamouzig R, Sabaté JM, Bouchoucha M, et al. Association between self-reported gluten avoidance and irritable Bowel syndrome: findings of the nutrinet-santé study. *Nutrients*. 2021;13(11):4147.
29. Whelan K, Bancil AS, Lindsay JO, Chassaing B. Ultra-processed foods and food additives in gut health and disease. *Nat Rev Gastroenterol Hepatol.* 2024;21(6):406-427.
30. Losso JN. Food processing, dysbiosis, gastrointestinal inflammatory diseases, and antiangiogenic functional foods or beverages. *Annu Rev Food Sci Technol.* 2021;12:235-258.
31. Atzeni A, Martínez MÁ, Babio N, Konstanti P, Tinahones FJ, Vioque J, et al. Association between ultra-processed food consumption and gut microbiota in senior subjects with overweight/obesity and metabolic syndrome. *Front Nutr.* 2022;9:976547.
32. Nie JY, Zhao Q. Beverage consumption and risk of ulcerative colitis: systematic review and meta-analysis of epidemiological studies. *Medicine (Baltimore).* 2017;96(49):e9070.
33. Li F, Liu X, Wang W, Zhang D. Consumption of vegetables and fruit and the risk of inflammatory bowel disease: a meta-analysis. *Eur J Gastroenterol Hepatol.* 2015;27(6):623-633.
34. Faisal-Cury A, Leite MA, Escuder MML, Levy RB, Peres MFT. The relationship between ultra-processed food consumption and internalising symptoms among adolescents from São Paulo city, Southeast Brazil. *Public Health Nutr.* 2022;25(12):2498-2506.
35. Ülker İ, Çamli A. Does ultra-processed food consumption affect hedonic hunger? *Bes Diy Derg.* 2024;52(1):68-76.
36. Açık M, Durmaz SE. Ultra işlenmiş besinler ve mental sağlık. *Turk Klin Nutr Diet-Spec Top.* 2025;11(1):68–73.
37. Vainik U, Eun Han J, Epel ES, Janet Tomiyama A, Dagher A, Mason AE. Rapid assessment of reward-related eating: the RED-X5. *Obesity (Silver Spring).* 2019;27(2):325-331.
38. Lee Y, Kim YK. Understanding the connection between the gut-brain axis and stress/anxiety disorders. *Curr Psychiatry Rep.* 2021;23(5):22.
39. De la Roca-Chiapas JM, Solís-Ortiz S, Fajardo-Araujo M, Sosa M, Córdova-Fraga T, Rosa-Zarate A. Stress profile, coping style, anxiety, depression, and gastric emptying as predictors of functional dyspepsia: a case-control study. *J Psychosom Res.* 2010;68(1):73-81.
40. Martínez Leo EE, Segura Campos MR. Effect of ultra-processed diet on gut microbiota and thus its role in neurodegenerative diseases. *Nutrition.* 2020;71:110609.

DOI: 10.4274/gulhane.galenos.2025.46872
Gulhane Med J 2026;68(2):81-86

Investigation of factors associated with the diagnosis process and delayed diagnosis in Familial Mediterranean fever patients: a single-center experience

Merve Öztürk[1], Yusuf Çetin Doğaner[2], Ümit Aydoğan[3], Sedat Yılmaz[3]

[1]Çayıralan Community Health Center, Yozgat, Türkiye
[2]University of Health Sciences Türkiye, Gülhane Faculty of Medicine, Department of Family Medicine, Ankara, Türkiye
[3]University of Health Sciences Türkiye, Gülhane Faculty of Medicine, Department of Rheumatology, Ankara, Türkiye

Cite this article as: Öztürk M, Doğaner YÇ, Aydoğan Ü, Yılmaz S. Investigation of factors associated with the diagnosis process and delayed diagnosis in Familial Mediterranean fever patients: a single-center experience. *Gulhane Med J.* 2026;68(2):81-86.

Date submitted:
01.07.2025
Date accepted:
28.11.2025
Epub:
21.05.2026
Publication Date:
16.06.2026

Corresponding Author:
Merve Öztürk, M.D., Çayıralan Community Health Center, Yozgat, Türkiye
merveozupak@hotmail.com

ORCID:
orcid.org/0009-0009-0622-2388

Keywords: Familial Mediterranean fever, diagnosis, diagnostic delay

ABSTRACT

Aims: Familial Mediterranean fever (FMF) is a common autoinflammatory disease in Türkiye and worldwide. Diagnosis may be delayed because it can present with diverse clinical phenotypes. This study aims to determine the initial symptoms of patients with FMF, the time from symptom onset to diagnosis, and factors associated with delayed diagnosis.

Methods: This cross-sectional study included patients with FMF who were under follow-up, receiving treatment, and who volunteered to participate. A face-to-face data collection form, including questions about the first symptoms of FMF, age at onset, and age at diagnosis, was administered to the patients.

Results: Of the 169 patients, 58% (n=98) were female, and the mean age was 34.31±10.96 years. The mean age at onset of symptoms was 17.26±11.43 years, and the mean age at diagnosis was 24.67±12.62 years. The diagnostic delay was 7.41±8.57 years. The most common initial symptom of FMF was abdominal pain (72.8%, n=123). Diagnostic delay was significantly longer in patients with joint pain than in patients without joint pain [6.00 (0-39) years vs. 3.00 (0-35) years; p=0.007]. Similarly, the diagnostic delay was significantly shorter in patients who had undergone surgery compared with those without a history of surgery [3.00 (0-39) years vs. 8.00 (0-37) years; p=0.002].

Conclusions: This study demonstrated that diagnostic delay remains a significant issue among patients with FMF, particularly those presenting with joint pain.

Introduction

Familial Mediterranean fever (FMF) is the most common hereditary autoinflammatory disease. FMF is an autoinflammatory disease of ethnic origin and genetic inheritance that presents with recurrent and self-limiting attacks of fever, peritonitis, pleuritis, arthritic pain, or rash (1). It is common in populations of Eastern Mediterranean origin, particularly among Turks, Jews, Arabs, and Armenians. While the carrier rate in Türkiye is 1/5, the disease incidence is reported to be 1/1000 (2,3).

FMF disease is caused by mutations on chromosome 16 (16p13.3) encoding the pyrin protein of the Mediterranean fever gene, which is inherited in an autosomal recessive manner (4). Excessive activation of the pyrin inflammasome because of these mutations and the resulting inflammation causes the typical febrile attacks observed in FMF (5-7). The most common symptoms are abdominal pain, fever, arthritis, chest pain, and erysipelas-like erythema (2).

Diagnosis is based on clinical symptoms. However, the disease can present with different clinical phenotypes. The signs and symptoms of the disease are not specific, and the differential diagnosis includes many diseases. This can make diagnosis difficult and lead to significant delays in starting treatment. Several studies have reported that diagnosis may be missed or delayed even in countries such as Israel and Türkiye, which are considered endemic regions for FMF (8-9). Misdiagnosis can lead to unnecessary surgery. Delayed diagnosis may increase the risk of amyloidosis. Delayed diagnosis of FMF can significantly increase morbidity and contribute to increased mortality and healthcare costs (10).

The existing literature reveals a paucity of studies specifically addressing the reasons for diagnostic delay or misdiagnosis (8). In this context, our study aimed to assess the initial symptoms of patients with FMF, determine the time from symptom onset to diagnosis, and identify factors associated with diagnostic delay.

Methods

Study design and participants

The cross-sectional study was conducted using a face-to-face data collection form on 169 patients who had applied to the Rheumatology Department and affiliated outpatient clinics of a hospital providing tertiary healthcare services in Türkiye between 01.11.2021 and 30.10.2022, who were being followed up and treated with a diagnosis of FMF, and who volunteered to participate in the study. The diagnosis of FMF in all patients was made by rheumatologists based on the Tel-Hashomer diagnostic criteria (11), which are widely accepted and validated for clinical use.

Data collection

The study collected information on the sociodemographic characteristics of the participants, their initial complaints related to FMF, the age at which their initial complaints began, and the age at which the diagnosis was made, the frequency of attacks before and after diagnosis, any diseases other than FMF, the healthcare institutions and specialist doctors they consulted before receiving a diagnosis, and the diagnosis for their initial complaints. Before the diagnosis, the patient was asked about their surgical history, history of amyloidosis, genetic testing, and family history of FMF or other rheumatological diseases. The FMF patient data collection form, comprising 38 questions related to the diagnostic process, was administered to patients via face-to-face interviews after obtaining their consent. Data were collected using a structured data collection form specifically developed for this study.

Statistical Analysis

The research data were analyzed using IBM SPSS Statistics for Windows, version 26.0 (IBM Corp., Armonk, NY, USA). The research data were examined for normality using the Kolmogorov-Smirnov test. In the analysis, the Mann-Whitney U test compared two independent groups, and the Kruskal-Wallis test compared three or more independent groups. Median (minimum-maximum) values were reported in the analysis. Multiple-comparison tests were performed using the Bonferroni correction to determine which groups differed. The relationships between variables were evaluated using Spearman correlation tests. A value of $p<0.05$ was considered statistically significant in the analyses.

Ethical approval

The University of Health Sciences Türkiye, Gülhane Non-Interventional Research Ethics Committee approved the study at the board meeting held on 21.10.2021 with decision number 2021/369. It was accepted at the board meeting number 16 of the University of Health Sciences Türkiye, Gülhane SBU Health Application and Research Center Medical Specialization Education Board dated 24.09.2021 and numbered E-50687469-799.

Results

Socio-demographic and clinical characteristics

The mean age of the 169 participants was 34.31±10.96 years. The mean age at onset of symptoms was 17.26±11.43 years, while the mean age at diagnosis was 24.67±12.62 years. The mean diagnostic delay was 7.41±8.57 years. Among the patients who participated in the study, 58% (n=98) were female; 62.7% (n=106) were married; 46.7% (n=79) were university graduates; 46.2% (n=78) were employed; and 79.9% (n=135) lived in urban areas (Table 1).

The participants' initial complaints of FMF were abdominal pain (72.8%, n=123), joint pain (59.2%, n=100), and fever (51.5%, n=87) (Figure 1). Of those with other diseases, 57.1% (n=16) had ankylosing spondylitis; 10.7% (n=3) had inflammatory bowel disease; 7.14% (n=2) had rheumatoid arthritis; and 17.8% (n=5) had other rheumatological diseases.

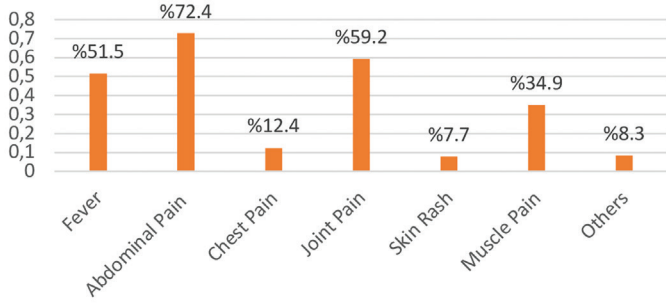

Figure 1. Distribution of initial complaints in patients with Familial Mediterranean fever
Others: Back pain (n: 5), weakness (n: 3), nausea (n: 3), syncope (n: 1), drowsiness (n: 1), bloody urine (n: 1)

The most common healthcare institutions to which patients in the study presented before diagnosis were public hospitals (57.4%) and training and research hospitals (56.8%); the most common specialties were internal medicine and rheumatology.

Following a thorough evaluation of participants' initial diagnoses, 92.9% (n=157) were found to have been misdiagnosed. In the present study, the subjects were diagnosed as follows: 33.7% (n=57) with gastrointestinal system diseases; 17.2% (n=29) with appendicitis; 12.4% (n=21) with arthritis; and 6.5% (n=11) with acute rheumatic fever (ARF) (Figure 2).

Table 1. Socio-demographic characteristics of patients with Familial Mediterranean fever (n=169)

Variables		n (%)
Gender	Male	71 (42)
	Female	98 (58)
Marital status	Married	106 (62.7)
	Single	63 (37.3)
Educational status	Primary school	26 (15.4)
	Middle school	12 (7.1)
	High school	52 (30.8)
	University	79 (46.7)
Working status	Employed	78 (46.2)
	Unemployed	91 (53.8)
Place of residence	Urban	34 (20.1)
	Rural	135 (79.9)
Physical activity	None	101(59.8)
	Irregular	46 (27.2)
	Regular	22 (13.0)
Smoking	No	116 (68.6)
	Yes	53 (31.4)
Alcohol use	No	158 (93.5)
	Yes	11 (6.5)

78.7% (n=133) of the participants had not undergone surgery before diagnosis. The most common surgical procedure was appendectomy (76.9%, n=30), followed by hernia surgery (2.5%, n=1), and gallbladder surgery (8%, n=3). The study examined the genetic testing status of the participants. Of the participants who underwent genetic testing (n=161), 87.6% (n=148) tested positive for a genetic mutation. Among those who tested positive, 64.5% (n=109) knew their specific genetic mutation. Of the participants whose genetic mutation was known, 22.9% (n=25) were M694V homozygous; 13.8% (n=15) were M694V heterozygous; 10.1% (n=11) were M694V/V726A compound heterozygous; 9.2% (n=10) were M694V/M680I compound heterozygous; and 8.3% (n=9) were M694V/E148Q compound heterozygous.

73.4% of the participants had a family history of FMF; among these, 62.1% (n=105) had a history of FMF in 1st-degree relatives, 26.7% (n=45) in 2nd-degree relatives, and 30.8% (n=52) in other relatives.

Diagnostic delay and associated factors

Correlation analysis showed that the length of diagnostic delay was positively and significantly associated with patients' current age (r=0.360, p<0.001) and with their age at diagnosis (r=0.436, p<0.001). In contrast, there was no significant correlation between the length of diagnostic delay and the age at which symptoms first appeared.

The results for diagnostic delay times by participants' socio-demographic characteristics are shown in Table 2.

In the results for diagnosis delay times according to the participants' initial complaints, a significant difference was found between participants with and without joint pain complaints [3.00 (0-35) years vs. 6.00 (0-39) years; p=0.007]. The diagnosis delay time for those with joint pain was found to be higher than the diagnosis delay time for those without joint pain (Table 2).

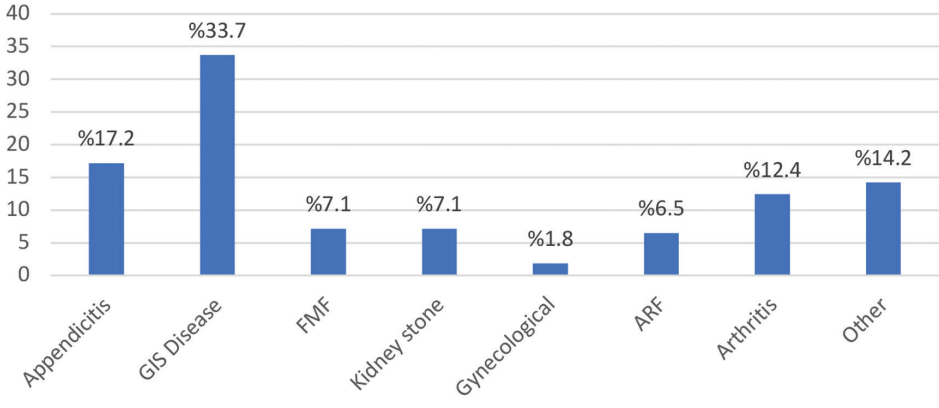

Figure 2. Distribution of initial diagnoses in patients with Familial Mediterranean fever
Others: Myalgia (n: 14), pericarditis (n: 4), Henoch-Schönlein Purpura (n: 2), cellulitis (n: 1), gout (n: 1), cholecystitis (n: 1)
FMF: Familial Mediterranean fever, ARF: Acute rheumatic fever, GIS: Gastrointestinal system

The results for diagnostic delay periods, stratified by the healthcare institutions patients visited before diagnosis, revealed a significant difference between participants who visited private hospitals and those who did not [3.50 (0-39) years vs. 6.00 (0-35) years; p=0.037]. The average diagnostic delay was found to be higher for participants who visited private hospitals than for those who did not. No significant difference was found in diagnostic delay for visits to other healthcare institutions.

The present study found no statistically significant correlation between diagnostic delay times and patients' initial diagnosis, genetic test status, genetic test result, gene mutation, and family history of FMF (p>0.05).

A significant difference in diagnostic delay time was found between participants who had undergone surgery and those who had not [3.00 (0-39) years vs. 8.00 (0-37) years; p=0.002]. Examination of the results revealed that diagnostic delay was longer in patients who underwent surgery than in those who did not.

Table 2. Comparison of diagnostic delay times by socio-demographic characteristics and patients' initial complaints

Characteristics		n	Diagnostic delay (years) Median (min-max)	Test statistic	p
Gender	Male	71	3.00 (0-29)	Z=-1.16	0.242[a]
	Female	98	5.00 (0-39)		
Marital status	Married	106	6.00 (0-39)	Z=-3.97	**<0.001**[a]
	Single	63	1.00 (0-37)		
Educational status	Primary school	26	9.50 (0-35)	X^2=15.49	**0.001**[b]
	Middle school	12	1.50 (0-39)		
	High school	52	2.00 (0-29)		
	University	79	6.00 (0-37)		
Working status	Employed	78	5.00 (0-30)	Z=-0.51	0.605[a]
	Unemployed	91	4.00 (0-39)		
Place of residence	Urban	34	5.50 (0-27)	Z=-0.04	0.962[a]
	Rural	135	4.00 (0-39)		
Physical activity	None	101	3.00 (0-35)	X^2=2.12	0.345[b]
	Irregular	46	5.50 (0-39)		
	Regular	22	3.50 (0-37)		
Smoking	No	116	3.50 (0-37)	Z=-1.16	0.246[a]
	Yes	53	7.00 (0-39)		
Alcohol use	No	158	4.00 (0-39)	Z=-0.04	0.962[a]
	Yes	11	4.00 (0-18)		
Fever	No	82	4.50 (0-39)	Z=-0.29	0.772[a]
	Yes	87	4.00 (0-37)		
Stomachache	No	46	5.00 (0-39)	Z=-0.24	0.806[a]
	Yes	123	4.00 (0-35)		
Chest pain	No	148	4.00 (0-39)	Z=-1.17	0.238[a]
	Yes	21	8.00 (0-18)		
Joint pain	No	69	3.00 (0-35)	Z=-2.69	**0.007**[a]
	Yes	100	6.00 (0-39)		
Skin rash	No	156	4.00 (0-39)	Z=-0.51	0.610[a]
	Yes	13	6.00 (0-17)		
Muscle pain	No	110	3.00 (0-35)	Z=-1.17	0.241[a]
	Yes	59	5.00 (0-39)		
Other	No	155	5.00 (0-39)	Z=-1.77	0.077[a]
	Yes	14	1.00 (0-28)		

[a]: Mann-Whitney U test, [b]: Kruskal-Wallis test
min-max: Minimum-maximum

Discussion

The diagnostic delay for patients included in the study was approximately 7.5 years. Diagnostic delay time increased with both patient age and age at diagnosis; it was significantly longer in married than in single patients, in patients whose first complaint was joint pain than in those without joint pain, and in patients who underwent surgery than in those who did not.

In the literature, the diagnostic delay time was reported to be approximately 7 years in the study of 2838 FMF patients in Türkiye, approximately 10 years in the multicentre study by Yaşar Bilge et al. (10), and approximately 8 years in the study by Hageman et al. (12), where it was known that the majority of the patients included were of Türk origin (2). It has been reported that the delay in diagnosis is longer outside the Mediterranean countries, with an average of 15 years in a study conducted in Germany, approximately 18 years in another study conducted in Italy, and an average time to diagnosis of approximately 9 years in another study conducted by Migita et al. (13) in Japan (14,15). The delay in diagnosis observed in our study is consistent with previous studies of patients of Turkish origin. It shows that, even in countries like Türkiye, where FMF is endemic and the disease is common, diagnostic delay remains a problem, and awareness of the disease needs to be increased.

The most common initial complaint in FMF was abdominal pain, followed by joint pain and fever. In a study of 197 FMF patients in Türkiye, abdominal pain was reported by 65%, fever by 47%, and joint symptoms by 43% when the first complaints were investigated (8). In the study by Samuels et al. (16), arthritis was reported as the third most common cause of clinical presentation after fever and abdominal pain, with a rate of 45%. Although the data obtained in our study are consistent with prevailing opinion, the second most common complaint—joint pain—appears to result from patients' inability to distinguish arthritis from arthralgia; consequently, they interpret all joint complaints as joint pain.

Our study found a significant difference in diagnostic delay time in those with joint pain compared to those without, and it was observed that the diagnostic delay time was longer in those with joint pain. A study by Erdogan et al. (8), stated that joint attacks play an important role in diagnosis delay and misdiagnosis, and it was reported that patients were less likely to have abdominal pain at the onset of FMF, while they were more likely to have joint involvement. A study by Barut et al. (17), reported that patients with symptoms of arthritis/arthralgia had longer diagnostic delays than those with symptoms of fever and serositis. The data obtained in our study are similar to those reported in the literature. Given the available data, it should be noted that complaints of joint pain may not initially be attributed to FMF; other diagnoses may be considered, and patients with FMF may present with isolated joint symptoms. This information should be considered when establishing the differential diagnosis of FMF.

We observed that the majority of patients (92.9%) were misdiagnosed. These were in order of frequency: gastrointestinal diseases, acute appendicitis, and arthritis. A study by Erdogan et al. (8) in 2019 reported that 84% of participants were misdiagnosed before diagnosis of FMF. It was reported that the two most common diagnoses in misdiagnosed patients were acute appendicitis and ARF. In another study of 143 patients in Türkiye, the misdiagnosis rate was 73%, and it was reported that appendicitis was the most common diagnosis, followed by gastrointestinal disease (18). In our study, the frequent occurrence of gastrointestinal disease as the first diagnosis may be explained by the fact that abdominal pain was the most common complaint: patients most often presented to emergency services with abdominal pain and were discharged without a clear diagnosis. The study did not find a significant association between the patients' initial diagnosis and the delay in diagnosis.

The results indicated that approximately one-fifth (21.3%) of the patients underwent surgical intervention; the most common intervention was appendectomy. In the study by Erdogan et al. (8), the surgical operation rate was 28%, and the most common operation was appendectomy in 91%. In a single-center retrospective study conducted in Amsterdam in 2019, appendectomy was the most common surgical operation (12). In the study by Kaşifoğlu et al. (19) to investigate the frequency of surgical operations in FMF patients, the surgical operation rate was reported to be 29.1% and the appendectomy rate was 91.8%. In our study, the surgical operation rate and the history of appendectomy were consistent with the literature. The heterogeneous and variable clinical course of FMF attacks, which can be mistaken for an acute abdomen, may lead to high rates of surgical intervention, including appendectomy, because of the disease's rarity and low awareness.

It was observed that those who underwent surgery had a longer delay in diagnosis than those who did not, suggesting that undergoing surgery may cause a diagnostic delay. In the literature, the study by Lidar et al. (9) found that surgery played an important role in misdiagnosis and delayed diagnosis. Increasing physicians' knowledge and awareness of FMF may contribute to the early diagnosis of FMF and to avoiding unnecessary surgery. A detailed medical history is important for a definitive diagnosis of FMF and other abdominal pathologies.

Study Limitations

Our study has several limitations. First, since it was conducted in a hospital providing tertiary health care in Türkiye, the results may be limited in that they are not generalizable to patients living in rural areas or to patients from other ethnic groups. Second, because the results are based on face-to-face patient responses, they may lack objectivity in this context. Third,

given the prevalence of this disease in Türkiye, our sample size could have been larger. Fourth, certain clinically important characteristics of FMF, such as attack severity, frequency, or multi-site attacks, were not evaluated.

Conclusion

The study found that patients waited a long time for a diagnosis, and this was longer for those with joint symptoms. This should always be considered when a patient presents with joint symptoms.

In light of these findings, it is challenging to pinpoint the causes of diagnostic delays. However, to prevent FMF complications, physicians need to be better informed.

Ethics

Ethics Committee Approval: The University of Health Sciences Türkiye, Gülhane Non-Interventional Research Ethics Committee approved the study at the board meeting held on 21.10.2021 with decision number 2021/369.

Informed Consent: All patients participating in the study provided informed consent.

Footnotes

Authorship Contributions

Surgical and Medical Practices: M.Ö., Concept: M.Ö., Y.Ç.D., S.Y., Design: M.Ö., Y.Ç.D., Ü.A., S.Y., Data Collection or Processing: M.Ö., Analysis or Interpretation: M.Ö., Y.Ç.D., Literature Search: M.Ö., Y.Ç.D., Writing: M.Ö., Y.Ç.D., Ü.A., S.Y.

Declaration of Interests: One authors of this article, Ümit Aydoğan, are a members of the Editorial Board of the Gulhane Medical Journal. However, they did not involved in any stage of the editorial decision of the manuscript.

Conflict of Interest: The authors declare that there is no conflict of interest.

Financial Disclosure: The authors declared that this study received no financial support.

References

1. Ben-Chetrit E, Levy M. Familial Mediterranean fever. *Lancet.* 1998;351(9103):659-564.
2. Familial Mediterranean fever (FMF) in Turkey: results of a nationwide multicenter study. *Medicine (Baltimore).* 2005;84(1):1-11.
3. Lidar M, Livneh A. Familial Mediterranean fever: clinical, molecular, and management advancements. *Neth J Med*. 2007;65(9):318-324.
4. Aksentijevich I, Centola M, Deng Z, Sood R, Balow J, Wood G, et al. Ancient missense mutations in a new member of the RoRet gene family are likely to cause familial Mediterranean fever. *The International FMF Consortium, Cell*. 1997;90(4):797-807.
5. Manukyan G, Aminov R. Update on pyrin functions and mechanisms of Familial Mediterranean fever. *Front Microbiol.* 2016;7:456.
6. Van Gorp H, Saavedra PHV, De Vasconcelos NM, Van Opdenbosch N, Walle L Vande, Matusiak M, et al. Familial Mediterranean fever mutations lift the obligatory requirement for microtubules in Pyrin inflammasome activation. *Proc Natl Acad Sci USA.* 2016;113(50):14384-14389.
7. Heilig R, Broz P. Function and mechanism of the pyrin inflammasome. *Eur J Immunol.* 2018;48(2):230-238.
8. Erdogan M, Ugurlu S, Ozdogan H, Seyahi E. Familial Mediterranean fever: misdiagnosis and diagnostic delay in Turkey. *Clin Exp Rheumatol.* 2019;37(Suppl 121)(6):119-124.
9. Lidar M, Tokov I, Chetrit A, Zaks N, Langevitz P, Livneh A. Diagnosis delay in familial Mediterranean fever (FMF): social and gender gaps disclosed. *Clin Exp Rheumatol.* 2005;23(3):357-363.
10. Yaşar Bilge Ş, Sarı İ, Solmaz D, Şenel S, Emmungil H, Kılıç L, et al. The distribution of MEFV mutations in Turkish FMF patients: multicenter study representing results of Anatolia. *Turk J Med Sci.* 2019;49(2):472-477.
11. Livneh A, Langevitz P, Zemer D, Zaks N, Kees S, Lidar T, et al. Criteria for the diagnosis of familial Mediterranean fever. *Arthritis Rheum.* 1997;40(10):1879-1885.
12. Hageman IMG, Visser H, Veenstra J, Baas F, Siegert CEH. Familial Mediterranean fever (FMF): a single centre retrospective study in Amsterdam. *Netherlands Journal of Medicine*. 2019;77(5):177-182.
13. Migita K, Uehara R, Nakamura Y, Yasunami M, Tsuchiya-Suzuki A, Yazaki M, et al. Familial Mediterranean fever in Japan. *Medicine (Baltimore).* 2012;91(6):337-343.
14. Giese A, Örnek A, Kilic L, Kurucay M, Şendur SN, Lainka E, et al. Disease severity in adult patients of Turkish ancestry with familial Mediterranean fever living in Germany or Turkey. Does the country of residence affect the course of the disease? *J Clin Rheumatol*. 2013;19(5):246-251.
15. La Regina M, Nucera G, Diaco M, Procopio A, Gasbarrini G, Notarnicola C, et al. Familial Mediterranean fever is no longer a rare disease in Italy. *Eur J Hum Genet.* 2003;11(1):50-56.
16. Samuels J, Aksentijevich I, Torosyan Y, Centola M, Deng Z, Sood R, et al. Familial Mediterranean fever at the millennium. Clinical spectrum, ancient mutations, and a survey of 100 American referrals to the National Institutes of Health. *Medicine (Baltimore).* 1998;77(4):268-297.
17. Barut K, Sahin S, Adrovic A, Sinoplu AB, Yucel G, Pamuk G, et al. Familial Mediterranean fever in childhood: a single-center experience. *Rheumatol Int.* 2018;38(1):67-74.
18. Erdogan M, Ozguler Y, Dincses E, Esatoglu SN, Guzelant G, Karatemiz G, et al. Problems in the diagnosis of Familial Mediterranean fever in Turkey. *Annals of the Rheumatic Diseases.* 2017; 76(2):719.3-720
19. Kaşifoğlu T, Cansu D, Korkmaz C. Frequency of abdominal surgery in patients with Familial Mediterranean fever. *Intern Med.* 2009;48(7):523-526.

DOI: 10.4274/gulhane.galenos.2025.34711
Gulhane Med J 2026;68(2):87-93

Age-related effects of smartphone and tablet reading on ocular surface parameters

Selcan Ekicier Acar, Zennure Özdemir Yıldız

University of Health Sciences Türkiye, Atatürk Sanatorium Training and Research Hospital, Clinic of Ophthalmology, Ankara, Türkiye

Cite this article as: Ekicier Acar S, Özdemir Yıldız Z. Age-related effects of smartphone and tablet reading on ocular surface parameters. *Gulhane Med J.* 2026;68(2):87-93.

Date submitted:
07.07.2025
Date accepted:
02.12.2025
Epub:
08.06.2026
Publication Date:
16.06.2026

Corresponding Author:
Selcan Ekicier Acar, M.D., University of Health Sciences Türkiye, Atatürk Sanatorium Training and Research Hospital, Clinic of Ophthalmology, Ankara, Türkiye
selcanekicier@gmail.com

ORCID:
orcid.org/0000-0002-7025-380X

Keywords: Handheld devices, visual discomfort, blinking, ocular surface

ABSTRACT

Aims: The use of handheld devices has increased rapidly over the past decade. Smartphones and tablets are commonly used for reading and work-related tasks. This study aims to compare the effects of smartphone and tablet screen sizes on the ocular surface of adolescents and young adults.

Methods: This was a prospective observational study involving 90 healthy volunteers divided into three age-based groups: adolescents (n=30, 10-18 years), young adults (n=30, 18-24 years), and adults (n=30, 24-40 years, control). Participants read for 30 minutes using a smartphone, a tablet, and a printed book. The Ocular Surface Disease Index©, the ocular discomfort questionnaire, fluorescein break-up time (FBUT), corneal fluorescein staining, the Schirmer test, and the blink rate were assessed before and after each reading session.

Results: Ninety participants (mean age for adolescents: 13.33±1.33 years; young adults: 20.77±2.32 years; adults: 33.47±5.38 years; sex distribution: 56%, 56%, 53% female, respectively) were included. FBUT values decreased significantly after reading in all groups ($p<0.01$). In adolescents, corneal fluorescein staining significantly increased after smartphone reading, from 0 to 0.30±0.46 ($p=0.001$). Schirmer test values did not change significantly ($p>0.05$) among all groups. Blink rate decreased from 18.2±2.7 to 9.8±1.8 blinks/min and incomplete blinking increased from 1.8±0.9 to 4.9±1.6 blinks/min during smartphone reading ($p<0.001$). Discomfort scores were highest after smartphone use (34.8±13.8) compared with tablet (24.8±10.1) and print reading (21.0±12.4) ($p<0.001$).

Conclusions: Reading from smartphones and tablets causes measurable alterations in ocular surface integrity, tear film stability, and blinking patterns. Ocular discomfort scores were highest after smartphone use, particularly in adolescents and young adults.These findings highlight the ocular strain associated with handheld devices and the need for preventive strategies, especially for younger populations with extended screen exposure.

Introduction

Electronic devices are commonly used in daily life. The use of handheld devices has been increasing rapidly. Smartphones, computers, tablets, and electronic reading devices have become necessary to read books and conduct work-related tasks (1). Electronic screen use increased during the coronavirus disease 2020 pandemic (2). Extended screen time during childhood adversely affects health and well-being and is associated with ocular changes, such as myopic progression and ocular surface alterations (3). This increasing trend in screen usage has resulted in national and international efforts to control screen time among young people (4-6).

Electronic displays, including laptops, tablets, and smartphones, have substantially changed methods of accessing information and are an important factor in daily human life compared with printed displays. Instead of pen and paper, students use software and tools to create presentations and projects. How varying screen sizes influence ocular surface parameters and blinking dynamics is not well understood, particularly in younger populations increasingly exposed to these devices. Prolonged reading from electronic displays is central to the onset of ocular symptoms and affects quality of life. After prolonged reading, the symptoms experienced are not specific to patients with dry eye disease (DED). Healthy individuals without a DED diagnosis experience eye-related complaints after prolonged reading (7).

High cognitive activity associated with reading can lead to dry eye symptoms caused by decreased and partial blinking (8). Similarly, prolonged screen time affects blinking dynamics, facilitating the onset and progression of ocular surface changes and causing dry eye symptoms. DED poses a substantial burden on patients' quality of life, productivity, learning, and economic well-being. Prolonged screen use from an early age and the inevitable role of screens in work environments predispose children, adolescents, and young adults to dry eyes and to an earlier, more rapid decline in quality of life (9,10).

Smartphones and tablets, as small handheld devices, typically feature larger, vertically oriented screens and lack external keyboards or mice, distinguishing them from traditional computers (11). Variations between computers and handheld devices in screen size, viewing distance and angle, usage modality, ambient light levels, screen reflection, and user posture may contribute to divergent ocular symptomatology. This study aims to elucidate these differences by investigating the effects of reading from handheld devices of varying screen sizes and from printed materials on ocular surface parameters and blink dynamics in adolescents and young adults. To the best of our knowledge, this is the first investigation to specifically assess the impact of screen size on the ocular surface in this population.

Methods

Study design and setting

This prospective, comparative study was conducted at the University of Health Sciences Türkiye, Atatürk Sanatorium Training and Research Hospitalfrom January to December 2024.

Participants were tested under standardized environmental conditions, including lighting. Screen brightness for all devices was adjusted to 50% of the maximum level. Font type and size were kept consistent across groups, and reading distance was set at 40 cm between the eyes and the screen. All participants undertook the reading test under comparable environmental conditions: temperatures ranged from 22 °C to 25 °C, without air conditioning, and testing occurred between 08.00 and 10.00 hours.

Participants

A total of adolescents (n=30), young adults (n=30), and adults (n=30) were included in the study. Volunteers underwent the following assessments: best-corrected visual acuity, tear break-up time, corneal fluorescein staining (assessed by the Oxford scale), Schirmer's test, Ocular Surface Disease Index© (OSDI©) questionnaire, and blink rate. A 15-minute interval was maintained between assessments. All volunteers had normal vision and were free of dry eye or significant accommodative or binocular vision abnormalities. Baseline readings served as controls.

Exclusion criteria included: (i) diminished near or distance visual acuity, (ii) use of multifocal spectacles, and (iii) use of contact lenses within 48 hours prior to the trial.

Ethical approval

The study protocol was approved by the Ankara Governorship Provincial Health Directorate, University of Health Sciences Türkiye, Atatürk Sanatorium Training and Research Hospital Ethics Committee (approval no: 2012-KAEK-15/2835, date: 27.12.2023). The study adhered to the tenets of the Declaration of Helsinki. All volunteers were informed about the purpose and procedures of the study and provided written informed consent.

Reading procedure

After the examination, volunteers read for 30 minutes in separate sessions from electronic devices with screen sizes of 6.1 inches (1) and 12.9 inches (2), and from A4-printed text (3). Blinking rates during the last 5 minutes of the reading sessions were recorded and analyzed.

OSDI©

The OSDI assesses dry eye symptoms through three subscales: (i) ocular symptoms, (ii) visual tasks, and (iii) environmental factors. The twelve items in the OSDI survey are evaluated on a scale from 0 to 4, with 0 indicating "never," 1 signifying "sometimes," 2 representing "half the time," 3 denoting "most of the time," and 4 meaning "always". The overall OSDI score is computed using the formula: OSDI=[(sum of all response scores)×100]/[(total number of answered questions)×4]. The Tear Film and Ocular Surface Society Dry Eye Workshop (DEWS) II Diagnostic Methodology Report categorizes OSDI scores for dry eye screening as follows: normal (0-12), mild (13-22), moderate (23-32), and severe (33-100).

Questionnaire about discomfort

During or after prolonged reading, ocular symptoms include blurred vision while reading and when looking away afterward,

difficulty or slowness in refocusing from one distance to another, irritation, dry eyes, eye strain, headache, watery eyes, sensitivity to bright lights, and eye discomfort. Each symptom was rated from 1 to 10, and the total scores were recorded.

Slit lamp biomicroscopy

Tear breakup time

A fluorescent strip (Liaoning Meizilin Pharmaceutical, China) was moistened with saline, and a droplet was administered to the lower fornix. The corneal surface was examined using a slit lamp with a cobalt blue filter at 10x magnification. fluorescein break-up time (FBUT) was defined as the interval between the last complete blink and the appearance of the first black patch on the corneal surface. An FBUT greater than 10 seconds was considered typical.

Oxford grading system

The corneal staining test was performed using the Oxford grading method two minutes after the assessment of FBUT. The system was validated by DEWS in 2007. Staining is depicted by a dotted line across panels A-E.

Schirmer's test

A strip of filter paper was positioned on the conjunctival sac of the temporal lower eyelid without the application of topical anesthetic. The length of the wetted segment was measured after 5 minutes. To mitigate the impact of corneal staining on the Schirmer's test, the testing interval was established at a minimum of 15 minutes. Hyposecretion was suspected in cases when strip moistening was less than 10 mm.

Blinking rate and pattern

The blinking rate was documented using a high-resolution camera (SJCAM SJ4000 Camera) positioned on the headband for 5 minutes. Intervals of blinking, as well as complete and incomplete blinks, were documented.

Statistical Analysis

The data were documented in a database and analyzed with SPSS software (version 22.0; IBM, Armonk, NY, 2013). Continuous data were presented as mean ± standard deviation. Differences among the three age groups and among reading modalities (smartphone, tablet, hard copy) were evaluated using one-way ANOVA or repeated-measures ANOVA. Categorical data, including Oxford grading scores, were compared using the chi-square test. The relationships between blinking parameters and discomfort scores were assessed using Pearson's correlation analysis. A p-value of <0.05 was considered statistically significant.

Results

This study included 180 eyes from 90 volunteers. The mean age was 13.33±1.33 years in adolescents, 20.77±2.32 years in young adults, and 33.47±5.38 years in adults. Female participants constituted 56%, 56%, and 53% of the adolescens, young adults and adults groups, respectively). Table 1 summarizes their baseline characteristics.

Before reading, all volunteers had good vision: the Schirmer's test, FBUT, and Oxford scale results were normal. Across all age groups, FBUT decreased compared with baseline. Corneal staining, based on the Oxford grading system, increased in adolescents after smartphone reading and in young adults after both smartphone and tablet reading (p=0.047). No statistically significant changes were observed in other groups (Table 2).

At rest, the blinking rate (n=90) was 18.24±2.66 blink/min and incomplete blinking rate was 1.82±0.91 blink/min. For different reading items, the changes in blinking frequency were as follows: 9.84±1.78 blink/min for smartphones, 13.78±3.13 blink/min for tablets, and 14.64±2.31 blink/min for hardcopy. The incomplete blinking rates were 4.88±1.63 blink/min for smartphones, 3.13±1.42 blink/min for tablets, and 2.31±1.14 blink/min for hardcopy (n=90). Discomfort scores after reading were 34.77±13.75 for smartphones, followed by 24.84±10.05 for tablets and 20.99±12.40 for hardcopy. When groups were divided by age, the blinking rate decreased across all groups (p<0.001). Among adolescents, the resting incomplete blinking rate increased in all groups (p<0.001). The incomplete blinking during smartphone reading was higher than during tablet and hard-copy reading. The discomfort score was higher for

Table 1. Comparison of baseline characteristics of different age groups

	Adolescents	Young adults	Adults
Age, years, mean ± SD	13.33±1.33	20.77±2.32	33.47±5.38
Gender, female/male, n	17/13	17/13	16/14
OSDI total, 0-100, mean ± SD	3.50±2.01	2.97±2.2	4.0±1.41
FBUT, seconds, mean ± SD	11.70±0.87	11.13±0.72	11.40±1.14
Schirmer's test, mm, mean ± SD	12.73±1.53	12.23±1.43	13.53±3.21
Self reported screen time, hours, mean ± SD	6.16±1.56	5.18±1.47	4.55±1.39

SD: Standard deviation, OSDI©: Ocular Surface Disease Index©, FBUT: Fluorescein break-up time

smartphones than for tablets and hard copy (p<0.001). Across all reading situations, young adults exhibited a lower blinking rate and a higher rate of incomplete blinking than at rest (p<0.001). The incomplete blinking rate was higher in smartphone reading (p<0.001); however, it did not differ between tablet and hardcopy reading. The discomfort score among young adults was higher for smartphone reading than for hardcopy reading (p<0.001) and for tablet reading (p=0.07). Among adults, the incomplete blinking rate was higher during tablet and smartphone reading than at rest (p<0.001); the rate did not differ from that during hardcopy reading. The discomfort score did not differ among the reading groups (Table 3).

When discomfort scores were compared across age groups, symptoms, including blurred vision, irritation, burning eyes, watery eyes, and eye discomfort, were more severe during smartphone reading. Among adolescents, the most prominent symptoms were: during smartphone reading, blurred vision and eye discomfort; during tablet reading, blurred vision, irritation, and burning eyes; and during hardcopy reading, blurred vision and watery eyes. In young adults, the prominent symptoms were watery and dry eyes during smartphone reading, dry eyes and eye strain during tablet reading, and blurred vision and eye strain during hard-copy reading. In adults, the prominent symptoms included blurred vision and eye discomfort during

Table 2. Changes in ocular surface and tear film parameters

		Smartphone		Tablet		Hardcopy	
	Baseline (mean ± SD)	After reading (mean ± SD)	p-value	After reading (mean ± SD)	p-value	After reading (mean ± SD)	p-value
Adolescents							
FBUT, seconds	11.70±0.87	9.07±0.96	**<0.01**	10.01±0.97	**<0.01**	10.22±1.04	**<0.01**
Schirmer's test, mm	12.73±1.53	12.40±1.61	0.33	12.63±2.37	0.76	12.80±2.32	0.89
Oxford grading system, 0-5	0	0.30±0.46	**0.001**	0.10±0.30	0.83	0.07±0.25	0.16
Young adults							
FBUT, seconds	11.13±0.72	9.55±0.90	**<0.01**	10.20±1.01	**<0.01**	10.24±0.61	**<0.01**
Schirmer's test, mm	12.23±1.43	12.40±1.99	0.68	12.56±2.44	0.41	12.83±2.42	0.19
Oxford grading system, 0-5	0	0.10±0.30	0.08	0.16±0.37	**0.02**	0.03±0.18	0.32
Adults							
FBUT, seconds	11.40±1.14	8.93±1.57	**<0.01**	9.86±1.16	**<0.01**	10.08±0.86	**<0.01**
Schirmer's test, mm	13.53±3.21	12.16±2.46	0.08	12.60±2.46	0.31	12.03±2.51	0.13
Oxford grading system, 0-5	0	0.16±0.37	0.23	0.1±0.30	0.83	0.23±0.43	0.06

SD: Standard deviation, FBUT: Fluorescein break-up time.

Table 3. Blinking rate, incomplete blinking rate, and discomfort scores during smartphone, tablet, and hardcopy reading across age groups

	Adolescents (mean ± SD)	Young adults (mean ± SD)	Adults (mean ± SD)
At rest			
Blinking rate, blinks/min	18.73±2.22	18.63±2.60	17.37±2.95
Incomplete blinking, blinks/min	1.70±0.98	1.67±0.80	2.10±0.88
Smartphone			
Blinking rate, blinks/min	9.57±1.81	9.83±1.51	10.13±2.01
Incomplete blinking, blinks/min	5.13±1.40	4.90±1.29	4.60±2.09
Discomfort score	38.40±10.50	29.63±9.13	36.27±18.53
Tablet			
Blinking rate, blinks/min	13.17±1.72	16.33±2.64	11.83±1.51
Incomplete blinking, blinks/min	3.30±1.31	2.53±1.07	3.57±1.63
Discomfort score 1-100	25.17±10.70	23.70±7.57	25.67±11.65
Hardcopy			
Blinking rate, blinks/min	14.97±2.91	16.73±2.87	12.23±2.60
Incomplete blinking, blinks/min	2.23±0.85	2.53±1.25	2.17±1.28
Discomfort score	11.87±6.98	21.17±8.25	29.93±13.65

SD: Standard deviation

smartphone reading, dry and watery eyes during tablet reading, and irritation, burning sensations, and eye discomfort during hardcopy reading. In adolescents, the most prominent symptom when looking away after smartphone reading was blurred vision (Figure 1). The blinking rate was not correlated with the incomplete blinking or discomfort scores.

Discussion

This study demonstrated that reading on different handheld devices and from hard copies significantly altered the ocular surface and blinking patterns in healthy adolescents, young adults, and adults.

Across all age groups, FBUT decreased after reading compared with baseline. Reading on smartphones affected corneal staining in adolescents and young adults. However, no significant changes were observed in the Schirmer's test scores.

Tablets and smartphones have gained popularity in daily life; nonetheless, their long-term effects on the ocular surface are unclear (12-14). Studies examining tear film secretion and amount have reported no change in tear meniscus levels 1 hour after smartphone or tablet reading (15). Another study reported an increase in Schirmer's test scores after watching a movie and playing a game on a smartphone; however, this increase could be attributed to reflex tear secretion (16). In contrast, studies conducted using computers reported a decrease in the tear volume (17,18). The tear volume appears to decrease with computer use; however, studies investigating the effects of handheld digital devices have generated contradictory results.

Studies evaluating tear film stability have demonstrated that FBUT decreases after 60 minutes of gaming on a tablet; however, no changes were recorded after smartphone reading (13,15). This study reported that, across all age groups, a decrease in FBUT was associated with corneal staining in children and adolescents. Children who used smartphones for an average of 3 hours per day demonstrated an FBUT <10 seconds and corneal punctate erosions. Conversely, children who used smartphones for <1 hour per day exhibited FBUT >10 seconds. Additionally, the group that used smartphones for 3 hours per day was 13 times more likely to have DED (12). In our study, the self-reported screen time among children and adolescents was 5 to 6 hours. Another study reported that screen time >4 hours per day negatively affected the quality of meibum expression (19). We did not evaluate meibomian gland function. FBUT decreased with computer use.

The observed reduction in FBUT after reading across all age groups underscores a common deleterious effect of digital screen exposure on tear film stability, an essential factor in maintaining ocular surface health. Notably, smartphone reading induced more pronounced corneal fluorescein staining in adolescents and young adults, whereas Schirmer's test results remained statistically unchanged. This suggests that short-term device use predominantly affects tear film quality and distribution rather than tear quantity, which aligns with the literature indicating that reflex tearing may mask basal tear film deficits in such scenarios.

Across all age groups, participants reported a lower blink rate and a higher rate of incomplete blinks when reading on a smartphone than when reading on a tablet or in hardcopy. The discomfort score was higher for smartphone reading, with blurred vision, irritation, burning eyes, watery eyes, and eye discomfort were the most prominent symptoms. Children predominantly reported visual symptoms, such as blurred vision; in contrast, young adults and adults most frequently reported dry eyes and eye discomfort. Short-term studies have reported symptoms related to the ocular surface and vision, such as blurred vision,

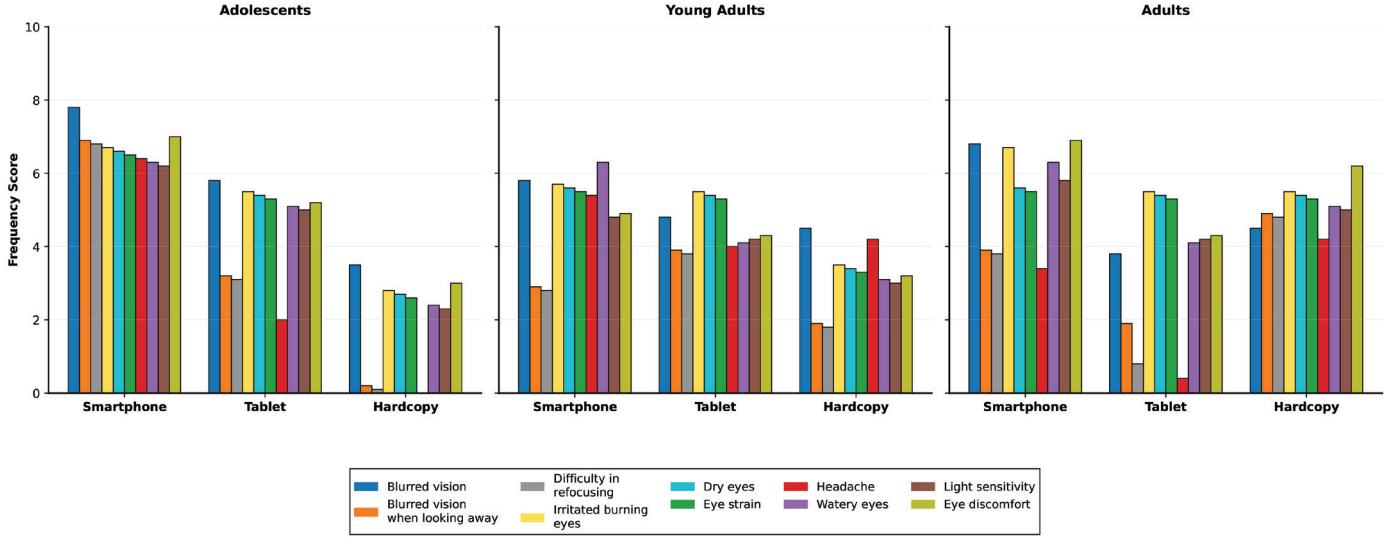

Figure 1. Comparison of digital device-related discomfort symtproms across age groups

headache, pain in the eyes, burning, and stinging (12,14). Dry eye symptoms improve after discontinuing phone use and double upon extending the screen time for 2 hours in adolescents (20). One hour of tablet or smartphone use increases eye fatigue and blurring up to five times in young adults (21). Among adolescents, blurred vision when looking away after reading is a prominent symptom in the smartphone-reading group. However, we did not evaluate the accommodation-vergence reflex or ocular deviation.

The mechanism by which smartphones and tablets disrupt accommodative flexibility is unclear. Additional cognitive demands from the multifunctionality of these devices may adversely affect accommodation, consequently affecting the ability to rapidly change focus (22). In our study, more adolescents with blurred vision looked away after reading in the smartphone-reading group. Smartphone use among adolescents results in dry eye symptoms and both immediate and sustained slowing of blinking, without changes in tear function for up to 1 hour. Considering the ubiquitous use of smartphones by adolescents, future studies should describe whether the mentioned effects persist or worsen over the long term, causing cumulative damage to the ocular surface (23). Our observation of frequent episodes of blurred vision in adolescents while reading on smartphones supports this hypothesis and highlights the need for detailed evaluations of accommodative and binocular visual function in this population.

Although adults demonstrated increased incomplete blinking with smartphone and tablet use, discomfort scores did not differ significantly across reading modalities. This may reflect greater ocular surface resilience and adaptive blinking patterns developed with age and prolonged exposure to digital devices, potentially mitigating subjective discomfort despite measurable ocular surface alterations. Nonetheless, these changes in blinking and tear film dynamics may still predispose adults to long-term ocular surface compromise if exposure continues unchecked.

Visual symptoms are the most common reading-related issues in patients without DED. Symptoms caused by dry eye substantially affect individuals' daily functioning and reduce their quality of life. In our study, adolescents and young adults demonstrated higher discomfort scores while reading on a smartphone. Healthy individuals without a DED diagnosis experience visual symptoms after prolonged reading (24). Given that incomplete blinking hinders the uniform spread of the tear film and exposes the ocular surface to desiccation, these results provide a mechanistic explanation for the increased ocular discomfort and visual symptoms reported, including blurred vision, irritation, and burning sensations. The higher discomfort scores associated with smartphone use reinforce the hypothesis that a smaller screen size and increased visual demands impose greater ocular strain than tablets or printed materials.

Study Limitations

Several limitations should be acknowledged. First, the sample size, although sufficient for detecting significant changes in blink rate and ocular surface parameters, was relatively small and limited to a single center, which may limit generalizability. Second, the study focused on short-term, 30 minute reading sessions; the long-term effects of chronic digital device use were not assessed. Third, only healthy participants without pre-existing ocular surface disease were included, which limits the extrapolation of these findings to populations with dry eye or other ocular conditions. Fourth, environmental factors, such as ambient light and screen reflection, were standardized; however, subtle variations could still influence ocular responses. Finally, subjective discomfort scores rely on self-reporting and may be influenced by individual perception, attention, or mood, thereby introducing potential bias. Future studies with larger, multi-center cohorts and extended monitoring periods are warranted to confirm and expand upon these findings.

Conclusion

These results emphasize that digital device use, particularly smartphone reading, constitutes a significant risk factor for ocular surface disruption and discomfort, with adolescents and young adults exhibiting greater susceptibility. Given the rising global prevalence of DED and its documented negative impact on quality of life, these findings underscore an urgent need for targeted clinical guidelines and public health strategies to minimize digital eye strain. Preventive interventions in vulnerable populations should include education on the importance of regular blinking, ergonomic optimization of screen use (e.g., viewing distance, screen angle), limiting continuous screen exposure, and possibly the use of artificial tears or other ocular surface therapies.

Future longitudinal studies are warranted to elucidate the cumulative effects of prolonged handheld device use on ocular surface health, accommodative function, and visual performance. Additionally, investigations into the interplay between device characteristics, user behavior, and individual ocular physiology will be critical to developing tailored recommendations to safeguard ocular health in the digital era.

Ethics

Ethics Committee Approval: The study protocol was approved by the Ankara Governorship Provincial Health Directorate, University of Health Sciences Türkiye, Atatürk Sanatorium Training and Research Hospital Ethics Committee (approval no: 2012-KAEK-15/2835, date: 27.12.2023).

Informed Consent: All volunteers were informed about the purpose and procedures of the study and provided written informed consent.

Footnotes

Authorship Contributions

Surgical and Medical Practices: Z.Ö.Y., Concept: S.E.A., Design: S.E.A., Data Collection or Processing: S.E.A., Analysis or Interpretation: Z.Ö.Y., Literature Search: Z.Ö.Y., Writing: S.E.A., Z.Ö.Y.

Conflict of Interest: The authors declared no conflict of interest.

Financial Disclosure: The authors declared that this study received no financial support.

References

1. Uchino M, Uchino Y, Dogru M, Kawashima M, Yokoi N, Komuro A, et al. Dry eye disease and work productivity loss in visual display users: the Osaka study. *Am J Ophthalmol.* 2014;157(2):294-300.
2. Wong CW, Tsai A, Jonas JB, Ohno-Matsui K, Chen J, Ang M, et al. Digital screen time during the covıd-19 pandemic: risk for a further myopia boom? *Am J Ophthalmol.* 2021;223:333-337.
3. Wang J, Li Y, Musch DC, Wei N, Qi X, Ding G, et al. Progression of myopia in school-aged children after covid-19 home confinement. *JAMA Ophthalmol.* 2021;139(3):293-300.
4. World Health Organization. WHO Guidelines Approved by the Guidelines Review Committee. Guidelines on physical activity, sedentary behaviour and sleep for children under 5 years of age. Geneva: WHO; [cited 2019; 2019]. Available from: https://www.who.int/publications/i/item/9789241550536
5. Ishii K, Shibata A, Adachi M, Mano Y, Oka K. School grade and sex differences in domain-specific sedentary behaviors among Japanese elementary school children: a cross-sectional study. *BMC Public Health.* 2017;17(1):318.
6. Republic of Turkey Ministry of Health. Technology addiction parent guide. Ankara: Ministry of Health; 2023. Available from: https://sggm.saglik.gov.tr/TR-101322/teknoloji-bagimliligi-ebeveyn-rehberi-2023.html
7. Chu CA, Rosenfield M, Portello JK. Blink patterns: reading from a computer screen versus hard copy. *Optom Vis Sci.* 2014;91(3):297-302.
8. Altalhi A, Khayyat W, Khojah O, Alsalmi M, Almarzouki H. Computer vision syndrome among health sciences students in Saudi Arabia: prevalence and risk factors. *Cureus.* 2020;12(2):e7060.
9. Cremers SL, Khan ARG, Ahn J, Cremers L, Weber J, Kossler AL, et al. New Indicator of children's excessive electronic screen use and factors in meibomian gland atrophy. *Am J Ophthalmol.* 2021;229:63-70.
10. Wang MT, Muntz A, Wolffsohn JS, Craig JP. Association between dry eye disease, self-perceived health status, and self-reported psychological stress burden. *Clin Exp Optom.* 2021;104(8):835-840.
11. Jaiswal S, Asper L, Long J, Lee A, Harrison K, Golebiowski B. Ocular and visual discomfort associated with smartphones, tablets and computers: what we do and do not know. *Clin Exp Optom.* 2019;102(5):463-477.
12. Moon JH, Kim KW, Moon NJ. Smartphone use is a risk factor for pediatric dry eye disease according to region and age: a case control study. *BMC Ophthalmol.* 2016;16(1):188.
13. Kim DJ, Lim CY, Gu N, Park CY. Visual fatigue induced by viewing a tablet computer with a high-resolution display. *Korean J Ophthalmol.* 2017;31(5):388-393.
14. Long J, Cheung R, Duong S, Paynter R, Asper L. Viewing distance and eyestrain symptoms with prolonged viewing of smartphones. *Clin Exp Optom.* 2017;100(2):133-137.
15. Golebiowski B, Long J, Harrison K, Lee A, Chidi-Egboka N, Asper L. Smartphone use and effects on tear film, blinking and binocular vision. *Curr Eye Res.* 2020;45(4):428-434.
16. Park JS CM, Ma JE, Choi J, Ma JE, Moon JH, Moon HJ. Influence of cellular phone videos and games on dry eye syndrome in university students. *J Korean Acad Nurs.* 2014;25:12-23.
17. Ribelles A, Galbis-Estrada C, Parras MA, Vivar-Llopis B, Marco-Ramírez C, Diaz-Llopis M. Ocular surface and tear film changes in older women working with computers. *Biomed Res Int.* 2015;2015:467039.
18. Yazici A, Sari ES, Sahin G, Kilic A, Cakmak H, Ayar O, et al. Change in tear film characteristics in visual display terminal users. *Eur J Ophthalmol*. 2015;25(2):85-89.
19. Wu H, Wang Y, Dong N, Yang F, Lin Z, Shang X, Li C. Meibomian gland dysfunction determines the severity of the dry eye conditions in visual display terminal workers. *PLoS One.* 2014;9(8):e105575.
20. Kim J, Hwang Y, Kang S, Kim M, Kim TS, Kim J, et al. Association between exposure to smartphones and ocular health in adolescents. *Ophthalmic Epidemiol.* 2016;23(4):269-276.
21. Maducdoc MM, Haider A, Nalbandian A, Youm JH, Morgan PV, Crow RW. Visual consequences of electronic reader use: a pilot study. *Int Ophthalmol.* 2017;37(2):433-439.
22. Park M, Ahn YJ, Kim SJ, You J, Park KE, Kim SR. Changes in accommodative function of young adults in their twenties following smartphone use. *J Korean Ophthalmic Opt Soc.* 2014;19:253-260.
23. Chidi-Egboka NC, Jalbert I, Golebiowski B. Smartphone gaming induces dry eye symptoms and reduces blinking in school-aged children. *Eye (Lond).* 2023;37(7):1342-1349.
24. Blehm C, Vishnu S, Khattak A, Mitra S, Yee RW. Computer vision syndrome: a review. *Surv Ophthalmol*. 2005;50(3):253-262.

DOI: 10.4274/gulhane.galenos.2025.03779
Gulhane Med J 2026;68(2):94-101

Comparison of positron emission tomography, computed tomography, magnetic resonance imaging and surgical staging in para-aortic lymph node sampling in cervical cancer

Tolga Çiftpınar[1], Faruk Köse[2], Mufit Cemal Yenen[3]

[1]*University of Health Sciences Türkiye, Kanuni Sultan Süleyman Training and Research Hospital, Clinic of Gynecological Oncology, İstanbul, Türkiye*
[2]*Acıbadem University Faculty of Medicine, Department of Gynecological Oncology, İstanbul, Türkiye*
[3]*Dr. Suat Günsel Kyrenia University Hospital, Department of Gynecology and Obstetrics, Kyrenia, Cyprus*

Cite this article as: Çiftpınar T, Köse F, Yenen MC. Comparison of positron emission tomography, computed tomography, magnetic resonance imaging and surgical staging in para-aortic lymph node sampling in cervical cancer. *Gulhane Med J.* 2026;68(2):94-101.

Date submitted:
08.06.2025
Date accepted:
25.12.2025
Epub:
08.06.2026
Publication Date:
16.06.2026

Corresponding Author:
Tolga Çiftpınar, M.D., University of Health Sciences Türkiye, Kanuni Sultan Süleyman Training and Research Hospital, Clinic of Gynecological Oncology, İstanbul, Türkiye
tolgaciftpinar@yahoo.com

ORCID:
orcid.org/0000-0001-7406-0629

Keywords: Cervical cancer, extraperitoneal lymphadenectomy, imaging

ABSTRACT

Aims: This study aimed to compare imaging-based evaluation of retroperitoneal nodal status with pathologic findings, and to identify the advantages and disadvantages of laparoscopy.

Methods: This retrospective study included patients with invasive cervical cancer who underwent laparotomy or extraperitoneal laparoscopy for evaluation of para-aortic nodal status between 2002 and 2006 at two tertiary care hospitals. The primary objectives were to compare the imaging modalities with pathological findings and laparoscopy with laparotomy.

Results: Forty-one women (mean age: 51±10 years) having invasive cervical cancer were included in the study. Laparoscopic extraperitoneal lymphadenectomy was performed in 26 patients [International Federation of Gynecology and Obstetrics (FIGO) stage IIB-IIIB], and laparotomic hysterectomy and para-aortic lymphadenectomy were performed in 15 patients (FIGO stage IB-IIB). Operation times (115.1 minutes vs. 182.0 minutes, p<0.001), the average length of hospital stay (6.1 days vs. 12.6 days, p<0.001), and the need for narcotic analgesics in the postoperative period (34.6% vs. 80.0%, p<0.005) were better in laparoscopy group. Lymphadenectomy times were similar (56.6 minutes vs. 52.2 minutes, p=0.07). Sensitivities of computed tomography, magnetic resonance imaging, and positron emission tomography (PET) for the para-aortic lymphatic region were 20%, 25%, and 33.3%, respectively; specificities were 92.3%, 96.2%, and 100%, respectively. PET was found to have 100% positive predictive value for both pelvic and para-aortic lymphatic evaluations. Extraperitoneal laparoscopic lymphadenectomy was found to have lower morbidity as a minimally invasive procedure for locally advanced cervical cancer.

Conclusions: Surgical staging is the gold standard for the retroperitoneal evaluation in cervical cancer. Laparoscopy appears to be a favorable option for surgical staging due to lower morbidity and faster recovery while maintaining comparable oncologic adequacy. PET was the most specific imaging modality.

Introduction

Cervical cancer is the third most common gynecological cancer in women worldwide. In the first half of the 20th century, cervical cancer was a leading cause of death. A significant decrease in incidence and mortality rates was achieved through the application of colposcopy by Hinselmann in the 1920s and of Pap smear screening by Papanicolaou in the 1940s. In general, cervical cancer and mortality caused by cervical cancer are seen more frequently in underdeveloped and developing countries (1). Staging, which has a very important place in treatment planning, was previously done clinically, but today it is done surgically, and nodal involvement has been included in staging in 2018 (2). Accuracy and consistency of preoperative imaging and postoperative pathology in evaluating nodal status for staging help us to guide appropriate treatment planning. Imaging provides additional information for our clinical evaluation of staging. In this study, we compared nodal involvement assessed by preoperative imaging with histopathological data obtained from surgical specimens. During surgical evaluation, we compared minimally invasive, laparoscopic, extraperitoneal lymphadenectomy with para-aortic lymphadenectomy performed via laparotomy.

Methods

Study design and population

This multicentric, retrospective study included patients diagnosed with invasive cervical cancer between 2002 and 2006 at the Gülhane Military Medical Academy (GATA) Gynecology and Obstetrics Clinic and the University of Health Sciences, Türkiye, Etlik Zübeyde Hanim Women's Health Training and Research Hospital, Clinic of Gynecological Oncology. Ethics committee approval was obtained from Gülhane Military Medical Academy (approval no: 1491-227-06, date: 22.05.2006), and institutional approval was granted by the Education and Planning Committee of Etlik Zübeyde Hanım Women's Health Training and Research Hospital (approval no: 73, date: 24.05.2006).

Patients who underwent surgery for invasive cervical carcinoma and patients who underwent para-aortic lymphadenectomy by laparotomy or laparoscopy were included in the study. Patients who had not underwent surgery (received only radiotherapy), who had not been diagnosed with invasive cervical cancer (carcinoma *in situ*), who had underwent surgery but had not underwent para-aortic lymph node dissection, who had distant metastasis, or who had a condition that prevented surgery were not included in the study.

Surgical technique

Patients with locally advanced cervical cancer (staged IIB-IIIB) have underwent laparoscopic extraperitoneal lymphadenectomy, whereas patients with early-stage disease (IB-IIB) have underwent hysterectomy with pelvic and para-aortic lymphadenectomy via laparotomy. All laparoscopic extraperitoneal lymphadenectomy operations were performed by the same surgeon, and all extraperitoneal laparotomy operations were performed by the gynecological oncology team, using the same procedure and surgical technique.

Data collection and data assessment

Informed consent was obtained from all patients for the operation. Additional gynecological pathology was investigated through a detailed patient history and pelvic evaluation, including transvaginal ultrasonography (TVUSG). International Federation of Gynecology and Obstetrics (FIGO) clinical staging was performed on patients using hemograms, biochemical values, chest radiography, examination under general anesthesia, and cystoscopy.

Imaging methods

The retroperitoneal area was evaluated using one or more imaging modalities in the patients: computed tomography (CT), magnetic resonance imaging (MRI), and positron emission tomography (PET). The interval between imaging and surgery did not exceed 1 month. All imaging interpretations were performed blinded to other imaging methods and to pathology results. MRI and CT scans were evaluated by the same radiologist. For lymphatic evaluation on imaging, the common, external iliac, internal iliac, and obturator lymph nodes of the pelvic region and any lymph node between the renal vein and common iliac vessels of the para-aortic region were scanned. In lymph node evaluation on MRI and CT, a short-axis dimension greater than 1 cm was accepted as the threshold for malignancy.

PET imaging

On the day of the PET imaging, blood glucose levels of all patients were measured after 6-8 hours of fasting. Patients with serum glucose levels ≤150 mg/dL proceeded to imaging. All patients were injected intravenously with 300-400 MBq F-18 fluorodeoxyglucose (FDG) and were given hydration to reduce urinary tract activity. After 45 minutes, images from the base of the skull to the proximal femur were obtained in the supine position using a PET scanner (ECAT EXACT 47, Siemens CTI). All FDG-PET images were evaluated by the same nuclear medicine specialist, blinded to the other radiological and pathological results. Maximum standardized uptake values (SUV_{max}) were calculated for metabolic foci deemed non-physiological, and areas of metabolic activity with SUV_{max} values of 2.5 or greater were considered positive for malignancy.

Lymphadenectomy

The lymph nodes removed after the operation and those identified on imaging were divided into two groups: pelvic and para-aortic. In the laparoscopic group (n=26), 11 patients underwent para-aortic lymphadenectomy alone,

while 15 patients underwent both para-aortic and pelvic lymphadenectomies. In the laparotomy group (n=15), all patients underwent both pelvic and para-aortic lymphadenectomies.

After the removed lymph nodes were divided into pelvic and para-aortic regions, the diameters of the lymph nodes in both regions were recorded as the per-patient average (in millimeters). The relationship between lymph node diameter and pathology results was examined. All histopathological evaluations were performed by two pathologists experienced in gynecological oncology.

The laparoscopic extraperitoneal and laparotomic para-aortic lymphadenectomy techniques were compared in terms of blood loss, operative and lymphadenectomy times, length of hospital stay, need for narcotic analgesics, and complications.

Lymphadenectomy results were compared with the imaging findings, and sensitivity, specificity, and predictive values were calculated for each imaging modality.

Statistical Analysis

Statistical analyses were performed using SPSS, version 11.0 (SPSS Inc., Chicago, USA). In addition to descriptive statistical methods (mean, standard deviation), the distribution of variables was examined with the Shapiro-Wilk normality test; the independent t-test was used to compare normally distributed variables between two independent groups; the Kruskal-Wallis test was used to compare variables with non-normal distributions between groups; Dunn's multiple comparison test was used for subgroup comparisons; the Mann-Whitney U test was used to compare two independent groups; and the chi-square and Fisher's exact tests were used to compare qualitative data. A p-value of <0.05 was considered statistically significant in all calculations.

Results

Socio-demographic characteristics

Forty-one patients diagnosed with invasive cervical cancer underwent surgery. Laparoscopic extraperitoneal lymphadenectomy was performed in 26 patients (FIGO stage IIB-IIIB); laparotomy with pelvic and para-aortic lymphadenectomy, hysterectomy, and salpingo-oophorectomy, as indicated, were performed in 15 patients (FIGO stage IB-IIB). When the demographic characteristics of the patients were examined, no statistically significant difference was found between the groups. The most common presenting complaint among the patients was vaginal bleeding (31 cases, 75.6%). The average age of all patients was 51±10 years (range 30-69), median parity values were 4 (range 0-12), and average body mass index was 27.4±3.7.

Regarding histological type distribution, squamous cell carcinoma was the most frequent in our study, consistent with the literature: 82.9% (34 cases). Adenocarcinoma was detected in 4 cases (9.8%), undifferentiated epithelial tumor in 2 cases (4.9%), and adenoma malignum in 1 case (2.4%).

When we examined the stages, 17.1% (7 cases) of the patients were stage IB, 7.3% (3 cases) were stage IIA, 61% (25 cases) were stage IIB, 4.9% (2 cases) were stage IIIA, and 9.8% (4 cases) were stage IIIB. 24.4% (10 cases) of patients were classified as stage IIA or lower, and 75.6% (31 cases) as stage IIB or higher.

Operative results

Operation times were found as 115.1±51.9 minutes (range 60-290 minutes) in the laparoscopy group and 182.0±60.5 minutes (range 120-320 minutes) in the laparotomy group. The difference between the two groups was statistically significant (p<0.001).

Lymphadenectomy times were found to be 56.6±8.3 minutes in the laparoscopy group and 52.2±4.6 minutes in the laparotomy group. No significant difference in lymphadenectomy times was detected between the two groups (p=0.07).

The average length of hospital stay was 6.1±3.8 days (2-17 days) in the laparoscopy group and 12.6±4.2 days (5-20 days) in the laparotomy group. The difference between the two groups was found to be statistically significant (p<0.001).

Narcotic analgesics in the postoperative period were required in only 9 of 26 patients (34.6%) in the laparoscopy group and in 12 of 15 patients (80.0%) in the laparotomy group. The difference between the two groups was statistically significant (p<0.005).

A total of 7 of 41 patients (17.1%) experienced complications. It developed in 7.7% (2 cases), of patients who underwent laparoscopy and in 33.3% (5 cases) of those who underwent laparotomy. Two complications in the laparoscopy group were identified as peritoneal ruptures, and both underwent laparotomy. In the laparotomy group, a bladder injury occurred in one patient and was repaired intraoperatively. Ureteral injury occurred in two cases, and a double-J catheter was placed intraoperatively. One patient developed peripheral nerve damage in the left lower extremity and experienced spontaneous regression within 3 weeks. In one patient, incision failure was observed at the Maylard incision site on the 7th day and was debrided and resutured on the 17th day. The difference between the two groups was not statistically significant (p=0.08).

Laparotomy was performed in 4 (4/26) patients who underwent laparoscopy. One was a peritoneal defect; another was due to both a peritoneal defect and a bulky tumor; and in the other two cases, the peritoneal defect prevented continuation of laparoscopy. Peritoneal defects occurred in 8 patients (8/26). In 6 of them, no laparotomy with intraoperative intervention was required.

The average follow-up period in the postoperative period was 18.2±14.9 months (1-44 months). Recurrence was observed in

2 of 41 patients (4.9%) during this follow-up period. One of the patients developed a central recurrence in the 17th month and received treatment with cisplatin and 5-fluorouracil. In the other patient, a 6 cm tumoral mass was observed in the vulvar region at the 16th month, and it was excised. In 12 (29.3%) cases, patients received chemotherapy. External pelvic radiotherapy was applied to 11 (26.8%) cases; external pelvic radiotherapy and brachytherapy were applied to 13 (31.7%) cases; and pelvic and para-aortic therapy was applied to 5 (12.2%) cases.

Lymphadenectomy results

The average number of para-aortic lymph nodes removed in the laparoscopy group was 11.2±6.4, and the average number of para-aortic lymph nodes removed in the laparotomy group was 10.3±4.0. There was no significant difference between the laparotomy and laparoscopy groups in terms of the number of para-aortic lymph nodes removed (p=0.63).

Histopathologic results

The pathology results were reported as metastatic in 5 (12.5%) of 40 patients who underwent para-aortic lymphadenectomy, while 35 (87.5%) were reported as reactive. Pelvic lymphadenectomy pathology results showed metastasis in 7 (26.9%) of 26 patients, while 19 (73.1%) were reported as reactive (Figure 1). Three of the patients with metastatic para-aortic lymph nodes were stage IIB, and two were stage IIIB. Of the seven patients with metastatic pelvic lymph nodes, two were stage IIA, four were stage IIB, and one was stage IIIB. The distribution of lymph node status by stage is shown in Figure 2. When we look at the lymphatic metastasis rates according to stage: of 3 patients with stage IIA, 2 (66.7%) had pelvic metastases; of 25 patients with stage IIB, 4 (16.0%) had pelvic and 3 (12%) had para-aortic metastases; and of 4 patients with stage IIIB, 1 (25%) had pelvic and 2 (50.0%) had para-aortic metastases (Table 1).

While the average total number of lymph nodes collected in all patients was 21.8±15.5 (range 4-59), the number of para-aortic lymph nodes was 10.8±5.6 (1-28), and the number of pelvic lymph nodes was 17.1±15.2 (1-48). In the pelvic group, lymph node diameters were 8.5±4.3 mm (range 3.6-18.6 mm) for reactive patients and 12.3±5.7 mm (range 9-25 mm) for metastatic patients (p=0.016). However, other studies found no relationship between lymph node metastasis and lymph node diameters. Because of this, studies with larger series are needed. In the para-aortic group, it was 8.5±4.2 mm (range 1.5-18.75 mm) for reactive patients and 10.4±2.9 mm (range 6.5-14.5 mm) for metastatic patients (p=0.13). While metastatic lymph node diameters were larger in the pelvic group, no significant association was found between lymph node diameters and pathology in the para-aortic group.

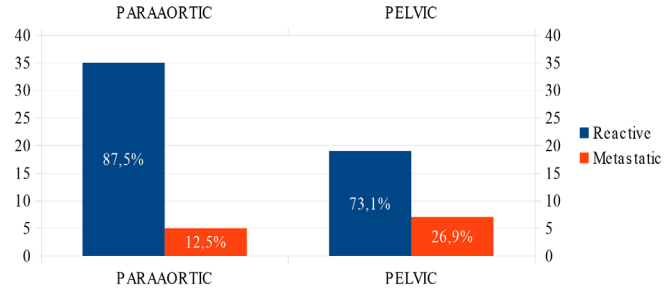

Figure 1. Metastatic and reactive lymph nodes rates of pelvic and para-aortic region according to pathologic findings

Imaging results

In examining the pelvic area; for CT (n=14) sensitivity, specificity, positive predictive value (PPV) and negative predictive value (NPV) were found to be 16.7%, 87.5%, 50% and 58.3%; for MRI (n=19) sensitivity, specificity, PPV and NPV were found to be 40%, 92.9%, % 66.7 and 81.3%; for PET (n=7) sensitivity, specificity, PPV and NPV were found to be 60%, 100%, 100%, 50% respectively. In examining the para-aortic area; for CT (n=18) sensitivity, specificity, PPV and NPV were found to be 20%, 92.3%, 50%, 75%; for MRI (n=30) sensitivity, specificity, PPV, NPV were found to be 25%, 96.2%, 50%, 89.3%; for PET (n=8) sensitivity, specificity, PPV and NPV were found to be 33.3%, 100%, 100% and 71.4% respectively (Table 2).

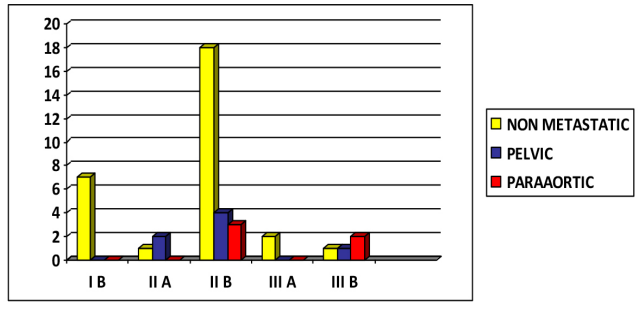

Figure 2. Lymph node status according to stages

Table 1. Pelvic and para-aortic metastasis rates according to stages (n=32)

Lymphatic involvement according to the stages		
Stage	**Pelvic (%)**	**Para-aortic (%)**
IIA (n=3)	66.7	-
IIB (n=25)	16	12
IIIB (n=4)	25	50

Table 2. Sensitivity, specificity, PPV and NPV values of imaging methods for the pelvic and the para-aortic region

	Sensitivity (%)	Specificity (%)	PPV (%)	NPV (%)
Pelvic				
CT (n=14)	16.7	87.5	50	58.3
MRI (n=19)	40	92.9	66.7	81.3
PET (n=7)	60	100	100	50
Para-aortic				
CT (n=18)	20	92.3	50	75
MRI (n=30)	25	96.2	50	89.3
PET (n=8)	33.3	100	100	71.4

PPV: Positive predictive value, NPV: Negative predictive value, CT: Computed tomography, MRI: Magnetic resonance imaging, PET: Positron emission tomography.

Discussion

This study demonstrated that surgical staging remains the most valuable option for evaluating the nodal status of the retroperitoneum in cervical cancer. In particular, the laparoscopic approach stands out for enabling histopathological examination and faster recovery. Imaging methods, which offer an alternative way to evaluate the nodal status of the retroperitoneum, stand out as non-invasive methods. With technological advances in recent years, its effectiveness has increased, and PET/CT, in particular, has come to the fore in this field.

Surgical staging allows us to understand and accurately evaluate the spread of the disease in gynecological cancers. Because of the clinical staging used in previous years, staging errors could have occurred in patients with cervical cancer. In a recent study by Marnitz et al. (3), the operative staging showed an upstaging in 33% of the patients. Imaging methods such as CT, MRI, and PET were not included in the standard staging procedures in FIGO 2009 staging (4).

With FIGO 2018 (2), imaging methods have been included in staging procedures. This new staging system has introduced evaluation using appropriate ultrasonography and cross-sectional imaging methods, each of which may be superior in different stages and patients, rather than a single standard imaging method. Transrectal or TVUSG and cross-sectional imaging methods such as CT, MRI, and PET may be used (5). Today, hybrid molecular oncology imaging applications such as PET/MRI, where radiomic features are used, are also starting to enter our practical lives (6,7). PET technology, which has just begun to enter our lives in the 2000s, can further increase diagnostic performance in the oncological field with its rapid technological developments, such as the use of PET/MRI, time of flight-PET, and digital detectors (8). As imaging methods have developed, diagnostic parameters in MRI have changed. A meta-analysis conducted by Xiao et al. (9), showed that MRI imaging is consistent in determining stromal infiltration and parametrial invasion, but is limited in diagnosing lymph node involvement.

Woo et al. (10) evaluated the results of a meta-analysis comparing conventional and advanced imaging methods in cervical cancer. MRI was found to be superior in determining local spread, but for nodal metastasis, CT, MRI, and PET were found to have low sensitivity and high specificity. This limitation in recognizing micro metastases still cannot replace lymphatic sampling for high-risk patients (10).

Although sensitivity and specificity have increased over the years, the order of the imaging methods has not changed. While CT has the lowest rate, PET has the best performance. With the advances in molecular imaging technology, fusion of PET and MRI has begun to give more detailed images with higher sensitivity and specificity; 84% and 90% for PET/CT and 9% and 93% for PET/MRI, respectively (11). In the literature, reported sensitivity and specificity for all three methods vary widely. The preoperative evaluation provided by imaging for detecting metastases remains suboptimal. Although it approaches the gold-standard test for pelvic evaluation, it remains far below the expected performance for the para-aortic region. In our study, PET imaging yielded the highest sensitivity and specificity values in both the pelvic and para-aortic regions. This was followed by MRI and CT. Sensitivity was slightly better in the pelvic region, while specificity was slightly better in the para-aortic region. The number of patients who underwent PET (n=8 for para-aortic evaluation) was very small. This small sample size limits statistical power, particularly for estimating sensitivity and PPV. Although PET demonstrated 100% specificity, its sensitivity was relatively low (33.3%). This may be due to small nodal size, micrometastases, or absence of the CT component.

There have been advances in both imaging and surgical methods. Primary surgical treatment is suitable for patients with early-stage disease. However, the majority of patients are at advanced stages. These patients with advanced-stage disease do not require surgical treatment, except for evaluation of nodal involvement. The laparoscopic approach prevents patients from experiencing the morbidity associated with laparotomy. Blood loss, major trauma, intraoperative and postoperative complications, immobilization, long-term hospitalization, prolonged recovery, delay in adjuvant treatment, and psychological effects are some of the extra burdens that major surgery brings to patients.

Extraperitoneal laparoscopic lymphadenectomy, introduced in the mid-1990s, shed new light on the staging of cervical cancer. The technique described by LeBlanc et al. (12) is a technique that can be quickly adapted, especially for those with experience in transperitoneal laparoscopic lymphadenectomy. Laparoscopic application is a method that should be preferred because it is more cosmetically acceptable, involves shorter hospitalization, allows quicker recovery, and facilitates final treatment planning.

In our study, we found shorter operation time, shorter hospitalization period, and a reduced need for narcotic analgesics in the laparoscopy group. Even with respect to the lymphadenectomy time and the number of para-aortic lymph nodes collected, the results were similar in both groups. These findings support the advantages of minimally invasive surgery.

In the study of Kerbage et al. (13), laparoscopic transperitoneal and extraperitoneal, robotic transperitoneal and extraperitoneal, and laparotomy were compared. They found that laparoscopy was associated with less blood loss, shorter operative time, and shorter hospitalization. Fewer complications were seen in the transperitoneal group than in the extraperitoneal group. Most complications were seen in the laparotomy group. Lymphoceles were the most common complication caused by the extraperitoneal approach, and they were commonly treated by marsupialization.

In our study, lymphocele formation was not observed in any patient because peritoneal marsupialization was performed routinely after the operation. However, we observed peritoneal defects in approximately 1/3 of the patients who underwent laparoscopy. Intraoperative intervention was sufficient in most cases, but we had to convert to laparotomy because the peritoneal defect adversely affected the procedure. Transfusion due to blood loss was more likely to occur during major surgery. The transfusion rate in the laparoscopy group was less than half that in the laparotomy group.

Disadvantages of laparotomy also include the formation of intestinal adhesions, intestinal complications due to immobilization resulting from radiotherapy, delays in initiating post-op radiotherapy while awaiting recovery, and difficulty in resection in obese patients. In the extraperitoneal laparoscopic approach, these problems do not exist because there are no intestines in the field (14).

Surgical staging has helped us detect upstaging, especially in locally advanced cervical cancer. Puga et al. (15), showed stage migration in 24% of the patients and change of the initially planned radiotherapy areas in 43% of the patients.

Thelissen et al. (16), reported upstaging in 11% of patients after negative imaging by para-aortic dissection. This rate increased to 21% in patients with para-aortic dissection with positive pelvic nodes but negative para-aortic nodes on imaging.

Marnitz et al. (3), found upstaging in 33% of patients through operative staging in the UTERUS-11 study. Laparoscopy did not delay the initiation of primary chemoradiotherapy because recovery after laparoscopy was rapid. Despite upstaging in 33% of patients with locally advanced cervical cancer, disease-free and overall survival rates were similar between surgical and clinical staging. The only benefit from surgical staging prior to primary chemoradiation was found in the patient group of FIGO stage IIB.

In our study, lymphatic metastasis was detected in 20% of early-stage and 25.8% of advanced-stage disease cases. These results are somewhat similar to the 33% staging error reported by Marnitz et al. (3,5).

The presence of para-aortic metastasis is important for determining the radiotherapy field. Radiology is less useful than histopathological examination for diagnosing small or microscopic diseases. Detailed microscopic examination and ultrastaging techniques can reveal micrometastatic disease. The term “low-volume metastases” refers to micrometastases and isolated tumor cells. Its incidence varies from 4% to 20% (17). In the SENTICOL 1 and 2 studies, serial sectioning for ultrastaging identified low-volume metastases in 7.5% of the patients. But there was no statistically significant difference in disease-free survival between the node-negative group and low volume metastases group (18). Buda’s study reported the same result for relapse and disease-free survival. And they found micro metastases or isolated tumor cells in 3.6% of patients (19). On the contrary, Guani et al. (18) and Kocian et al. (20) have found negative effects on disease-free survival in the low-volume metastases group. This controversial situation has not yet been resolved. However, since ultra staging cannot be performed systemically on all lymph nodes, lower uptake may be observed in low-volume disease (21). Therefore, surgical staging and careful pathological evaluation are necessary to determine the extent of the disease and plan treatment.

With information obtained from the surgical-pathological examination, treatment can be personalized and clinical outcomes improved. Determining the para-aortic lymph node status prevents unnecessary or inadequate treatment of the para-aortic region. Contrary to previous studies showing that prophylactic extended-field radiotherapy does not improve survival and increases morbidity, recent studies suggest that the widespread use of PET/CT and advances in radiotherapy techniques make it unlikely that surgical identification and removal of microscopic nodal involvement will clearly improve oncological outcomes. The increasing use of intensity-modulated radiotherapy is associated with less toxicity and leads to questioning the future place of surgical staging (22).

Study Limitations

The limitations of the study are a small sample size and heterogeneity among the imaging groups. This may affect the sensitivity and specificity rates. Not all patients had underwent the same imaging method. Because PET scan was newly introduced for use in malignancies, there was no standard protocol for preoperative staging using imaging. Since it was not statistically powered, no comparisons were made between the imaging modalities. A striking aspect of the study is that it is one of the first to use laparoscopic extraperitoneal lymphadenectomy and oncologic PET scanning in Türkiye.

Conclusion

This study examined radiological and surgical methods for evaluating retroperitoneal lymphatic status in patients with cervical cancer. Para-aortic lymphatic involvement may affect the staging and treatment of locally advanced cervical cancer. Among the imaging methods, PET was found to be the most effective, followed by MRI and, finally, CT. Sensitivity and specificity were higher in the pelvic area, whereas imaging accuracy was lower in the para-aortic area. Although MRI and PET/CT are prominent imaging methods, surgical evaluation of the para-aortic area and histopathological results will continue to be the gold standard. Since lymphatic evaluation alone is sufficient in patients with advanced cervical cancer, minimally invasive laparoscopic extraperitoneal lymphadenectomy should be performed to surgically evaluate the para-aortic area and avoid exposing patients to the stress and trauma of major surgery.

Ethics

Ethics Committee Approval: Ethics committee approval was obtained from Gülhane Military Medical Academy (approval no: 1491-227-06, date: 22.05.2006), and institutional approval was granted by the Education and Planning Committee of Etlik Zübeyde Hanım Women's Health Training and Research Hospital (approval no: 73, date: 24.05.2006).

Informed Consent: This retrospective study.

Footnotes

Authorship Contributions

Surgical and Medical Practices: T.Ç., F.K., M.C.Y., Concept: T.Ç., F.K., M.C.Y., Design: T.Ç., F.K., M.C.Y., Data Collection or Processing: T.Ç., F.K., M.C.Y., Analysis or Interpretation: T.Ç., F.K., M.C.Y., Literature Search: T.Ç., F.K., M.C.Y., Writing: T.Ç., F.K., M.C.Y.

Conflict of Interest: No conflict of interest was declared by the authors.

Financial Disclosure: The authors declare that this study received no financial support.

References

1. Sung H, Ferlay J, Siegel RL, Laversanne M, Soerjomataram I, Jemal A, et al. Global Cancer Statistics 2020: GLOBOCAN estimates of incidence and mortality worldwide for 36 cancers in 185 countries. *CA Cancer J Clin*. 2021;71(3):209-249.
2. Bhatla N, Berek JS, Cuello Fredes M, Denny LA, Grenman S, Karunaratne K, et al. Revised FIGO staging for carcinoma of the cervix uteri. *Int J Gynaecol Obstet.* 2019;145(1):129-135. Erratum in: *Int J Gynaecol Obstet.* 2019;147(2):279-280.
3. Marnitz S, Tsunoda AT, Martus P, Vieira M, Affonso Junior RJ, Nunes J, et al. Surgical versus clinical staging prior to primary chemoradiation in patients with cervical cancer FIGO stages IIB-IVA: oncologic results of a prospective randomized international multicenter (Uterus-11) intergroup study. *Int J Gynecol Cancer.* 2020;30(12):1855-1861.
4. Pecorelli S. Revised FIGO staging for carcinoma of the vulva, cervix, and endometrium. *Int J Gynaecol Obstet.* 2009;105(2):103-104.
5. Dhamija E, Gulati M, Manchanda S, Singhal S, Sharma D, Kumar S, et al. Imaging in carcinoma cervix and revised 2018 FIGO staging system: implications in radiology reporting. *Indian J Radiol Imaging.* 202131(3):623-634.
6. Esfahani SA, Torrado-Carvajal A, Amorim BJ, Groshar D, Domachevsky L, Bernstine H, et al. PET/MRI and PET/CT radiomics in primary cervical cancer: a pilot study on the correlation of pelvic PET, MRI, and CT derived ımage features. *Mol Imaging Biol.* 2022;24(1):60-69.
7. Nazir A, Matthews R, Chimpiri AR, Henretta M, Varughese J, Franceschi D. Fluorodeoxyglucose positron-emission tomography-magnetic resonance hybrid imaging: An emerging tool for staging of cancer of the uterine cervix. *World J Nucl Med.* 2020;20(2):150-155.
8. Surti S, Karp JS. Update on latest advances in time-of-flight PET. *Phys Med.* 2020;80:251-258.
9. Xiao M, Yan B, Li Y, Lu J, Qiang J. Diagnostic performance of MR imaging in evaluating prognostic factors in patients with cervical cancer: a meta-analysis. *Eur Radiol.* 2020;30(3):1405-1418.
10. Woo S, Atun R, Ward ZJ, Scott AM, Hricak H, Vargas HA. Diagnostic performance of conventional and advanced imaging modalities for assessing newly diagnosed cervical cancer: systematic review and meta-analysis. *Eur Radiol.* 2020;30(10):5560-5577.
11. Zhu Y, Shen B, Pei X, Liu H, Li G. CT, MRI, and PET imaging features in cervical cancer staging and lymph node metastasis. *Am J Transl Res.* 2021;13(9):10536-10544.
12. LeBlanc E, Caty A, Dargent D, Querleu D, Mazeman E. Extraperitoneal laparoscopic para-aortic lymph node dissection for early stage nonseminomatous germ cell tumors of the testis with introduction of a nerve sparing technique: description and results. *J Urol.* 2001;165(1):89-92.
13. Kerbage Y, Kakkos A, Kridelka F, Lambaudie E, Bats AS, Hébert T, et al. Lomboaortic lymphadenectomy in gynecological oncology: laparotomy, laparoscopy or robot-assisted laparoscopy? *Ann Surg Oncol.* 2020;27(10):3891-3897.

14. Huang M, Slomovitz BM, Ramirez PT. Transperitoneal versus extraperitoneal para-aortic lymphadenectomy in patients with cervical cancer. *Rev Obstet Gynecol.* 2009;2(2):101-106.

15. Puga O, Retamales J, Saez N, Urzúa M, Saavedra M, Pérez MV, et al. The role of pre-treatment para-aortic surgical staging for cervical cancer in the EMBRACE criteria. *Ecancermedicalscience.* 2022;16:1463.

16. Thelissen AAB, Jürgenliemk-Schulz IM, van der Leij F, Peters M, Gerestein CG, Zweemer RP, et al. Upstaging by para-aortic lymph node dissection in patients with locally advanced cervical cancer: a systematic review and meta-analysis. *Gynecol Oncol.* 2022;164(3):667-674.

17. Bianchi T, Grassi T, Di Martino G, Negri S, Trezzi G, Fruscio R, et al. Low-volume metastases in cervical cancer: does size matter? *Cancers (Basel).* 2024;16(6):1107.

18. Guani B, Balaya V, Magaud L, Lecuru F, Mathevet P. The clinical impact of low-volume lymph nodal metastases in early-stage cervical cancer: the senticol 1 and senticol 2 trials. *Cancers (Basel).* 2020;12(5):1061.

19. Buda A, Casarin J, Mueller M, Fanfani F, Zapardiel I, Mereu L, et al. The impact of low-volume metastasis on disease-free survival of women with early-stage cervical cancer. *J Cancer Res Clin Oncol.* 2021 Jun;147(6):1599-1606. Erratum in: *J Cancer Res Clin Oncol.* 2021;147(6):1607.

20. Kocian R, Slama J, Fischerova D, Germanova A, Burgetova A, Dusek L, et al. Micrometastases in sentinel lymph nodes represent a significant negative prognostic factor in early-stage cervical cancer: a single-institutional retrospective cohort study. *Cancers (Basel).* 2020;12(6):1438.

21. Martinez A, Angeles MA, Querleu D, Ferron G, Pomel C. How should we stage and tailor treatment strategy in locally advanced cervical cancer? Imaging versus para-aortic surgical staging. *Int J Gynecol Cancer.* 2020;30(9):1434-1443.

22. Nasioudis D, George EM, Tanyi JL. Controversies in the staging of patients with locally advanced cervical cancer. *Diagnostics (Basel).* 2023;13(10):1747.

DOI: 10.4274/gulhane.galenos.2025.47855
Gulhane Med J 2026;68(2):102-108

The predictive role of hemoglobin-albumin-lymphocyte-platelet (HALP) score and serum inflammatory markers in intrahepatic cholestasis of pregnancy

Özge Öztürk[1], Seval Yılmaz Ergani[1], Recep Taha Ağaoğlu[1], Figen Günday[1], Aysu Yeşim Tezcan[2], Kadriye Yakut Yücel[1], Zehra Vural Yılmaz[1]

[1]University of Health Sciences Türkiye, Ankara Etlik City Hospital, Clinic of Perinatology, Ankara, Türkiye
[2]University of Health Sciences Türkiye, Ankara Etlik City Hospital, Clinic of Obstetrics and Gynecology, Ankara, Türkiye

Cite this article as: Öztürk Ö, Yılmaz Ergani S, Ağaoğlu RT, Günday F, Tezcan AY, Yakut Yücel K, et al. The predictive role of hemoglobin-albumin-lymphocyte-platelet (HALP) score and serum inflammatory markers in intrahepatic cholestasis of pregnancy. *Gulhane Med J.* 2026;68(2):102-108.

Date submitted:
13.06.2025
Date accepted:
25.12.2025
Epub:
11.06.2026
Publication Date:
16.06.2026

Corresponding Author:
Özge Öztürk, M.D., University of Health Sciences Türkiye, Ankara Etlik City Hospital, Clinic of Perinatology, Ankara, Türkiye
drozgeozturk06@hotmail.com

ORCID:
orcid.org/0009-0004-1134-9950

Keywords: HALP, SIRI, AISI, intrahepatic cholestasis of pregnancy

ABSTRACT

Aims: To date, no studies have examined the relationship between the hemoglobin-albumin-lymphocyte-platelet (HALP) score and the systemic inflammatory response index (SIRI) in pregnancy. The aim of this study was to compare HALP, SIRI, and other systemic inflammatory indices, including the neutrophil-to-lymphocyte ratio (NLR), monocyte-to-lymphocyte ratio (MLR), platelet-to-lymphocyte ratio (PLR), systemic immune-inflammation index (SII), and aggregate index of systemic inflammation (AISI), between pregnant women with intrahepatic cholestasis of pregnancy (ICP) and healthy pregnant controls.

Methods: This retrospective cross-sectional study included pregnant women diagnosed with ICP and healthy controls matched for age and pregnancy. Participants were screened using complete blood count data collected at diagnosis. The primary endpoint was a comparison of systemic inflammatory markers, including NLR, MLR, PLR, SII, SIRI, AISI, and HALP score.

Results: A total of 143 pregnant women with a mean age of 29.3 years were included. Of these, 73 were in the ICP group and 70 were in the control group. PLR, SII, and HALP scores were significantly higher in the ICP group than in the control group (p=0.026, p=0.019, and p=0.016, respectively), while NLR, MLR, SIRI, and AISI showed no significant differences between the groups. Weak positive correlations were found between the presence of ICP and each of PLR (r=0.187, p=0.025), SII (r=0.197, p=0.019), and HALP (r=0.201, p=0.016). Receiver operating characteristic analysis showed that HALP [area under the curve (AUC)=0.616, sensitivity 97%, p=0.016], SII (AUC=0.614, specificity 94%, p=0.019), and PLR (AUC=0.608, specificity 89%, p=0.026) had significant predictive value.

Conclusions: HALP and selected systemic inflammatory indices can serve as helpful biomarkers for the diagnosis of ICP.

Introduction

Intrahepatic cholestasis of pregnancy (ICP) is a pregnancy-specific condition. It is characterized by impaired bile flow, resulting in elevated maternal bile acid (BA) levels. The underlying causes of ICP are believed to include hormonal changes during gestation, genetic and environmental factors affecting bile transport, and inflammatory mechanisms (1). The literature reports a role for inflammation in the pathogenesis of the disease (2). This condition mainly manifests in the third trimester of pregnancy and is concomitantly associated with severe fetal complications. These include premature labor, fetal distress, and an increased number of stillbirths (3-5). The disease has been observed to resolve spontaneously after delivery; however, it has also been reported to reappear in a more severe form in 45-90% of subsequent pregnancies (6,7). Cholestatic liver injury, whether caused by endogenous or exogenous factors, may present with elevated cholestatic enzymes such as alkaline phosphatase and gamma-glutamyl transferase, and is frequently accompanied by pruritus and hyperbilirubinemia (8).

In recent years, the hemoglobin-albumin-lymphocyte-platelet (HALP) score has demonstrated potential as a predictive biomarker. This score, which involves the analysis of hemoglobin, albumin, lymphocytes, and platelets, has demonstrated its potential to assess systemic inflammation and nutritional status. It is currently being investigated for its ability to predict a range of clinical outcomes associated with various neoplastic diseases (9-12).

Although numerous studies have investigated the association between HALP scores and various types of cancer, the HALP score during pregnancy remains poorly studied. A study was conducted to investigate the sensitivity of the HALP level in predicting preterm delivery. The study included a comparison of the HALP score with other serum markers for the prediction of preterm labor (13). Soykan Sert and Bertizlioğlu (14) found higher HALP scores in patients with severe preeclampsia. Low HALP scores were shown to be associated with hyperemesis gravidarum severity by Bayram et al. (15). However, there are no data on the HALP score and on ICP disease in pregnancy. In addition to pregnancy-related causes such as ICP, drug-induced liver injury must be considered in the differential diagnosis of cholestatic elevations of liver enzymes during gestation. Başgöz et al. (8) reported two cases of cholestatic hepatitis triggered by meropenem, emphasizing the importance of recognizing medication-induced liver injury that may mimic ICP symptoms.

The hematological system plays a pivotal role in preserving the structural integrity and physiological function of the placenta. This system serves as a conduit between the foetus, the placenta, and the maternal circulation. A number of changes associated with post-term pregnancies have been shown to diminish nutrient and oxygen transport to the foetus. Markers such as the neutrophil-to-lymphocyte ratio (NLR) and the platelet-to-lymphocyte ratio (PLR) are strong indicators of an acute inflammatory state. They are commonly used as diagnostic and prognostic markers for cardiovascular events, including myocardial infarction. Recent evidence supports the use of these haematological indices as valuable biomarkers in obstetrics and gynaecology. It has been demonstrated by means of research that as gestation progresses, there is an increase in neutrophil levels and a decrease in lymphocyte levels, which results in an elevated NLR (16). The main objective of the current study was to evaluate the HALP score together with other inflammatory markers obtained from the blood count, such as the systemic inflammatory response index (SIRI), aggregate index of systemic inflammation (AISI), and systemic immune-inflammation index (SII). The aim of this study was to assess the ability of these markers to predict disease severity in pregnant women with ICP.

Methods

Study design, setting, duration, participants, and ethical approval

This cross-sectional study was conducted from October 2022 to February 2024 in the Perinatology Clinic of University of Health Sciences Türkiye, Ankara Etlik City Hospital, a tertiary referral center affiliated with the Turkish Ministry of Health in Ankara. A total of 143 pregnant women were included. Seventy-three women were diagnosed with ICP, and 70 were healthy pregnant women of the same age group and gestational age. Ethical approval was granted by the University of Health Sciences Türkiye, Ankara Etlik City Hospital Ethics Committee (approval no: AEŞH-BADEK-2024-069, date: 31.01.2024). All participants provided written informed consent. The study was conducted in accordance with the standards of the Declaration of Helsinki.

Inclusion and exclusion criteria

Pregnant women with ICP, as determined by clinical and laboratory findings, were included. The diagnosis was based on the presence of pruritus (especially on the palms and soles), elevated total BA levels (>10 μmol/L) and/or increased liver transaminases [alanine aminotransferase (ALT) or aspartate aminotransferase (AST)>40 U/L], in the absence of dermatological or other pathological conditions that could explain these symptoms (17,18).

Clinical and laboratory assessments

The clinical parameters collected included maternal age, gravidity, parity, body mass index (BMI) (BMI, kg/m^2), and gestational age at diagnosis. Haematological and biochemical

parameters obtained from maternal peripheral venous blood samples included haemoglobin (g/dL), leukocytes (white blood cell), neutrophils, lymphocytes, monocytes, platelets (10^3/μL), AST, ALT, fasting BAs (μmol/L), and albumin (g/L).

All laboratory data were retrieved from the hospital's electronic medical records system. Based on BA values, patients with ICP were categorised into two groups: mild (10-40 μmol/L) and severe (≥40 μmol/L) (18).

Outcome measures

The primary aim of our study was to compare systemic inflammatory indices between pregnant women with ICP and a healthy control group. The secondary outcome was to determine the diagnostic efficacy of these indices in distinguishing between mild and severe ICP.

Inflammatory index calculations

The systemic inflammatory indices were calculated as follows: (9,19,20)

HALP score=(hemoglobin×albumin×lymphocyte)/platelet

AISI=(neutrophil×monocyte×platelet)/lymphocyte

NLR=neutrophil/lymphocyte

PLR=platelet/lymphocyte

SIRI=(neutrophil×monocyte)/lymphocyte

MLR=monocyte/lymphocyte

SII=(neutrophil×platelet)/lymphocyte

Statistical Analysis

Statistical analyses were conducted using SPSS version 27.0 (IBM Corp., Armonk, NY, USA). The Shapiro-Wilk test was utilized to evaluate the distribution of continuous variables. The data concerning variables distributed normally were characterized in accordance with the mean ± standard deviation, after which a comparison was made between said variables using an Independent Samples t-test. Non-normal variables were expressed as medians and interquartile ranges and subsequently evaluated using the Mann-Whitney U test.

Spearman's rank correlation coefficient was used to analyze the correlations between the variables. Diagnostic accuracy was evaluated using receiver operating characteristic (ROC) curve analysis. The area under the curve (AUC) and optimal cut-off values were reported. A p-value of less than 0.05 was considered significant

Results

Study population and demographics

A total of 143 pregnant women were included in the study: 73 diagnosed with ICP and 70 healthy pregnant women who served as controls. The median age of the mothers was 28 years [interquartile range (IQR): 25-32] in the ICP group and 26 years (IQR: 23-31) in the control group. No subjects were excluded after enrollment due to data inaccessibility or eligibility issues. Among the patients with ICP, 87.7% (n=64) had mild disease (defined as serum BA levels between 10 and 40 μmol/L), while 12.3% (n=9) had severe ICP (BA levels ≥40 μmol/L).

Basic clinical and laboratory characteristics

The demographic and laboratory data of the study groups are presented in Table 1. The results indicate that there were no statistically significant differences between the two groups regarding maternal age, gravidity, or BMI (p>0.05 for all). However, parity was significantly lower in the ICP group than in the control group (p=0.024).

Regarding the laboratory parameters, the present study found that the liver enzymes, ALT and AST, were significantly elevated in the ICP group (p<0.001 for both). The investigation showed that the concentrations of haemoglobin, neutrophils, monocytes, lymphocytes, platelets, and serum albumin did not differ significantly between groups (p>0.05).

Regarding the calculated inflammatory indices, SII and the PLR were significantly higher in the ICP group than in the control group (p=0.026 and p=0.019, respectively). No significant differences were observed between the groups for the NLR, AISI, SIRI, or MLR. However, the HALP score was significantly higher in the ICP group compared to the controls [26.60 (18.96-36.30) vs. 23.94 (3.21-36.68); p=0.016].

Primary and secondary outcomes

The correlations between the inflammatory indices and the presence of ICP are summarized in Table 2. The correlation analysis showed slight but statistically significant positive correlations of ICP with PLR (r=0.187, p=0.025), SII (r=0.197, p=0.019), and HALP score (r=0.201, p=0.016). No statistically significant correlations were observed between fasting BA levels and biomarkers of inflammation, including SIRI, SII, AISI, NLR, PLR, MLR, and HALP score (p>0.05).

The effectiveness of these measures in identifying ICP was evaluated using ROC analysis. The results are presented in Figure 1 and Table 3. Figure 1 illustrates the ROC analysis. The HALP score demonstrated the highest sensitivity (97%) at a cut-off value of ≥7.565, with an AUC of 0.616 [95% confidence interval (CI): 0.522-0.711; p=0.016]. The SII had a cut-off value of ≥1432.674, resulting in a sensitivity of 30% and a specificity of 94% (AUC=0.614, 95% CI: 0.521-0.706; p=0.019). The PLR had a cut-off of ≥174.820, with a sensitivity of 34% and a specificity of 89% (AUC=0.608, 95% CI: 0.515-0.701; p=0.026).

Table 1. Descriptive and comparative analysis of demographic and laboratory data between ICP and control groups

Variables	ICP (n=73)	Control (n=70)	p-value
Age (year)	28 (25-32)	26 (23-31)	0.407[a]
Gravidity (n)	2 (1-2)	2 (1-3)	0.208[a]
Parity (n)	0 (0-1)	1 (0-2)	**0.024[a]**
BMI (kg/m²)	27.86±2.95	25.03±3.67	0.230[b]
GA at time of blood sampling (weeks)	34 (31-36)	35 (32-36)	0.149[a]
Hb (g/dL)	11.7±1.5	11.6±1.3	0.458[b]
Thrombocyte (10^3/μL)	265.1±65.3	252.7±66.0	0.259[b]
Neutrophile (10^3/μL)	7.31 (6.06-8.76)	6.98 (6.12-8.40)	0.516[a]
Monocyte (10^3/μL)	0.66±0.33	0.7±0.25	0.433[b]
Lymphocyte (10^3/μL)	1.82±0.71	1.96±0.51	0.174[b]
Albumin (g/L)	35.0 (32.7-36.3)	33.0 (31.0-36.0)	0.088[a]
ALT (U/L)	78 (39-190)	15 (12-20)	**<0.001[a]**
AST (U/L)	54 (28-134)	13 (9-17)	**<0.001[a]**
FBA (μmol/L)	27.7±23.4	-	-
Mild ICP (FBA=10-40)	64 (87.7%)	-	-
Severe ICP (FBA>40)	9 (12.3%)	-	-
PLR	141.82 (117.39-190.05)	128.97 (107.65-151.15)	**0.026[a]**
NLR	3.92 (3.24-5.49)	3.80 (3.130-4.405)	0.101[a]
MLR	0.33 (0.25-0.450)	0.35 (0.28-0.43)	0.605[a]
SII (10^9/L)	1007.75 (762.50-1535.76)	857.40 (717.50-1099.58)	**0.019[a]**
SIRI	2.379 (1.54-3.88)	2.58 (1.88-3.32)	0.818[a]
AISI	635.55 (394.25-955.03)	592.50 (423.44-901.66)	0.784[a]
HALP score	26.60 (18.96-36.30)	23.94 (3.21-36.68)	0.016[a]

[a]: The Mann-Whitney U test was used, with results presented as median and quartiles (25^{th}-75^{th} percentiles), [b]: The Student's t-test for independent samples was used to compare the measured values between two independent groups, with the results expressed as mean ± standard deviation
ICP: Intrahepatic cholestasis of pregnancy, BMI: Body mass index, GA: Gestational age, Hb: Hemoglobin, ALT: Alanine aminotransferase, AST: Aspartate amino transferase, FBA: Fasting bile acid, NLR: Neutrophil-to-lymphocyte ratio, PLR: Platelet-to-lymphocyte ratio, MLR: Monocyte-to-lymphocyte ratio, SII: Systemic immune inflammation index, SIRI: Systemic inflammation response index, AISI: Aggregate index of systemic inflammation, HALP: Hemoglobin-albumin-lymphocyte-platelet

Discussion

This study investigated the association of the HALP score, a novel immune-nutritional biomarker, with ICP and with various systemic inflammatory indices derived from complete blood counts. The main finding was that pregnant women with ICP had significantly higher HALP, SII, and PLR levels than healthy pregnant controls. This is the first study to evaluate the diagnostic potential of the HALP score in the context of ICP.

In this study, inclusion and exclusion criteria were strictly defined to avoid bias, and blood samples were uniformly collected at the time of diagnosis. Although the sample size was modest, it was sufficient to detect statistically significant differences in certain inflammatory indices, which indicates adequate representativeness and internal validity.

The primary endpoint of this study was to determine whether HALP, SII, and PLR values differed significantly between pregnant women with ICP and healthy controls. The present study found that these indices were significantly elevated in the ICP group, supporting the hypothesis that ICP is associated with systemic inflammation. The secondary endpoint included comparison of other inflammatory indices (NLR, MLR, SIRI, AISI), none of which differed significantly. Previous studies have also reported associations between elevated SIRI and ICP (21), and have highlighted PLR as a meaningful marker in ICP diagnosis (22). Moreover, studies by Huang et al. (23) and Gul and Callioglu (24) provided evidence of inflammatory changes in similar cohorts. In this study, Huang et al. (23) demonstrated that increased levels of the pro-inflammatory mediator interleukin-8 (IL-8) and decreased levels of the anti-inflammatory cytokines IL-4, IL-6, and tumor necrosis factor-α (TNF-α) occurred together, thus supporting the notion that ICP is associated with inflammatory processes. The researchers concluded that TNF-α, while providing significant diagnostic value on its own, achieves optimal diagnostic accuracy when used together with IL-4 and IL-8.

In light of previous research, this study makes several contributions. First, the assessment of HALP and AISI scores in the context of ICP is novel, as no previous studies have addressed this relationship (25,26). Second, our finding of elevated PLR is consistent with previous results by Çallıoğlu et al. (22) and Irak et al. (27), confirming its association with ICP. Third, our results contrast with those of Wang et al. (28), who reported significantly increased NLR values in ICP patients. The absence of NLR elevation in our study may be attributed to differences in population characteristics, sample size, or timing of sampling. Furthermore, MLR was investigated in studies such as Shen (29), but produced varying conclusions. As demonstrated by Shen (29), there was a considerable increase in platelet parameters and inflammatory indices in pregnant women with ICP. It was reported that the MLR increased; although there was an upward trend in the early period, its predictive value was not as strong as that of the NLR and SII. However, when the MLR is evaluated alongside these indices, it supports the immunological mechanisms of ICP as a complementary marker reflecting the systemic inflammatory response (30).

The HALP score has previously demonstrated predictive value in oncological and obstetric conditions, such as preeclampsia and hyperemesis gravidarum (9,14,15). In these contexts, both increased and decreased HALP levels were associated with disease severity, depending on the inflammatory profile of the disease. In the present study, the higher HALP scores observed in ICP cases may reflect an inflammatory phenotype distinct from that of chronic inflammatory diseases, indicating disease-specific immune responses. The diagnostic utility of the HALP score was further emphasized by the ROC analysis, which showed higher sensitivity compared to other indices. In addition, previous studies have suggested an association between ICP and gestational diabetes mellitus overlap syndromes, which may provide a rationale for future investigations evaluating composite inflammatory biomarkers such as HALP (31).

Recent evidence suggests an association between systemic inflammatory indices and hepatic and immune dysregulation

Table 2. Correlation analysis of inflammatory markers with ICP and fasting bile acid levels

Variables	r	p-value
ICP		
PLR	0.187	**0.025**[a]
SII	0.197	**0.019**[a]
HALP	0.201	**0.016**[a]
FBA levels		
NLR	-0.064	0.591[b]
MLR	0.078	0.512[b]
PLR	-0.024	0.841[b]
SII	-0.085	0.476[b]
SIRI	-0.010	0.935[b]
AISI	0.011	0.928[b]
HALP	-0.096	0.419[b]

[a]: Spearman's rank correlation analysis was used. Statistically significant correlations are shown in bold, [b]: Pearson correlation analysis was used to assess the relationship between inflammatory markers and FBA levels
ICP, Intrahepatic cholestasis of pregnancy, PLR: Platelet-to-lymphocyte ratio, SII: Systemic immune-inflammation index, HALP: Hemoglobin, albumin, lymphocyte, and platelet, FBA: Fasting bile acid, NLR: Neutrophil-to-lymphocyte ratio, MLR: Monocyte-to-lymphocyte ratio, SIRI: Systemic inflammation response index, AISI: Aggregate index of systemic inflammation

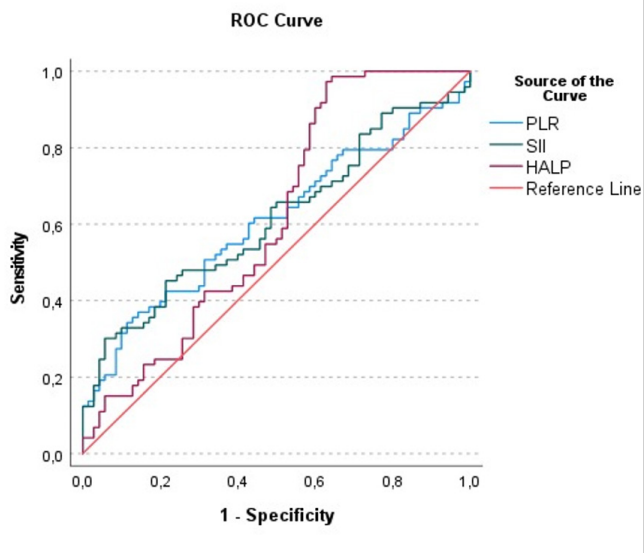

Figure 1. ROC curve analysis of biomarkers for ICP prediction
ICP: Intrahepatic cholestasis of pregnancy, NLR: Neutrophil-to-lymphocyte ratio, PLR: Platelet-to-lymphocyte ratio, MLR: Monocyte-to-Lymphocyte Ratio, SII: Systemic Immune Inflammation Index, HALP: Hemoglobin, albumin, lymphocyte, and platelet score, ROC: Receiver-operating characteristic

Table 3. Logistic regression analysis of data for the prediction of cholestasis and ROC analysis table for the cut-off value of the HALP score for the prediction of ICP

Variables	Cut-off value	AUC	Sensitivity (%)	Specificity (%)	95% CI	p-value*
PLR	≥174.820	0.608	34	89	0.515-0.701	**0.026**
SII	≥1432.674	0.614	30	94	0.521-0.706	**0.019**
HALP	≥7.565	0.616	97	37	0.522-0.711	**0.016**

*: ROC analyses were performed, and the results were accepted with a 95% CI, with statistical significance set at p<0.05
ICP: Intrahepatic cholestasis of pregnancy, NLR: Neutrophil-to-lymphocyte ratio, PLR: Platelet-to-lymphocyte ratio, MLR: Monocyte-to-lymphocyte ratio, SII, Systemic immune-inflammation index, HALP: Hemoglobin, albumin, lymphocyte, and platelet, AUC: Area under the curve, ROC: Receiver-operating characteristic, CI: Confidence interval

in cases of ICP. Elevated PLR and SII values in our cohort may indicate increased platelet activation and neutrophil-driven inflammation. These, in turn, contribute to cholestatic hepatocellular injury and microcirculatory disturbance. It has been established that platelet-derived mediators can amplify oxidative stress and cytokine release, thereby exacerbating BA-induced hepatocyte damage. Our findings are consistent with previous research indicating that indices of platelet function reflect subclinical inflammatory changes associated with pregnancy-related hepatic disorders.

The HALP score, which integrates haemoglobin, albumin, lymphocyte, and platelet counts, demonstrated the highest diagnostic sensitivity among the evaluated markers. This may be attributable to the dual nutritional and inflammatory components in its formula. Decreased albumin and lymphocyte levels, commonly observed in cholestatic conditions, indicate hepatic synthetic dysfunction and systemic inflammation. In contrast, reactive thrombocytosis leads to an elevated HALP value. Therefore, the hypothesis that HALP may serve as a composite biomarker reflecting both inflammatory and metabolic stress in ICP is supported by these results and the literature. These findings highlight the potential clinical relevance of HALP, alongside PLR and SII, as a cost-effective method for identifying systemic inflammatory activity in cases of ICP.

Study Limitations

Despite the revealing results, the study has some limitations. The retrospective design, combined with the absence of longitudinal follow-up, limits the ability to draw causal conclusions and establish temporal relationships. In addition, the lack of subgroup analysis based on disease severity and the absence of dynamic biomarker measurements restrict the generalizability and depth of the conclusions. However, the strengths of the study lie in its structured methodology, well-matched control group, and novel investigation of HALP and AISI in ICP.

Conclusion

The primary objective of this study was to evaluate the diagnostic value of haematological indices reflecting the systemic inflammatory response, particularly HALP and SIRI, in pregnant women with ICP. The findings of this study demonstrated that the HALP score was significantly higher in the ICP group and exhibited high diagnostic potential and sensitivity. This result demonstrates, for the first time in the literature, an association between the HALP score and ICP, suggesting that the HALP score—previously examined only in obstetric conditions such as preeclampsia and hyperemesis gravidarum—may also be useful in pregnancy-related hepatobiliary pathologies. In addition, classical inflammatory indices, such as NLR, MLR, and SIRI, do not always show significant differences in diagnosing ICP, whereas immune-nutritional parameters, such as HALP, may provide a stronger diagnostic contribution. In this context, this study emphasizes that the HALP score, a novel biomarker in ICP, can be used as a cost-effective, easily accessible, and complementary diagnostic tool in clinical practice, especially in cases where BA measurements are delayed or inaccessible.

Ethics

Ethics Committee Approval: Ethical approval was granted by the University of Health Sciences Türkiye, Ankara Etlik City Hospital ethics committee (approval no: AEŞH-BADEK-2024-069, date: 31.01.2024). The study was conducted in accordance with the standards of the Declaration of Helsinki.

Informed Consent: All participants provided written informed consent.

Footnotes

Authorship Contributions

Surgical and Medical Practices: Ö.Ö., S.Y.E., R.T.A., F.G., A.Y.T., K.Y.Y., Z.V.Y., Concept: Ö.Ö., K.Y.Y., Z.V.Y., Design: Ö.Ö., K.Y.Y., Z.V.Y., Data Collection or Processing: Ö.Ö., R.T.A., F.G., A.Y.T., Analysis or Interpretation: S.Y.E., R.T.A., Literature Search: Ö.Ö., Writing: Ö.Ö., R.T.A., K.Y.Y., Z.V.Y.

Conflict of Interest: The authors declared no conflict of interest.

Financial Disclosure: The authors declared that this study received no financial support.

References

1. Kıncı MF, Şehirli Kıncı Ö, Karakaş Paskal E. Intrahepatic cholestasis of pregnancy. *MMJ.* 2021;8(2):158-162.
2. Biberoglu E, Kirbas A, Daglar K, Kara O, Karabulut E, Yakut HI, et al. Role of inflammation in intrahepatic cholestasis of pregnancy. *J Obstet Gynaecol Res.* 2016;42(3):252-257.
3. Abdul Waheed MI, Jaiswal A, Yelne S, Nandanwar V. Navigating perinatal challenges: a comprehensive review of cholestasis of pregnancy and its impact on maternal and fetal health. *Cureus.* 2024;16(4):e58699.
4. Pillarisetty LS, Sharma A. Pregnancy Intrahepatic Cholestasis. In: StatPearls [Internet]. Treasure Island (FL): StatPearls Publishing; 2024 [cited 2024 Aug 16]. Available from: http://www.ncbi.nlm.nih.gov/books/NBK551503/
5. Society for Maternal-Fetal Medicine (SMFM). Electronic address: pubs@smfm.org; Lee RH, Mara Greenberg, Metz TD, Pettker CM. Society for Maternal-Fetal Medicine Consult Series #53: Intrahepatic cholestasis of pregnancy: Replaces Consult #13, April 2011. *Am J Obstet Gynecol.* 2021;224(2):B2-B9.
6. Piechota J, Jelski W. Intrahepatic cholestasis in pregnancy: review of the literature. *J Clin Med.* 2020;9(5):1361.
7. Luo M, Wang L, Yao H, Wen Y, Cao D, Shen W, et al. Diagnostic and prognostic value of blood inflammation and biochemical indicators for intrahepatic cholestasis of pregnancy in Chinese pregnant women. *Sci Rep.* 2022;12(1):20833.

8. Başgöz BB, Mehmetzade N, Ediboğlu E, Taşçı İ, Sağlam K. Meropenem induced mixed hepatocellular and cholestatic hepatitis: a report of two cases. *Gulhane Med J.* 2018;60(2):64-66.

9. Farag CM, Antar R, Akosman S, Ng M, Whalen MJ. What is hemoglobin, albumin, lymphocyte, platelet (HALP) score? A comprehensive literature review of HALP's prognostic ability in different cancer types. *Oncotarget*. 2023;14:153-172.

10. Eskin F, Köseoğlu H, Düzenli T, Özden M, Bebek B, Kaya M, et al. A new index for predicting malignant causes in patients with extrahepatic biliary obstruction: the hemoglobin, albumin, lymphocyte, and platelet (HALP) score. *Eur Rev Med Pharmacol Sci.* 2023;27(6):2514-2521.

11. Tian M, Li Y, Wang X, Tian X, Pei LL, Wang X, et al. The hemoglobin, albumin, lymphocyte, and platelet (HALP) score is associated with poor outcome of acute ischemic stroke. *Front Neurol.* 2021;11:610318.

12. Antar R, Farag C, Xu V, Drouaud A, Gordon O, Whalen MJ. Evaluating the baseline hemoglobin, albumin, lymphocyte, and platelet (HALP) score in the United States adult population and comorbidities: an analysis of the NHANES. *Front Nutr.* 2023;10:1206958.

13. Hrubaru I, Motoc A, Dumitru C, Bratosin F, Fericean RM, Alambaram S, et al. Assessing the utility of hemoglobin, HALP score, FAR ratio, and coagulation parameters as predictors for preterm birth. *Children (Basel)*. 2023;10(3):527.

14. Soykan Sert Z, Bertizlioğlu M. Predictive value of the HALP score for pre-eclampsia with severe features. *Postgrad Med.* 2024;136(4):468-473.

15. Bayram F, Ozgen G, Karasın SS, Ozgen L. The predictive value of HALP score and systemic immune inflammation (SII) index in hyperemesis gravidarum. *J Obstet Gynaecol Res.* 2023;49(7):1729-1735.

16. Akbas O, Balci MF, Karaduman AB, Odabas O, Yurtkul AA, Kinci MF, et al. Determination of systemic inflammatory markers and determination of possible risk factors in post-term pregnancies. *Perinatal Journal.* 2025;33(2):15-22.

17. Kothari S, Afshar Y, Friedman LS, Ahn J. AGA clinical practice update on pregnancy-related gastrointestinal and liver disease: expert review. *Gastroenterology.* 2024;167(5):1033-1045.

18. Viswanathan L, Sthaneshwar P, Razali N, Thambiah SC. Diagnosis and management of intrahepatic cholestasis of pregnancy- a retrospective clinical audit. *Malays J Med Health Sci.* 2022;18(SUPP21):73-79.

19. Ou S, Lu H, Qu R, Cui X, Xiong Z, Fan F, et al. The clinical value of systemic immune inflammatory index in predicting the prognosis of patients with bloodstream infection. *J Inflamm Res.* 2025;18:10181-10192.

20. Jin M, Xu J, Liu H, Zhou Y, Hao H, Yuan Y, et al. Association of multiple inflammatory index markers with overactive bladder syndrome: a cross-sectional study results from the NHANES 2005 to 2018. *Medicine (Baltimore)*. 2025;104(41):e45154.

21. Kanza Gul D, Callioglu N. The role of the systemic inflammatory response index (SIRI) and other maternal biochemical markers in determining the severity of intrahepatic cholestasis of pregnancy. *Ginekol Pol.* 2025;96(5):379-384.

22. Çallıoğlu N, Tuna G, Tandoğan Ö, Ersan F, Atalay S, Bilirer KK. Systemic immune-inflammatory index and platelet-to-lymphocyte ratio in intrahepatic cholestasis of pregnancy. *Saudi Med J.* 2024;45(11):1217-1222.

23. Huang S, Liu Y, Guo N, Liu X, Li G, Du Q. Serum profiles of inflammatory cytokines associated with intrahepatic cholestasis of pregnancy. *J Matern Fetal Neonatal Med.* 2022;35(25):10072-10081.

24. Gul DK, Callioglu N. Does amnioumbilicocerebral ratio better predict adverse neonatal outcomes in comparison to other doppler parameters in late-onset fetal growth restriction? *Clin Exp Obstet Gynecol.* 2023;50(12):261.

25. Lin QX, Huang WW, Shen W, Deng XS, Tang ZY, Chen ZH, et al. Intrahepatic cholestasis of pregnancy increases inflammatory susceptibility in neonatal offspring by modulating gut microbiota. *Front Immunol.* 2022;13:889646.

26. Asensio M, Ortiz-Rivero S, Morente-Carrasco A, Marin JJG. Etiopathogenesis and pathophysiology of cholestasis. *Explor Dig Dis.* 2022;1(2):97-117.

27. Irak K, Bayram M, Becerik TF. The role of inflammatory markers derived from complete blood count results in the diagnosis of intrahepatic cholestasis of pregnancy. *J Health Sci Med / JHSM.* 2022;5(2):640-645.

28. Wang L, Lu Z, Zhou X, Ding Y, Guan L. Effects of intrahepatic cholestasis of pregnancy on hepatic function, changes of inflammatory cytokines and fetal outcomes. *Exp Ther Med.* 2019;17(4):2979-2984.

29. Shen C. Analysis of changes in platelet parameters and inflammatory markers in intrahepatic cholestasis of pregnancy before disease development. *Am J Transl Res.* 2024;16(12):7448-7457.

30. Hosseninia S, Ghobadi H, Garjani K, Hosseini SAH, Aslani MR. Aggregate index of systemic inflammation (AISI) in admission as a reliable predictor of mortality in COPD patients with COVID-19. *BMC Pulm Med*. 2023;23:107.

31. Martineau M, Raker C, Powrie R, Williamson C. Intrahepatic cholestasis of pregnancy is associated with an increased risk of gestational diabetes. *Eur J Obstet Gynecol Reprod Biol.* 2014;176:80-85.

DOI: 10.4274/gulhane.galenos.2026.42223
Gulhane Med J 2026;68(2):109-117

Hematological indices in children with *Helicobacter pylori* infection: a retrospective analysis

Yasin Maruf Ergen, Selçuk Teke

University of Health Sciences Türkiye, Gülhane Training and Research Hospital, Clinic of Pediatrics, Division of Pediatric Gastroenterology, Ankara, Türkiye

Cite this article as: Ergen YM, Teke S. Hematological indices in children with *Helicobacter pylori* infection: a retrospective analysis. *Gulhane Med J.* 2026;68(2):109-117.

Date submitted:
22.10.2025
Date accepted:
20.01.2026
Publication Date:
16.06.2026

Corresponding Author:
Yasin Maruf Ergen, M.D., University of Health Sciences Türkiye, Gülhane Training and Research Hospital, Clinic of Pediatrics, Division of Pediatric Gastroenterology, Ankara, Türkiye
yasinmaruf@gmail.com

ORCID:
orcid.org/0000-0002-3689-6852

Keywords: *Helicobacter pylori*, children, hematological indices, PLR, MPVLR

ABSTRACT

Aims: *Helicobacter pylori (H. pylori)* infection is a frequent chronic condition in childhood, and determining whether it provokes a systemic inflammatory imprint is clinically relevant. This study aimed to evaluate whether pediatric *H. pylori* infection was associated with alterations in complete blood count (CBC)-derived inflammatory indices, particularly the platelet-to-lymphocyte ratio (PLR) and the mean platelet volume-to-lymphocyte ratio (MPVLR).

Methods: This retrospective cross-sectional study included children aged 6-18 years who underwent upper gastrointestinal endoscopy for dyspeptic symptoms and had histopathological confirmation of *H. pylori* infection. Pre-procedural CBC and serum albumin levels were recorded, and CBC-derived inflammatory indices (such as the PLR and the MPVLR) were calculated. The primary endpoint was the association between *H. pylori* positivity and these inflammatory indices.

Results: A total of 453 children were included, of whom 171 were *H. pylori* positive and 282 were *H. pylori* negative [median age 13.4 years (interquartile range 10.8-15.7); predominantly female (65.6%)]. Children with *H. pylori* infection had significantly higher PLR (127.45 vs. 113.50; p<0.001) and MPVLR (4.45 vs. 4.02; p<0.001) values compared with controls. Neutrophil, lymphocyte, and monocyte counts were lower in the positive group (p<0.01 for all), while no meaningful differences were observed in other composite indices.

Conclusions: Pediatric *H. pylori* infection is associated with a measurable, low-grade systemic inflammatory response, as reflected by elevated PLR and MPVLR values.

Introduction

Helicobacter pylori (H. pylori) is a common bacterial pathogen in childhood; in the absence of treatment, it may persist in the host for many years. In children, the infection is frequently silent or accompanied only by vague, non-specific complaints; however, the resulting persistent gastric inflammation can facilitate the development of peptic ulcer disease and may elevate the long-term risk of malignancy later in life (1). In addition to gastric involvement, the organism has been linked to several extra-intestinal consequences, including impaired growth, iron deficiency anemia, and immune-mediated thrombocytopenia, which highlights the need for timely detection and management in childhood (2). Consequently, it is important to evaluate not only whether the bacterium is present but also how it influences the host's overall biology. In children, the immunological reaction elicited by *H. pylori* generally manifests as a mild, predominantly cell-mediated inflammatory response.

In pediatric patients, the immune response to *H. pylori* typically reflects a low-grade, cell-mediated inflammatory pattern. Sustained antigenic stimulation promotes persistent mucosal inflammation while simultaneously altering the balance of circulating neutrophils, lymphocytes, and platelets (3,4). These systemic changes indicate that the infection is not confined to the gastric mucosa but may also be indirectly monitored through peripheral hematological parameters.

In this context, hematological indices derived from the complete blood count (CBC) have gained increasing attention as non-invasive biomarkers for the evaluation of chronic inflammatory processes in children. Various CBC-derived ratios, including the neutrophil-to-lymphocyte ratio (NLR), platelet-to-lymphocyte ratio (PLR), and lymphocyte-to-monocyte ratio (LMR), have been explored as indirect markers of systemic immune activation in a range of pediatric disorders (5). However, existing pediatric studies on *H. pylori* have reported heterogeneous diagnostic performance, and data correlating these indices with histopathological severity or bacterial density remain limited (6,7). This uncertainty highlights the need to better define the clinical utility of CBC-based composite markers in the non-invasive assessment of *H. pylori*-associated gastric inflammation in the pediatric population.

In light of these gaps, the present study was designed to characterize the hematological alterations associated with *H. pylori* infection in children with dyspeptic complaints and to determine whether CBC-based composite indices can support the identification of infection and approximate the histopathological severity. Through this investigation, we aimed to clarify the potential clinical value of these easily obtainable, inexpensive, and non-invasive parameters in routine pediatric practice.

Methods

Study design and participants

This study employed a descriptive retrospective cross-sectional design and used clinical data from pediatric patients who underwent endoscopic evaluation for dyspeptic complaints at a tertiary pediatric gastroenterology referral center between August 2023 and August 2025. Eligible participants were children aged 6-18 years who underwent upper gastrointestinal (GI) endoscopy under general anesthesia and whose gastric biopsy specimens were assessed for *H. pylori* status by histopathological examination. All information was extracted retrospectively from the institutional electronic medical records and analyzed after full de-identification.

As part of the standard pre-endoscopy anesthesia protocol at our center, a CBC and a routine biochemistry panel (including albumin) were obtained after an overnight fast of approximately eight hours. For inclusion in the present analysis, these laboratory assessments had to have been performed no more than one week before endoscopy.

The *H. pylori*-positive group consisted of patients in whom the bacterium was identified by Giemsa or hematoxylin-eosin (H&E) staining of biopsy specimens. The control group was selected from children who presented with the same dyspeptic complaints and underwent endoscopy for clinical indications, but were histologically negative for *H. pylori* and showed no endoscopic abnormalities other than mild non-specific hyperemia. Individuals were not considered eligible if they had chronic systemic illnesses; had abnormalities in the esophagus or duodenum on endoscopy or histology; were taking medications such as antibiotics, corticosteroids, or immunosuppressants; an acute infection within the preceding four weeks; had signs of active systemic inflammation; or had missing laboratory or pathology data.

Endoscopic evaluation

All procedures were carried out while the children were under general anesthesia, which was administered and monitored by a pediatric anesthesia team. Upper GI endoscopy was performed by an experienced pediatric gastroenterologist using the Fujinon ELUXEO VP-7000/BL-7000 videoendoscopy system (Fujifilm Corporation, Tokyo, Japan); the endoscope diameter was selected according to the child's age and body size, and the procedure was performed in a child-friendly environment. The procedures were conducted in accordance with the recommendations of the 2023 ESPGHAN/NASPGHAN *H. pylori* guideline (8). Mucosal findings observed during the procedure (e.g., hyperemia, edema, nodularity, erosion, and ulceration) were recorded using a standardized protocol. From each patient, six gastric biopsies were systematically collected: three from the antral region and three from the corpus, to allow adequate histopathological evaluation. Additional biopsies were collected from macroscopically abnormal areas when present. All biopsy samples were labeled appropriately and fixed in 10% neutral-buffered formalin before being transferred to the pathology laboratory.

Histopathological evaluation

Gastric biopsy samples obtained from both the antrum and corpus were evaluated using the criteria defined in the Updated Sydney System (9). Diagnosis of *H. pylori* infection was based on these standardized histopathological findings. Rapid urease testing or culture/PCR is not routinely included in the initial diagnostic workflow for pediatric endoscopy at our center. To reduce the risk of misclassification, cases with equivocal histological findings were excluded. The degree of mucosal inflammation, inflammatory activity, glandular atrophy, intestinal metaplasia, and H. pylori burden were recorded using a four-tier grading system ranging from 0 (absent) to 3 (severe). The presence of *H. pylori* was evaluated using H&E and/or Giemsa

staining, and immunohistochemical confirmation was performed when deemed necessary. All evaluations were conducted by experienced pathologists at the institution.

Laboratory parameters and calculated hematological indices

All laboratory data were obtained retrospectively from the hospital information system. CBC and biochemistry results obtained as part of the standard pre-endoscopy anesthesia protocol constituted the laboratory dataset for this study. Only patients with laboratory tests performed during the same admission as the endoscopy were included in the analysis.

CBC parameters were measured using an automated hematology analyzer (Mindray BC-6000, Shenzhen Mindray Bio-Medical Electronics Co., Ltd., China) following routine quality-control procedures. The recorded parameters included white blood cell count, neutrophil count, lymphocyte count, monocyte count, erythrocyte count, hemoglobin, hematocrit, mean corpuscular volume (MCV), red cell distribution width (RDW), platelet count, mean platelet volume (MPV), platelet distribution width, and plateletcrit. Serum albumin levels were measured in the hospital biochemistry laboratory using the COBAS C8000 analyzer system (Roche Diagnostics, Mannheim, Germany), and all values were assessed according to internationally accepted laboratory standards.

In addition to raw CBC values, a set of CBC-derived inflammatory indices reflecting neutrophil-, lymphocyte-, and platelet-based systemic immune activity was calculated. Based on these measurements, CBC-derived hematological and composite inflammatory indices were calculated, including NLR, PLR, LMR, dNLR, systemic immune-inflammation index (SII), systemic inflammation response index (SIRI), aggregate index of systemic inflammation (AISI), MPV-to-lymphocyte ratio (MPVLR), mean platelet volume-to-platelet ratio (MPR), RDW-to-platelet ratio (RPR), prognostic nutritional index (PNI), neutrophil-to-albumin ratio (NAR), and platelet-to-albumin ratio (PAR), with the corresponding formulas summarized in Table 1. All calculated ratios and raw laboratory values were included in the statistical analysis.

Ethical Approval

The study was conducted in accordance with the ethical principles of the Declaration of Helsinki (1975), as revised in 2013. Because this research was conducted as a retrospective chart review with no direct patient contact or intervention, the approving ethics committee waived the requirement for written informed consent. The study protocol was reviewed and approved by the University of Health Sciences Türkiye, Gülhane Scientific Research Ethics Committee (approval no: 2025-417, date: 30.09.2025).

Statistical Analysis

All statistical computations were carried out with IBM SPSS Statistics software (version 26.0; IBM Corp., Armonk, NY, USA). The distribution of continuous variables was assessed using the Shapiro-Wilk test. Non-normally distributed data were presented as median (minimum-maximum), whereas categorical variables were presented as frequencies and percentages.

Comparisons between the *H. pylori* positive and negative groups were performed using the Mann-Whitney U test for continuous variables and the chi-square test or Fisher's exact test for categorical variables. Multiple comparisons were controlled using the Benjamini-Hochberg false discovery rate (FDR) procedure. Effect sizes, together with 95% confidence intervals, were calculated to complement p-values.

Table 1. Calculation formulas of hematological and composite inflammatory indices

Abbreviation	Full name	Formula
NLR	Neutrophil-to-lymphocyte ratio	NEU/LYM
PLR	Platelet-to-lymphocyte ratio	PLT/LYM
LMR	Lymphocyte-to-monocyte ratio	LYM/MON
dNLR	Derived neutrophil-to-lymphocyte ratio	NEU/(WBC-NEU)
SII	Systemic immune-inflammation index	(PLT×NEU)/LYM
SIRI	Systemic inflammation response index	(NEU×MON)/LYM
AISI	Aggregate index of systemic inflammation	(NEU×MON×PLT)/LYM
MPR	Mean platelet volume-to-platelet ratio	MPV/PLT
MPVLR	Mean platelet volume-to-lymphocyte ratio	MPV/LYM
RPR	Red cell distribution width-to-platelet ratio	RDW/PLT
PNI	Prognostic nutritional index	(10×Alb [g/dL])+(0.005×LYM [/µL])
NAR	Neutrophil-to-albumin ratio	NEU/Alb
PAR	Platelet-to-albumin ratio	PLT/Alb

NEU: Neutrophil, LYM: Lymphocyte, MON: Monocyte, PLT: Platelet, RDW: Red cell distribution width, MPV: Mean platelet volume, Alb: Serum albumin

The discriminatory ability of each index was evaluated using receiver operating characteristic (ROC) curve analysis; in addition, area under the curve (AUC), optimal cut-off values, sensitivity, specificity, positive predictive value, negative predictive value, and likelihood ratios (LR^+ and LR^-) were reported with 95% confidence intervals. Variables that remained significant in univariate analyses were subsequently included in a multivariable logistic regression model, adjusted for age, sex, hemoglobin, and albumin, to identify independent predictors of *H. pylori* positivity. A two-tailed p-value <0.05 was considered statistically significant.

In a subgroup of patients for whom a post-eradication hemogram was available in the hospital electronic records, a short-term within-patient comparison was conducted to evaluate the responsiveness of PLR and MPVLR following eradication. Because the distribution of paired differences deviated from normality (Shapiro-Wilk test), the Wilcoxon signed-rank test was applied to both indices, and effect sizes were summarized using Cliff's delta.

Results

Demographic and histopathological characteristics

A total of 453 children were included in the study, of whom 171 were *H. pylori* positive and 282 were *H. pylori* negative. The median age was 14.0 years (IQR 11.0-16.0) in the *H. pylori* positive group and 13.0 years (IQR 10.0-15.0) in the control group (difference: +1 year; 95% CI: -0.3 to +2.1; p=0.152). Sex distribution was comparable between the two groups (36.2% vs. 34.0% boys; p=0.545).

Among *H. pylori* positive patients, histopathological grading according to the Updated Sydney System demonstrated mild (17.5%), moderate (53.8%), and severe (28.7%) inflammation; mild (29.8%), moderate (50.3%), and severe (19.9%) activity; and mild (25.7%), moderate (47.4%), and severe (26.9%) bacterial density.

Hematological and biochemical parameters

There were no significant differences in hemoglobin, platelet count, MCV, mean corpuscular hemoglobin (MCH), MCH concentration, MPV, eosinophil count, or serum albumin levels between the groups (all p_FDR >0.05). In contrast, neutrophil, lymphocyte, monocyte, and RDW values were significantly higher in the *H. pylori* negative group (all p_FDR <0.05). The distribution of these differences is illustrated in Figure 1 using box-plot visualizations, and the detailed hematological and biochemical measurements are presented in Table 2.

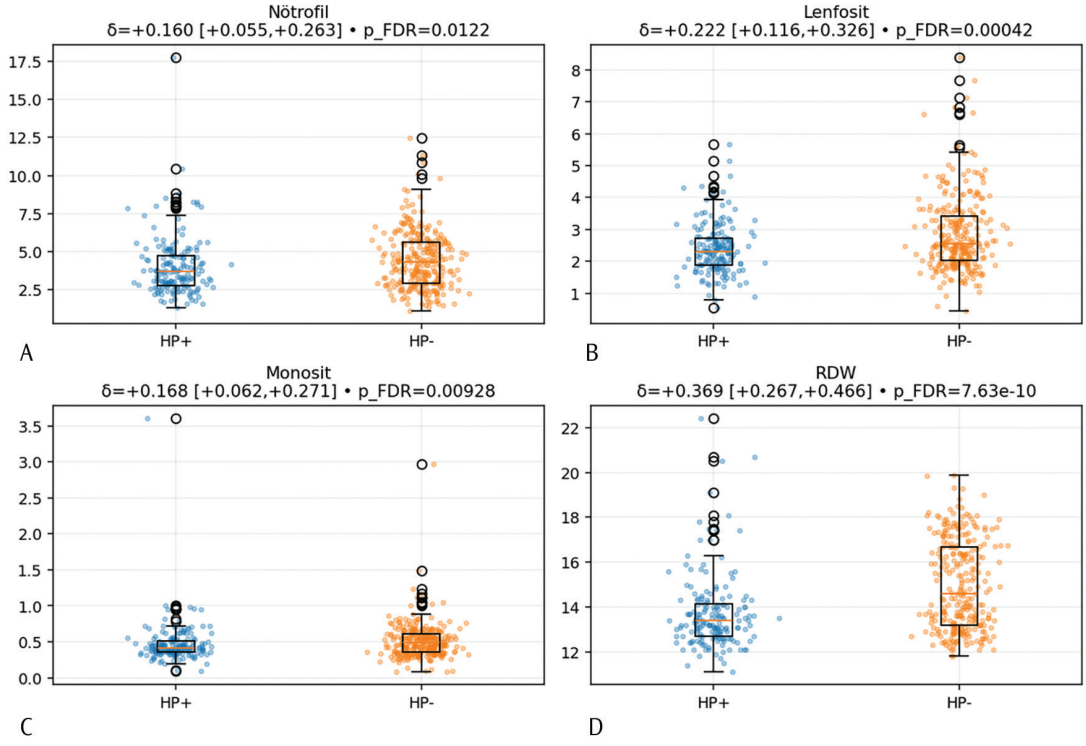

Figure 1. Hematological and biochemical parameters with significant differences

Boxplots showing hematological and biochemical parameters with significant intergroup differences between HP positive and HP negative groups: (A) Neutrophil, (B) Lymphocyte, (C) Monocyte, and (D) RDW. Boxes indicate interquartile ranges and median values, while individual jittered dots represent the distribution of observations. All p-values were adjusted for multiple comparisons using the Benjamini-Hochberg FDR method, and effect sizes are reported as Cliff's δ with 95% confidence intervals

FDR: False discovery rate, RDW: Red cell distribution width, HP: *Helicobacter pylori*

Table 2. Comparison of hematological and biochemical parameters between HP positive and HP negative groups

Parameter	HP positive (n=171)	HP negative (n=282)	Cliff's δ (95% CI)	p_FDR
Hb (g/dL)	13.40 (12.55-14.10)	13.40 (12.70-14.30)	+0.057 (-0.053 to +0.168)	0.427
Platelet (×10³/μL)	294.00 (255.00-338.00)	298.00 (259.00-350.00)	+0.042 (-0.069 to +0.152)	0.557
MCV (fL)	84.40 (80.40-87.95)	85.00 (81.50-88.20)	+0.055 (-0.054 to +0.160)	0.427
MCH (pg)	27.70 (26.00-29.00)	27.90 (26.50-29.10)	+0.066 (-0.046 to +0.175)	0.409
MCHC (g/dL)	32.60 (31.85-33.30)	32.80 (32.10-33.30)	+0.086 (-0.028 to +0.197)	0.232
MPV (fL)	10.20 (9.60-10.95)	10.20 (9.60-10.90)	-0.008 (-0.123 to +0.103)	0.891
Neutrophil (×10³/μL)	3.68 (2.77-4.76)	4.31 (2.93-5.62)	**+0.160 (+0.055 to +0.263)**	**0.012**
Lymphocyte (×10³/μL)	2.31 (1.88-2.73)	2.54 (2.04-3.42)	**+0.222 (+0.116 to +0.326)**	**0.0004**
Monocyte (×10³/μL)	0.41 (0.36-0.52)	0.49 (0.36-0.61)	**+0.168 (+0.062 to +0.271)**	**0.009**
Eosinophil (×10³/μL)	0.12 (0.07-0.21)	0.12 (0.06-0.21)	-0.013 (-0.126 to +0.098)	0.863
RDW (%)	13.40 (12.70-14.20)	14.60 (13.20-16.70)	**+0.369 (+0.268 to +0.466)**	**<0.0001**
Albumin (g/dL)	4.70 (4.50-4.80)	4.70 (4.50-4.90)	+0.030 (-0.079 to +0.136)	0.701

Values are presented as median (interquartile range). Statistical comparisons were performed using the Mann-Whitney U test
This table summarizes peripheral blood hematological and biochemical findings in the HP-positive and HP-negative (control) groups. Although hemoglobin, erythrocyte indices (MCV, MCH, MCHC), platelet count, MPV, eosinophil count, and albumin levels were comparable between the two groups, neutrophil, lymphocyte, monocyte, and RDW values were significantly higher in the HP-negative group
Hb: Hemoglobin, MCV: Mean corpuscular volume, MCH: Mean corpuscular hemoglobin, MCHC: Mean corpuscular hemoglobin concentration, MPV: Mean platelet volume, RDW: Red cell distribution width, HP: *Helicobacter pylori*, FDR: False discovery rate

Hematological indices

When hematological indices derived from CBC parameters were compared, PLR and MPVLR were significantly higher in the *H. pylori* positive group, whereas RPR, NAR and PNI were significantly higher in the *H. pylori* negative group (all p_FDR <0.05). Detailed comparative results are presented in Table 3, and representative distributions of the significant indices are illustrated in Figure 2. Although PLR and MPVLR values showed statistically significant differences between groups, the effect sizes were small, and therefore, their biological relevance should be interpreted with caution.

Among *H. pylori* positive patients, post-eradication hemogram data were available in the electronic hospital records for 36 patients, enabling a paired short-term evaluation. In this subgroup, neither PLR nor MPVLR showed a significant change following treatment. PLR decreased from a mean of 139.86 to 128.00 (mean difference -11.86; Wilcoxon W=305; p=0.870; Cliff's δ=-0.086), whereas MPVLR decreased from a mean of 4.754 to 4.477 (mean difference -0.277; Wilcoxon W=315; p=1.000; Cliff's δ=0.029). These findings indicate that only a small fraction of the *H. pylori* positive cohort had system-level post-eradication CBC follow-up data available; in this subset, no early measurable shift in PLR/MPVLR was observed.

Correlation between hematological parameters and histopathological findings

Spearman's correlation analysis demonstrated only weak and non-significant associations between the evaluated indices (NLR, PLR, LMR, SII, SIRI, AISI, MPVLR, MPR, RPR, NAR, PAR, and PNI) and *H. pylori* density, histological activity, or inflammation scores (all p>0.05). Similarly, conventional laboratory parameters such as RDW, MPV, and albumin showed no significant relationships with histopathological severity. The correlation coefficients (ρ) ranged from -0.10 to +0.23, indicating minimal effect sizes that were neither clinically nor statistically significant. These findings suggest that peripheral hematological and biochemical markers do not reliably reflect the histological severity or inflammatory activity of *H. pylori* associated gastritis in children; see Supplementary Figure S1.

ROC analysis

Exploratory ROC analysis showed that PLR and MPVLR had the highest, yet still modest, discriminative performance in identifying *H. pylori* infection, with AUC values around 0.60. Other indices, including NAR, RPR, and PNI, demonstrated poor diagnostic ability (AUC ≤0.43). Accordingly, the complete ROC curves are presented in the Supplementary Material (Supplementary Figure S2).

Discussion

In this study, we observed that both primary hematological parameters and CBC-derived inflammatory indices significantly differed between *H. pylori* positive and *H. pylori* negative children. The *H. pylori* positive group exhibited significantly higher PLR and MPVLR values, whereas neutrophil, lymphocyte, and monocyte counts were lower than those in controls. In contrast, RDW values were significantly higher in the *H. pylori* negative group, while hemoglobin and MCV levels remained comparable between the two groups.

Table 3. Comparison of hematological indices between HP positive and HP negative groups

Parameter	HP positive (n=171)	HP negative (n=282)	Cliff's δ (95% CI)	p_FDR
NLR	1.56 (1.12-2.23)	1.49 (1.11-2.13)	+0.017 (-0.093 to +0.125)	0.547
dNLR	0.86 (0.82-0.89)	0.87 (0.83-0.90)	+0.010 (-0.102 to +0.121)	0.491
LMR	5.41 (4.30-6.80)	5.58 (4.35-6.86)	+0.018 (-0.094 to +0.130)	0.485
SII	461.19 (334.60-692.72)	449.59 (322.94-629.40)	-0.008 (-0.119 to +0.103)	0.547
SIRI	0.65 (0.44-0.97)	0.71 (0.48-1.10)	+0.044 (-0.067 to +0.156)	0.485
AISI	186.94 (133.37-318.31)	218.10 (131.00-352.67)	+0.040 (-0.072 to +0.154)	0.491
MPR	0.03 (0.03-0.04)	0.03 (0.03-0.04)	+0.022 (-0.094 to +0.136)	0.603
PAR	63.83 (53.55-73.92)	63.71 (54.06-75.62)	+0.012 (-0.098 to +0.123)	0.870
PLR	127.45 (102.24-165.81)	113.50 (88.92-145.09)	**-0.205 (-0.308 to -0.098)**	**0.0004**
MPVLR	4.45 (3.57-5.70)	4.02 (3.02-5.05)	**-0.210 (-0.316 to -0.106)**	**0.0004**
RPR	0.05 (0.04-0.06)	0.05 (0.04-0.05)	**+0.152 (+0.044 to +0.259)**	**0.007**
NAR	0.76 (0.60-1.05)	0.91 (0.63-1.18)	**+0.150 (+0.045 to +0.256)**	**0.007**
PNI	58.60 (55.62-61.75)	60.25 (57.11-64.21)	**+0.229 (+0.122 to +0.330)**	**<0.001**

Values are presented as median (interquartile range). Statistical comparisons were performed using the Mann-Whitney U test. p-values were adjusted for multiple comparisons using the Benjamini-Hochberg FDR method, and effect sizes were reported as Cliff's δ with 95% confidence intervals. Bold p-values indicate statistically significant differences after FDR correction (p_FDR <0.05)

Among CBC-derived indices, PLR and MPVLR were significantly higher in the HP-positive group, while RPR, NAR, and PNI were significantly higher in the HP-negative group (all remained significant after FDR correction). No significant intergroup differences were observed for NLR, dNLR, LMR, SII, SIRI, AISI, MPR, or PAR

NLR: Neutrophil-to-lymphocyte ratio, dNLR: Derived neutrophil-to-lymphocyte ratio, PLR: Platelet-to-lymphocyte ratio, LMR: Lymphocyte-to-monocyte ratio, SII: Systemic immune-inflammation index, SIRI: Systemic inflammation response index, AISI: Aggregate index of systemic inflammation, MPVLR: Mean platelet volume-to-lymphocyte ratio, MPR: Mean platelet volume-to-platelet ratio, RPR: Red cell distribution width-to-platelet ratio, NAR: Neutrophil-to-albumin ratio, PAR: Platelet-to-albumin ratio, PNI: Prognostic nutritional index, HP: *Helicobacter pylori*, FDR: False discovery rate, CI: Confidence interval

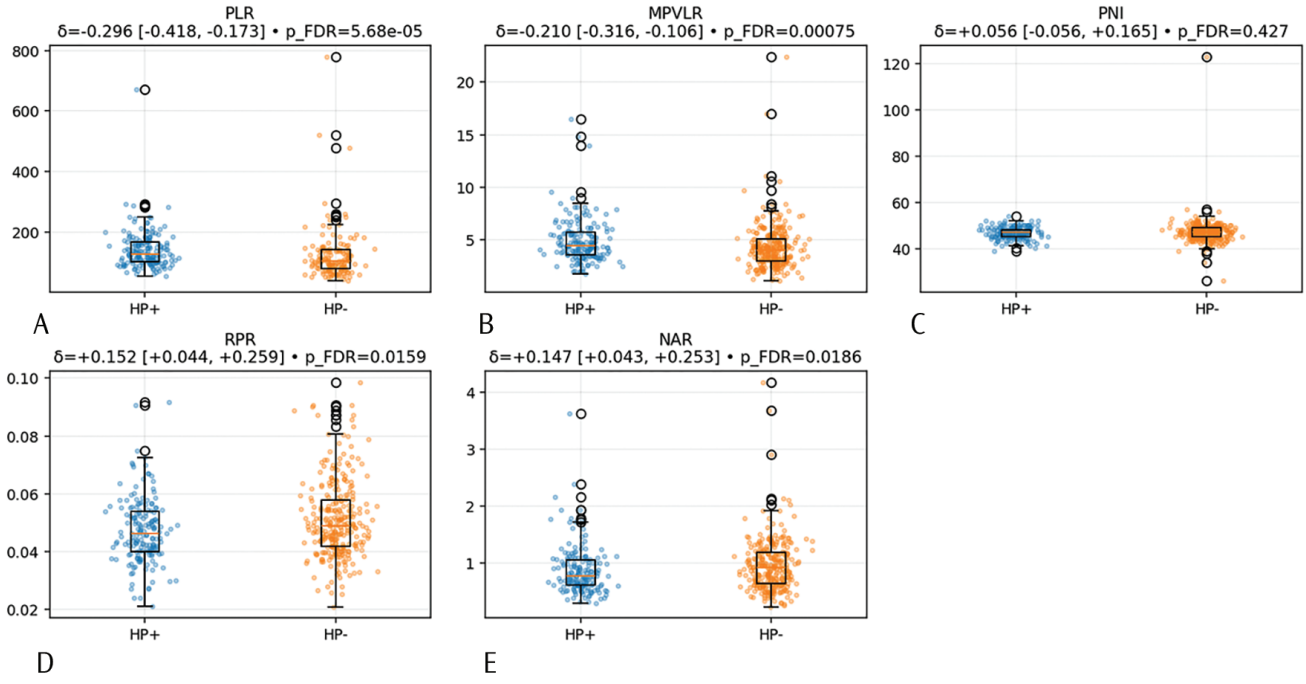

Figure 2. Significant hematological indices between HP positive and HP negative groups

Boxplots of hematological indices with significant intergroup differences between HP positive and HP negative groups: (A) PLR, (B) MPVLR, (C) PNI, (D) RPR, and (E) NAR. Boxes indicate interquartile ranges and medians; individual jittered dots show the distribution of observations. All p-values were adjusted for multiple comparisons using the Benjamini-Hochberg FDR method, and effect sizes are reported as Cliff's δ with 95% confidence intervals

PLR: Platelet-to-lymphocyte ratio, MPVLR: Mean platelet volume-to-lymphocyte ratio, RPR: Red cell distribution width-to-platelet ratio, NAR: Neutrophil-to-albumin, PNI: Prognostic nutritional index, HP: *Helicobacter pylori*, FDR: False discovery rate

During *H. pylori* infection, pro-inflammatory cytokines such as interleukin-1β (IL-1β), IL-6, tumor necrosis factor- α (TNF-α), and IL-8 are upregulated within the gastric mucosa, initiating a local immune response that subsequently influences hematopoietic pathways. Among these, IL-6-mediated upregulation of hepatic thrombopoietin enhances megakaryocyte activation and platelet production, whereas TNF-α and IL-8 promote lymphocyte recruitment to the site of inflammation, leading to a relative decline in peripheral lymphocyte counts (10). The combined effect of increased platelet activity and reduced lymphocyte levels translates into higher PLR and MPVLR values. Conversely, the absence of a pronounced neutrophil-dominant response and the predominantly low-grade, mucosa-restricted inflammatory pattern of *H. pylori* gastritis explain why neutrophil-weighted markers such as NLR did not differ significantly between groups. This pathophysiological mechanism may partially explain the lack of correlation between histopathological severity and hematological indices observed in our cohort, given that CBC-based markers reflect systemic inflammatory activity, whereas histopathology reflects strictly local inflammatory activity.

Previous studies assessing the relationship between *H. pylori* infection and hematological indices have yielded heterogeneous findings. Some reports have demonstrated elevated NLR, whereas others with larger sample sizes have found no meaningful differences in NLR or MPV. This heterogeneity is also evident across the limited pediatric literature, where some cohorts report mild elevations in CBC-derived indices while others demonstrate no significant systemic signal. The absence of a difference in NLR in our study aligns with the latter group and suggests that pediatric *H. pylori* infection may be characterized by a limited systemic inflammatory imprint without a dominant neutrophilic response. In contrast, the significant elevation in PLR parallels findings from studies emphasizing platelet-driven immune activation (11-13). Notably, the concomitant increase in MPVLR observed in our cohort appears to be the first reported evidence of this finding in the pediatric population, underscoring its potential relevance as a surrogate marker of platelet functional activation in this age group.

A key contribution of our study is the first demonstration that MPVLR is significantly elevated in pediatric *H. pylori* infection. In the adult literature, MPVLR has been proposed as a marker of pro-inflammatory activation in cardiovascular and autoimmune disorders; however, its clinical relevance in childhood disease has not previously been explored (14). The elevation of MPVLR in *H. pylori* positive children reflects the combined effect of enhanced platelet activation and reduced peripheral lymphocyte counts. This finding further supports the view that inflammation in childhood *H. pylori* infection is not neutrophil-dominant but rather is organized along a platelet-lymphocyte axis, which in turn reinforces the observed increase in PLR and suggests that MPVLR may serve as a marker of this pathway. Rather than indicating definitive systemic inflammation, our findings might reflect subtle hematological alterations associated with *H. pylori* infection and should be interpreted as hypothesis-generating.

Although an expanded RDW has been reported in conditions associated with gastric inflammation, it is noteworthy that RDW was higher in the *H. pylori* negative group in our cohort (15). This finding suggests that RDW is influenced more strongly by non-infectious factors, such as micronutrient status, dietary variation, or subtle alterations in erythropoiesis, than by serving as a reliable marker of the inflammatory response specific to *H. pylori*.

The absence of correlation between *H. pylori* density and hematological indices, according to the Sydney classification, further supports the notion that *H. pylori* infection in children is characterized by a predominantly local rather than systemic inflammatory response. A similar observation has been reported in adults, where hematological markers were able to reflect the presence of infection but not the histological severity of mucosal injury (16). This parallel reinforces the concept that these indices lack sufficient sensitivity to gauge the extent of mucosal damage in both pediatric and adult populations.

ROC analysis demonstrated that although PLR and especially MPVLR achieved statistical significance in discriminating *H. pylori* positivity, their diagnostic performance remained modest. AUC values hovering around 0.60 indicate that these markers are unlikely to serve as stand-alone diagnostic tools and should, at best be interpreted as adjunctive indicators. The post-hoc power analysis, which confirmed adequate statistical power for medium effect sizes (power ≈ 0.87), further supports the interpretation that the limited AUC values stem not from sample size constraints but from the intrinsically limited diagnostic capacity of these biomarkers.

A short-term paired analysis in the subgroup with available post-eradication CBCs likewise showed no significant reduction in PLR or MPVLR, indicating that these indices do not meaningfully improve in the early post-treatment period. This supports the interpretation that their utility is limited to cross-sectional detection rather than follow-up monitoring.

Among the main strengths of this study are its large sample size (n=453), the histopathological confirmation of *H. pylori* infection, and the exclusion of potential confounders such as active infection, immunosuppressive therapy, and systemic disease. Furthermore, the simultaneous assessment of multiple hematological and composite indices allowed for a comprehensive characterization of the systemic immune profile associated with *H. pylori* infection in children.

Study Limitations

However, several limitations should be considered. The retrospective, cross-sectional design precludes the establishment of causality. Moreover, the absence of additional

biomarkers, such as ferritin, iron indices, CRP, or cytokine panels, limited the biological interpretability of the hematological alterations. In our center, these biomarkers are not routinely collected prior to endoscopy, which limits their availability for analysis. Although this may reduce the granularity of systemic inflammatory profiling, the lack of intergroup imbalance in baseline measures such as body mass index, hemoglobin, and albumin suggests that any residual confounding is likely minimal. Additionally, *H. pylori* infection was diagnosed solely on the basis of histopathological findings. Although standardized antral and corpus sampling enhances diagnostic accuracy, the absence of a second confirmatory invasive test, such as a rapid urease test or culture, as recommended by the current ESPGHAN and NASPGHAN guidelines, may have resulted in diagnostic misclassification in cases with low bacterial density, which could have biased the associations observed in this study toward the null. Finally, the control group consisted of children undergoing endoscopy for dyspeptic symptoms rather than completely healthy subjects; non-specific markers, such as RDW, may have been influenced by factors unrelated *to H. pylori*.

Conclusion

From a clinical perspective, CBC-derived indices such as PLR and MPVLR may reflect subtle hematological alterations associated with *H. pylori* infection; however, given their low discriminative performance, they cannot serve as diagnostic tools and should be interpreted with caution. These indices may provide supportive information during preliminary assessment, but cannot replace histopathological confirmation via endoscopy or biopsy. Prospective studies incorporating post-eradication follow-up could better elucidate the temporal dynamics of these hematological markers, while the integration of data on iron metabolism, nutritional indices, and cytokine profiles would help delineate the true systemic boundaries of *H. pylori*-associated inflammation in children.

Our findings indicate that pediatric *H. pylori* infection may be associated with subtle hematological alterations, particularly in platelet- and lymphocyte-related indices. These changes likely reflect a mild and predominantly mucosa-restricted inflammatory response rather than definitive systemic inflammation. Although PLR and MPVLR demonstrated statistically significant differences between groups, their limited discriminative accuracy precludes any diagnostic application. Therefore, these markers should be considered exploratory and hypothesis-generating rather than clinically actionable parameters. Prospective studies incorporating systemic inflammatory biomarkers and post-eradication follow-up are required to clarify whether such hematological alterations have meaningful clinical implications for this population.

Ethics

Ethics Committee Approval: The study protocol was reviewed and approved by the University of Health Sciences Türkiye, Gülhane Scientific Research Ethics Committee (approval no: 2025-417, date: 30.09.2025).

Informed Consent: This retrospective study.

Footnotes

Authorship Contributions

Concept: Y.M.E., Design: Y.M.E., S.T., Data Collection or Processing: Y.M.E., S.T., Analysis or Interpretation: Y.M.E., S.T., Literature Search: Y.M.E., Writing: Y.M.E., S.T.

Conflict of Interest: The authors declared no conflict of interest.

Financial Disclosure: The authors declared that this study received no financial support.

Supplementary Figures: https://d2v96fxpocvxx.cloudfront.net/688d2d00-d207-464d-89b6-73f393f4f50c/content-images/696c2741-2bb7-4a3a-87c1-6ea82a52a3ce.pdf

References

1. Seo JH, Bortolin K, Jones NL. Review: Helicobacter pylori infection in children. *Helicobacter*. 2020;25 (Suppl 1):e12742.
2. Manfredi M, Ravikumara M. Helicobacter pylori infection in children: to eradicate or not to eradicate? *Helicobacter*. 2024;29(6):e70002.
3. Săsăran MO, Meliț LE, Dobru ED. MicroRNA modulation of host immune response and inflammation triggered by *Helicobacter pylori*. *Int J Mol Sci.* 2021;22(3):1406.
4. Helmin-Basa A, Wiese-Szadkowska M, Szaflarska-Popławska A, Kłosowski M, Januszewska M, Bodnar M, et al. Relationship between *Helicobacter pylori* infection and plasmacytoid and myeloid dendritic cells in peripheral blood and gastric mucosa of children. *Mediators Inflamm.* 2019;2019:7190596.
5. Moosmann J, Krusemark A, Dittrich S, Ammer T, Rauh M, Woelfle J, et al. Age- and sex-specific pediatric reference intervals for neutrophil-to-lymphocyte ratio, lymphocyte-to-monocyte ratio, and platelet-to-lymphocyte ratio. *Int J Lab Hematol.* 2022;44(2):296-301.
6. Lucero Y, Lagomarcino AJ, Torres JP, Roessler P, Mamani N, George S, et al. Helicobacter pylori, clinical, laboratory, and noninvasive biomarkers suggestive of gastric damage in healthy school-aged children: a case-control study. *Int J Infect Dis.* 2021;103:423-430.
7. Săsăran MO, Meliţ LE, Mocan S, Ghiga DV, Dobru ED. Pediatric gastritis and its impact on hematologic parameters. *Medicine (Baltimore).* 2020;99(35):e21985.
8. Homan M, Jones NL, Bontems P, Carroll MW, Czinn SJ, Gold BD, et al. Updated joint ESPGHAN/NASPGHAN guidelines for management of Helicobacter pylori infection in children and adolescents (2023). *J Pediatr Gastroenterol Nutr.* 2024;79(3):758-785.

9. Dixon MF, Genta RM, Yardley JH, Correa P. Classification and grading of gastritis. The updated Sydney System. International workshop on the histopathology of gastritis, Houston 1994. *Am J Surg Pathol.* 1996;20(10):1161-1181.

10. Meliţ LE, Mărginean CO, Săsăran MO, Mocan S, Ghiga DV, Bogliş A, et al. Innate immunity - the hallmark of *Helicobacter pylori* infection in pediatric chronic gastritis. *World J Clin Cases*. 2021;9(23):6686-6697.

11. Meliţ LE, Mărginean MO, Mocan S, Mărginean CO. The usefulness of inflammatory biomarkers in diagnosing child and adolescent's gastritis: STROBE compliant article. *Medicine (Baltimore).* 2019;98(26):e16188.

12. Sahin Y, Gubur O, Tekingunduz E. Relationship between the severity of Helicobacter pylori infection and neutrophil and lymphocyte ratio and mean platelet volume in children. *Arch Argent Pediatr.* 2020;118(3):e241-e245. English, Spanish.

13. Yalın EA, Kayataş K. Investigation of neutrophil to lymphocyte ratio and platelet to lymphocyte ratio parameters in chronic gastritis with Helicobacter pylori. *Haydarpasa Numune Med J*. 2022;62(3):342-345.

14. Niu MH, Liu PH, Liu ZH, Zhu JW, Guo R, He F. The relationship between mean platelet volume lymphocyte ratio and collateral circulation in patients with chronic total coronary occlusion. *Front Cardiovasc Med.* 2022;9:1008212.

15. Goyal H, Lippi G, Gjymishka A, John B, Chhabra R, May E. Prognostic significance of red blood cell distribution width in gastrointestinal disorders. *World J Gastroenterol.* 2017;23(27):4879-4891.

16. Guclu M, Faruq Agan A. Association of severity of *Helicobacter pylori* infection with peripheral blood neutrophil to lymphocyte ratio and mean platelet volume. *Euroasian J Hepatogastroenterol.* 2017;7(1):11-16.

DOI: 10.4274/gulhane.galenos.2026.65668
Gulhane Med J 2026;68(2):118-126

Short-term effects of +Gz exposure on respiratory functions: results from human centrifuge training

Abdurrahman Engin Demir[1], Menduh Savaş İlbasmış[2], Nuran Küçük[3], Şükrü Hakan Gündüz[1], Cantürk Taşçı[4]

[1]*University of Health Sciences Türkiye, Institute of Defensive Health Sciences, Department of Aerospace Medicine, Ankara, Türkiye*
[2]*University of Health Sciences Türkiye, Kayseri City Hospital, Clinic of Aerospace Medicine, Kayseri, Türkiye*
[3]*Aeromedical Research and Training Center, Eskişehir, Türkiye*
[4]*University of Health Sciences Türkiye, Gülhane Training and Research Hospital, Clinic of Pulmonary Diseases, Ankara, Türkiye*

Cite this article as: Demir AE, İlbasmış MS, Küçük N, Gündüz ŞH, Taşçı C. Short-term effects of +Gz exposure on respiratory functions: results from human centrifuge training. *Gulhane Med J.* 2026;68(2):118-126.

Date submitted:
23.09.2025
Date accepted:
29.01.2026
Epub:
11.06.2026
Publication Date:
16.06.2026

Corresponding Author:
Asst. Prof. Abdurrahman Engin Demir, University of Health Sciences Türkiye, Institute of Defensive Health Sciences, Department of Aerospace Medicine, Ankara, Türkiye
aengindmr@hotmail.com

ORCID:
orcid.org/0000-0003-0949-1734

Keywords: +Gz accelerations, respiratory functions, hypergravity, high G, pulmonary system

ABSTRACT

Aims: Military jet pilots are mandated to undergo human centrifuge training (HCT) to experience the adverse effects of +Gz acceleration during flight. The present study aimed to analyze short-term respiratory changes following +Gz exposure via pulmonary function testing (PFT) among jet pilots.

Methods: This single-center, cross-sectional study was conducted among healthy military jet pilots. Participants were classified as smokers or non-smokers. Each participant underwent PFTs immediately before and after the HCT. Forced vital capacity (FVC), forced expiratory volume in 1 second (FEV_1), FEV_1/FVC, maximal voluntary ventilation (MVV), peak expiratory flow rate (PEFR), and forced expiratory flow at 25-75% ($FEF_{25-75\%}$) have been measured. The participants' PFT parameters were evaluated to assess potential +Gz-related alterations.

Results: The study included 21 male pilots with a mean age of 27.95±3.60 years. Ten (47.6%) pilots were active smokers. After HCT, significant improvements were observed in the mean values of FEV_1 (4.45±0.55 vs. 4.55±0.57, p=0.001), FEV_1/FVC (80.0±0.6 vs. 83.0±0.7, p=0.002), $FEF_{25-75\%}$ (4.72±1.43 vs. 4.96±1.52, p=0.007), and MVV (169.3±28.6 vs. 181.5±32.4, p=0.002); however, no significant changes were observed in FVC or PEFR (p>0.05). Among smokers, significant post-training improvements were observed in FEV_1, the FEV_1/FVC ratio, and PEFR (p<0.05), whereas no significant changes were detected in FVC, $FEF_{25-75\%}$, or MVV (p>0.05). In non-smokers, significant increases were observed in FEV_1, FEV_1/FVC, and MVV (p<0.05), while the remaining parameters showed no significant changes.

Conclusions: This study revealed that +Gz exposure was associated with short-term improvements in expiratory flow parameters and effort-dependent ventilatory performance in jet pilots. Additionally, subgroup analysis demonstrated that smokers predominantly exhibited significant increases in flow-dependent parameters.

Introduction

While the human physiology is well-suited to a gravity of 1 G (9.8 m/s^2), it is barely adapted to cope with numerous unusual conditions during flight, including discrete flight maneuvers that create "G" forces with varying amplitudes and directions. The +Gz force, generated during an inside loop maneuver, is a force experienced from the head to the feet, resulting in a downward displacement of intrathoracic and intra-abdominal organs and the redistribution of bodily fluids. In the initial moments of elevated +Gz, arterial blood pressure declines due to a decrease in total peripheral resistance induced by passive dilation of the lower extremity arteries and a reduction in venous return due to venous dilation. Stimulation of baroreceptors triggers sympathetic activation within 6-10 seconds, leading to an increase in arterial blood pressure due to elevated heart rate and peripheral resistance. This adjustment requires a few additional seconds at cardiac level compared with sympathetic activation. A delay during high +Gz loads (up to 9 G) results in an acute reduction of cerebral blood flow, which eventually results in a temporary condition of unconsciousness, G-induced loss of consciousness (G-LOC) (1,2). These effects may pose a significant risk during flight, potentially leading to incapacitation and jeopardizing flight safety.

During air combat maneuvers with high-performance aircraft, such as the F-16, Jet pilots are generally exposed to forces of +7 to +9 Gz for about 5-10 seconds and to levels beyond +5 Gz for over one minute. A significant quantity of medical incapacitations and military jet accidents has resulted from the hazardous effects of G-forces, especially during high-performance missions that involve maneuvers characterized by rapid onset and sustained high G levels (3,4). +Gz additionally causes various adverse effects including respiratory impairments and musculoskeletal injuries (1). To raise pilots' awareness of these G-related consequences, a ground-based human centrifuge training (HCT) platform with a free-swinging gondola is used to generate +Gz by rotational motion (Figure 1). During this training, pilots are taught how to cope with the hazardous physiological effects of G forces.

+Gz alone has various effects on the pulmonary system, potentially causing alterations in lung volume and capacities. A rise of about 500 mL is observed at +3 Gz. Total lung capacity and vital capacity remain unchanged at accelerative forces up to +3 Gz; however, they undergo a 15% decline when accelerative forces exceed +5 Gz. The diaphragm and intra-abdominal organs also descend, which results in a rise in the functional residual capacity (6). Increased +Gz exposure also improves respiratory efforts and minute ventilation (7,8). Acceleration of +5 Gz may cause a 5 cm reduction in the heart and diaphragm level (2). To achieve effective respiration and adequate cerebral perfusion under high +Gz load, pilots execute the Anti-G Straining Maneuver (AGSM), which involves a rapid inspiration lasting less than one second, a forceful expiration against a partially closed glottis, and simultaneous contraction of all abdominal and limb muscle groups. Each respiratory cycle last for 2.5-3.0 seconds, providing the stability of intrathoracic pressure and respiratory regulation, thereby mitigating the negative respiratory effects of acceleration while supporting cardiovascular responses to increased +Gz. The anti-G suit provides another protective measure against +Gz. The suit provides full bladder coverage around the lower extremities and abdomen, inflating in response to increasing +Gz to apply pneumatic pressure that minimizes pooling of blood in the limbs (2). The inflation of the abdominal component additionally prevents the descent of the diaphragm to ensure adequate respiration (2,9). Contrary to the alterations

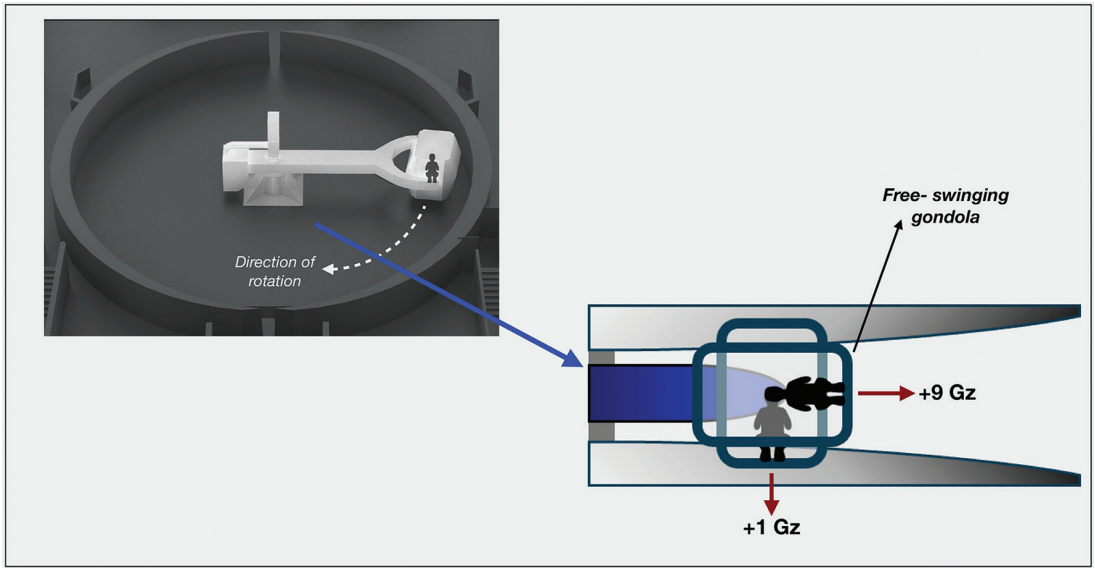

Figure 1. Human centrifuge training device. The device has a free-swinging gondola and is capable of producing high acceleration forces of up to 9 Gs [Adapted from the author's previously published presentation (5)]

caused by +Gz alone, vital capacity, functional residual capacity, and tidal volume have been shown to decline with the inflation of anti-G suit due to its restrictive mechanism (10,11). As is seen, hypergravity independently, as well as in conjunction with anti-G suit compression and AGSM, generates various physiological alterations within the respiratory mechanics.

While most of the research has focused on the changes occurring during high +Gz exposure (6,7,8,10,11), there is a lack of information about the persistence of these changes following the exposure. In this study, we aimed to analyze respiratory alterations immediately after exposure to +Gz acceleration using pulmonary function testing (PFT) in jet pilots.

Methods

Study design and participants

This single-center, cross-sectional study included military jet pilots who attended HCT at the Aeromedical Research and Training Center between December 2023 and March 2024.

The inclusion criteria were active military jet pilots who attended HCT and who consented to participate in the study. All these pilots were assessed to be in optimal health, having been deemed medically fit for flight duties and HCT following comprehensive aeromedical examinations (12). The exclusion criterion was the refusal to attend. Additionally, pilots who were unable to complete the HCT protocol and therefore did not experience the anticipated +Gz exposure were excluded from the post-training PFT. A total of 22 military jet pilots were enrolled in the study. One pilot suffered G-LOC during the training. The training was immediately stopped, and the HCT was rescheduled for another date. The pilot was excluded from the study procedures and post-training PFTs due to his incomplete HCT. Consequently, the PFT parameters of 21 pilots were measured both prior to and following HCT, and the statistical analysis was conducted on these pilots who completed the HCT and PFTs.

Ethical approval was taken from the University of Health Sciences Türkiye, Gülhane Training and Research Hospital (approval number: 2023/265, date: 22.11.2023). The study was conducted in accordance with the principles of the Declaration of Helsinki. Participants in the study provided informed consent after receiving thorough information via the consent forms.

Study protocol

Before PFT, a basic questionnaire was applied for collecting data, involving age, sex, height and weight, history of medication, and smoking status. A pilot was identified as a smoker who had smoked a minimum of 100 cigarettes in their lifespan and smoked regularly in the period of 30 days before the centrifuge training. A non-smoker was identified as an individual who had not smoked within the thirty days before the training day, had not consumed 100 cigarettes in their lifetime, or smoked over 100 cigarettes in their lifespan but had not smoked in the last 30 days (13).

The PFTs were performed using the Quark PFT device (Cosmed, Rome, Italy). An experienced technician conducted PFTs for each pilot in a sitting position. Just before (pre-training) and immediately after (post-training) the HCTs, each pilot performed PFTs. Forced vital capacity (FVC), forced expiratory volume in 1 second (FEV_1), FEV_1/FVC, maximal voluntary ventilation (MVV), peak expiratory flow rate (PEFR), and forced expiratory flow at 25-75% ($FEF_{25-75\%}$) values were measured and recorded. Pilots met the standardization requirements by performing a minimum of three PFT cycles, and the most accurate cycle was evaluated (14). The PFT unit and the HCT platform were adjacent within the same facility. Therefore, the pilots were immediately transferred to the PFT unit following the HCT, and PFTs were performed without delay.

The HCT protocol consisted of three profiles: the initial profile involved a +4.0 Gz load, starting from baseline with an onset rate of 0.1 $G \cdot s^{-1}$. The following profile included a +4.5 Gz load, administered at an onset rate of 3 $G \cdot s^{-1}$, and maintained for a 30-sec peak. The last profile included a +7.0 Gz load, administered at an onset rate of 3 $G \cdot s^{-1}$, and maintained for a 15-sec peak. Each pilot completed the training successfully, did not experience any G-related alterations, and had no pathological symptoms. Pre- and post-training PFT values were statistically compared.

Statistical Analysis

Statistical analysis was performed using IBM SPSS Statistics for Windows, version 29 (IBM Corp., Armonk, NY, USA). The Shapiro-Wilk test was utilized to determine the normality of numerical data. For within-group comparisons of pre- and post-training pulmonary function test parameters, paired t-tests were applied to normally distributed variables, while the Wilcoxon signed-rank test was applied to non-normally distributed variables. Changes in mean post-pre-training values were compared between smokers and non-smokers using Independent Samples t-tests or Mann-Whitney U tests, depending on the distribution of the data. Categorical variables were presented as percentages and frequencies. A p-value of less than 0.05 was considered statistically significant, and the data were evaluated at a 95% confidence level.

Results

Demographics and clinical measures

The mean ± standard deviation age of the 21 pilots was 27.95±3.60 years. After HCT, significant improvements were observed in the mean values of FEV_1 (4.45±0.55 vs. 4.55±0.57, p=0.001), FEV_1/FVC (80.0±0.6 vs. 83.0±0.7, p=0.002), $FEF_{25-75\%}$ (4.72±1.43 vs. 4.96±1.52, p=0.007), and MVV (169.3±28.6 vs.

181.5±32.4, p=0.002). No significant changes were observed in FVC or PEFR (p>0.05) (Table 1).

Among smokers, significant post-training improvements were observed in the mean values of FEV_1 (4.35±0.47 vs. 4.42±0.45, p=0.012), FEV_1/FVC (80%±0.06 vs. 83%±0.06, p=0.007), and PEFR (9.48±1.10 vs. 10.10±1.45, p=0.032), whereas no significant changes were detected in FVC, $FEF_{25-75\%}$, or MVV (p>0.05). In non-smokers, significant increases were observed in FEV_1 (4.54±0.61 vs. 4.68±0.67, p=0.008), FEV_1/FVC (80%±0.6 vs. 83%±0.7, p=0.05), and MVV (175.7±36.0 vs. 190.1±37.8, p=0.01), while the remaining parameters showed no significant changes.

No statistically significant differences were observed in the magnitude of pre-post training changes for FVC, FEV_1, FEV_1/FVC, $FEF_{25-75\%}$, PEFR, or MVV between smokers and non-smokers (all p>0.05).

Intragroup comparisons

Ten (47.6%) pilots were active smokers. The analysis comparing PFT values between smokers and non-smokers revealed distinct PFT response patterns to HCT. Among smokers, significant post-training improvements were observed in FEV_1, FEV_1/FVC ratio, and PEFR, while FVC, $FEF_{25-75\%}$, and MVV exhibited non-significant increases. Within non-smokers, significant increases were observed in FEV_1, FEV_1/FVC, and MVV; other variables exhibited no significant alteration (Table 2).

Discussion

This study suggests that short-term exposure to +Gz is correlated with rapid improvements in specific PFT measures in healthy military jet pilots. The observed changes in FEV_1, FEV_1/FVC, $FEF_{25-75\%}$, and MVV, primarily involving expiratory flow parameters and effort-sensitive lung volumes, reveal that high +Gz exposure induces temporary functional changes in

Table 1. Pulmonary function parameters measured before and after human centrifuge training among 21 pilots

Parameters	Pre-training	Post-training	p
FVC (L), mean ± SD	5.51±0.59	5.59±0.59	0.767
FEV_1 (L), mean ± SD	4.45±0.55	4.55±0.57	**0.001***
FEV_1/FVC (%), mean ± SD	80±0.6	83±0.7	**0.002****
PEFR (L/sec), mean ± SD	10.12±1.63	10.33±1.4	0.237
$FEF_{25-75\%}$ (L/sec), mean ± SD	4.72±1.43	4.96±1.52	**0.007****
MVV (L/min), mean ± SD	169.3±28.6	181.5±32.4	**0.002****

*: Wilcoxon signed-rank test, **: Paired t-test
FVC: Forced vital capacity, SD: Standard deviation, FEV_1: Forced expiratory volume in 1 second, PEFR: Peak expiratory flow rate, $FEF_{25-75\%}$: Forced expiratory flow at 25-75%, MVV: Maximal voluntary ventilation

Table 2. Comparison of pre- and post-training pulmonary function test parameters and magnitude of change among smoker and non-smoker pilots

Parameters	Group	Pre-training	Post-training	p1	p2
FVC (L), mean ± SD	s	5.39±0.43	5.33±0.44	0.386	0.372
	ns	5.63±0.71	5.64±0.69	0.722	
FEV_1 (L), mean ± SD	s	4.35±0.47	4.42±0.45	**0.012***	0.289
	ns	4.54±0.61	4.68±0.67	**0.008****	
FEV_1/FVC (%), mean ± SD	s	80±0.06	83±0.06	**0.007***	0.982
	ns	80±0.6	83±0.7	0.05	
PEFR (L/sec), mean ± SD	s	9.48±1.10	10.10±1.45	**0.032***	0.051
	ns	10.70±1.86	10.53±1.39	0.657	
$FEF_{25-75\%}$ (L/sec), mean ± SD	s	4.65±1.44	4.91±1.45	0.074	0.307
	ns	4.79±1.50	5.00±1.64	0.083	
MVV (L/min), mean ± SD	s	162.3±16.6	172±23.6	0.059	0.613
	ns	175.7±36.0	190.1±37.8	**0.010***	

*: Paired t-test, **: Wilcoxon signed-rank test
p1: Within-group comparison between pre-training and post-training values (paired analysis)
p2: Between-group comparison of mean post-pre training values among smokers and non-smokers
FVC: Forced vital capacity, SD: Standard deviation, s: Smoker, ns: Non-smoker, FEV_1: Forced expiratory volume in 1 second, PEFR: Peak expiratory flow rate, $FEF_{25-75\%}$: Forced expiratory flow at 25-75%, MVV: Maximal voluntary ventilation

respiratory dynamics. Furthermore, significant improvements have been observed in expiratory flow-related parameters, particularly FEV_1 and FEV_1/FVC, in both smokers and non-smokers, along with a substantial increase in MVV among non-smokers and in PEFR among smokers.

In our study, FEV_1, FEV_1/FVC, $FEF_{25-75\%}$, and MVV exhibited significant improvements, while FVC and PEFR demonstrated non-significant increases following HCT. These parameters are considered as effort-sensitive lung volumes, which are primarily determined by physical exertion, expiratory muscle strength, and air flow rate (15,16). Exposure to +Gz and performing AGSM can be considered as a form of physical exercise since it requires strong muscular effort and circulatory stress, resulting in higher levels of oxygen consumption and lactate generation in a short time, both of which are characteristic indicators of physical activity (17). The observed increase in plasma adrenaline levels during +Gz exposure was interpreted as indicative of the excessive physical exertion associated with hypergravity conditions (18). High +Gz load has also been shown to affect lung stretch receptors, regulating cardiovascular responses and enhancing respiratory dynamics, as well as increasing breathing effort through deeper and more rapid breathing cycles and a rise in minute ventilation (2,7,11). The AGSM involves a quick and deep inspiratory gasp and an expiration phase after the forced expiration stage, thereby serving as a short, intense physical exertion, which is suggested to improve pulmonary functions and cause larger lung volumes throughout this period (19,20). The anti-G suit concurrently exerts additional restrictions, causing physical strain (10,11). All these alterations eventually boost sympathetic response which in turn impacts respiratory dynamics inducing bronchodilation and thereby improving the ventilatory process (2). However, these physiological conditions alter immediately upon cessation of +Gz exposure. Upon the completion of +Gz loading and the deflation of the anti-G suit, external pressure is alleviated, resulting in a decline in stress levels and a rapid restoration of chest wall mobility to baseline levels. During this post-exposure period, the physical burden diminishes, while the physiological activation induced by +Gz load may persist. Miyamoto et al. observed increases in adrenaline and noradrenaline levels during and after a 1-minute exposure to +5 Gz, with a sustained increase lasting for 110 seconds post-exposure (18). In order to benefit from the short-term G tolerance gain induced by catecholamines, pilots are advised to execute maneuvers that generate short-term G exposures before conducting high-G maneuvering (21). A study evaluating pulmonary functions via impulse oscillometer revealed a significant decrease in small-airway resistance and the reactance area, indicating the stiffness or flexibility of the airways following high-Gz exposure (22). In the same study, these findings have been linked to a temporary increase in intrathoracic pressure during AGSM, which momentarily dilates and expands the small airways—offering a probable physiological rationale for the increases in FEV_1, FEV_1/FVC, $FEF_{25-75\%}$, and MVV observed in our study. Therefore, the elevated +Gz levels in our HCT protocol likely resulted in a short-term improvement in G tolerance via catecholamines, which in turn led to enhanced airway capacity, increased muscular effort, slight bronchodilation, and increased motivation, all of which caused a prolonged increase in respiratory dynamics following HCT.

Besides catecholamines, increased levels of serum cortisol have also been observed during +Gz exposure (23), mirroring those encountered during physical exercise and training (24,25). Any kind of stress triggers a cascade of physiological reactions, including an increase in heart rate due to the baroreceptor response- and cortisol levels in the blood (24). Although it takes longer than the baroreceptor reaction does, the endocrine response appears to play a greater role as G exposure intervals increase. Cortisol secretion was indicated to be “dose-dependent,” implying that increased +Gz acceleration correlates with higher cortisol release (26). Substantial data indicate that even short periods of vigorous resistance exercises can induce an immediate rise in blood cortisol levels that continues following exercise (27,28). Various research indicates that salivary cortisol levels significantly increase 15 to 30 minutes following brief +Gz exposures of around 6 +Gz lasting less than 1 minute (29,30). Given that +Gz exposure constitutes a form of physical exertion and that various hormone levels rise rapidly following intense physical activity, transient hormonal increases may have influenced post-training PFT outcomes in our study. The present study did not acquire hormonal measures or blood samples; thus, no endocrine inferences could be derived from our findings. The hormonal mechanisms discussed are conjectural, rely entirely on existing research detailing physiological responses to hypergravity and strenuous physical activity, and help to explain the observed pulmonary alterations following exposure, rather than to establish a proven causal relationship. Further studies utilizing repeated endocrine biomarkers with subsequent pulmonary evaluations would be helpful to find out if hormonal responses significantly influence pulmonary dynamics following HCT.

Subgroup analysis indicated that HCT provided small but significant increases in expiratory metrics, especially FEV_1 and FEV_1/FVC for both smokers and non-smokers, MVV considerably increased just in non-smokers, and PEFR in smokers. Considering the physiological similarities between +Gz loading and physical exertion, the current literature does not specifically compare the impact of smoking status on PFT alterations with respect to +Gz exposure, although it supports such a comparison in the context of physical exertion. While smoking was shown to have significant effects on the PFT parameters, indicating airflow restriction (FEV_1, FEV_1/FVC, PEFR, etc.) (31,32), respiratory muscle training and physical

exercise have been demonstrated to improve pulmonary functions among smokers. A study involving both smokers and non-smokers participating in an 8-week respiratory muscle training program revealed substantial improvements in basic spirometry measurements -FVC, FEV_1, PEF, and FEV_1/FVC- with smokers exhibiting greater increases in FEV_1/FVC (33). In another study, smokers who underwent six weeks of pulmonary muscle training had notable improvements in FVC, although starting with lower baseline levels compared to non-smokers, who demonstrated considerable improvements in FEV_1 (34). While smoking is linked to progressive and mostly irreversible airflow restriction, especially in chronic obstructive pulmonary disease (COPD) (35), the observed increases in FEV_1, FEV_1/FVC, and PEFR values among smokers may be said to indicate temporary and acute physiological modifications of airway functions that are triggered by sympathetic stimulation and effort-dependent respiratory mechanics, instead of structural airway alterations related to smoking. Additionally, the study cohort consisted of young, healthy, active pilots without any pulmonary disease (e.g., COPD), suggesting preserved basal respiratory reserve despite smoking. On the other hand, the MVV improvement observed in non-smokers may be indicative of a more enhanced baseline pulmonary reserve (36). Moreover, MVV is strongly influenced by respiratory muscle strength (37), and short-term high +Gz exposure might have functioned as a strong ventilatory stimulant, rapidly improving the efficacy of the ventilatory muscle and expiratory flow efficiency. Therefore, it is likely that the higher MVV increases among non-smokers may be said to demonstrate improved ventilatory muscle function on a normal airway background, while significant improvements in effort-dependent flow metrics in smokers indicate a temporary restoration of impairment in small airways due to smoking.

The long-term effects of repetitive or extended +Gz exposure have primarily been studied concerning cardiovascular functions (38,39), however, there is a lack of research specifically assessing whether repeated +Gz exposure results in cumulative improvements, fatigue-related impairments, or morphological alterations in the respiratory system. Although exposure to high +Gz likely results in significant improvements in effort-dependent flow metrics, airway capacity, and muscular effort, such exposure generally lasts for very short periods of 5 to 15 seconds, with prolonged durations barely exceeding 20 to 30 seconds and total cumulative exposure mostly not exceeding five minutes due to structural, operational, and physiological restrictions during aerial combat maneuvers in each sortie (1,2). On the other hand, considering the physiological similarities between high +Gz loads and intense physical activity, recurrent high-intensity physical exercise may induce respiratory muscle fatigue within minutes (40,41). It was shown that diaphragmatic fatigue develops in after just eight to ten minutes of high respiratory need with full-body exercise at or near peak effort (VO_2max >85%) and that both inspiratory and expiratory muscles become significantly fatigued several minutes after sustained excessive ventilation, which reduces the capacity for exercise and changes breathing patterns (40,42). In such a healthy population, these short exposure periods of high +Gz load appear inadequate to induce significant respiratory muscle fatigue that could lead to clinically relevant respiratory incapacitation, and are more likely to result in just mild, temporary fatigue levels as scientifically confirmed fatigue of the respiratory system typically needs longer periods of prolonged high ventilatory effort (1). Nonetheless, given the transient autonomic and hormonal responses that are likely to cause temporary changes in spirometry measurements following exposure, these alterations might be considered as acute physiological adaptations rather than actual improvements in the respiratory system. Consequently, it might be suggested that these improvements could obscure any underlying respiratory issue, especially among those with reduced pulmonary reserve, such as smokers or those with pre-existing subclinical airflow restrictions, whose impairments might only be observed under repeated stress or extended ventilatory exertion. While single episodes of high +Gz load are short-lasting, the cumulative mechanical strain on the respiratory system resulting from multiple exposures in a single sortie could otherwise unmask insidious physiological constraints which are not apparent following a single maneuver. In addition to +Gz, Pollock et al. (43) investigated the transient aftereffects of +Gx using a human centrifuge. Their findings revealed that sustained exposure to high-Gx acceleration- a force experienced from the chest to the back- during commercial suborbital spaceflight might cause substantial and rapidly developing respiratory mechanical stress, even in healthy individuals. This was stated to suggest that any temporary improvements observed in spirometry measurements could obscure underlying respiratory issues in individuals with medical conditions, such as coexisting cardiopulmonary disease and obesity. Therefore, further research involving extended or repeated high-Gz profiles, real-time ventilation assessments, and a wider range of aircrew populations would be useful to better and more comprehensively understand those mechanisms, and to identify how transient post-G changes obscure early signs of respiratory susceptibility.

Although such short-term respiratory improvements might not represent prolonged advancement in ventilatory capacity, they may provide a temporary boost in pulmonary functions that could assist individuals to execute maneuvers that require increased oxygenation, better ventilation, or more physical effort. Since moderate exercise was shown to improve cognitive and physical performance (44,45), high-Gz exposures can be beneficial in maintaining cognitive abilities, reaction times, and physical endurance throughout crucial mission periods by triggering an immediate burst in catecholamines and associated hormonal reactions. Understanding the short-term nature of

the respiratory improvements could benefit training supervisors in effectively regulating maneuver effectiveness, arranging sufficient recovery periods, and minimizing the overestimation of respiratory tolerance depending simply on acute post-G measurements. Furthermore, integrating regular respiratory measurements into HCT protocols may assist in identifying aircrew- even including passengers for commercial space flights- with insidious underlying conditions who might be at increased risk due to prolonged exposure patterns or inadequate recovery. Future operational investigations are needed to identify the optimal integration of these physiological responses into training procedures to improve both performance and safety.

Study Limitations

The present study has various limitations. First, the cohort size was relatively small, which might have limited the statistical power and generalizability of the results. Given the operational difficulties, this was the maximum achievable sample size. Pilots generally either leave the training center shortly after completing their physiological training tasks or continue to other modules of training (such as ejection seat, spatial disorientation, or night vision training), making their attendance in subsequent PTSs challenging. Second, PFT was performed immediately following centrifuge exposure, increasing the likelihood that the observed effects were short-term rather than long-term physiological alterations. However, additional testing was not possible due to the same practical concerns. Potential residual effects of +Gz exposure could be studied more thoroughly by conducting follow-up PFTs at specific subsequent time points. Another limitation of this study is the absence of a control group that did not undergo +Gz exposure. Without a control cohort, it is challenging to definitively attribute the observed improvements in pulmonary function solely to the high-G exposure, as opposed to other factors such as testing familiarity, psychological effects, or natural variability in respiratory function. Including a control group in future studies—such as pilots undergoing identical testing without +Gz exposure—would strengthen the causal inference and help distinguish true physiological changes from test-retest effects or placebo influences. Moreover, a control group could facilitate assessment of baseline stability of PFT parameters, thereby ensuring that the observed modifications are specifically related to the high-G stress.

Conclusion

Overall, respiratory responses to +Gz acceleration exposure resulted in improvements in several PFT values. Expiratory flow-dependent parameters (FEV_1, FEV_1/FVC, $FEF_{25-75\%}$) and MVV exhibited significant post-training improvements. Subgroup analysis demonstrated that non-smokers showed significantly greater increases in flow-dependent measures, while smokers had smaller yet significant improvements. Acute high-Gz exposure may be said to temporarily improve respiratory dynamics, especially in those who have preserved basal pulmonary reserve, through sympathetic stimulation, and improved activation of respiratory muscle groups. To confirm these outcomes and explain the mechanisms at work, further studies should better include larger cohorts, additional analyses of hormonal biomarkers' responses, and repeated post-exposure measures.

Ethics

Ethics Committee Approval: Ethical approval was taken from the University of Health Sciences Türkiye, Gülhane Training and Research Hospital (approval number: 2023/265, date: 22.11.2023).

Informed Consent: Participants in the study provided informed consent after receiving thorough information via the consent forms.

Footnotes

Authorship Contributions

Surgical and Medical Practices: M.S.İ., N.K., Ş.H.G., Concept: A.E.D., M.S.İ., N.K., Ş.H.G., Design: A.E.D., M.S.İ., N.K., C.T., Data Collection or Processing: A.E.D., M.S.İ., Ş.H.G., Analysis or İnterpretation: C.T., Literature Search: A.E.D., Writing: A.E.D., Ş.H.G., C.T.

Conflict of Interest: The authors declare that they have no conflict of interest regarding this study.

Financial Disclosure: The authors declared that this study received no financial support.

References

1. Banks RD, Somers JT, Chelette TL, Wood RL, Watson RA. Human Response to Acceleration. In: David JR, Johnson R, Stepanek J, Fogarty JA, eds. Fundamentals of aerospace medicine. 5th ed. Philadelphia, PA: Wolters Kluwer/Lippincott Williams & Wilkins; 2021. p. 1252-1134. Available from: https://www.wolterskluwer.com/en/solutions/ovid/fundamentals-of-aerospace-medicine-5421
2. Green DCN. Long-duration acceleration. In: Gradwell DP, Rainford DJ, editors. Ernsting's Aviation and Space Medicine, 5th ed. Taylor & Francis Group, LLC; 2016. p. 131-156. https://doi.org/10.1201/b13197
3. Metzler MM. G-LOC Due to the push-pull effect in a fatal F-16 mishap. *Aerosp Med Hum Perform*. 2020;91(1):51-55.
4. Sevilla NL, Gardner JW. G-induced loss of consciousness: case-control study of 78 G-Locs in the F-15, F-16, and A-10. *Aviat Space Environ Med.* 2005;76(4):370-374.
5. Demir AE. Ground-based simulation technologies in aerospace physiology trainings in turkey: current status and future aspects. In: Proceedings of the 12th Ankara International Aerospace Conference; 2023: Türkiye. Available from: http://aiac.ae.metu.edu.tr/paper.php?No=AIAC-2023-044

6. Glaister DH. The effects of gravity and acceleration on the lung. *The Advisory Group for Aerospace Research and Development*. NATO, London: 1970. Available from: https://apps.dtic.mil/sti/tr/pdf/AD0882903.pdf
7. Gustafsson PM, Eiken O, Grönkvist M. Effects of hypergravity and anti-G suit pressure on intraregional ventilation distribution during VC breaths. *J Appl Physiol (1985*). 2001;91(2):637-644.
8. Marek W, Rasche K, Mückenhoff K. Zur interaktion chemosensibler und vagaler afferenzen auf die respiratorische moto-aktivität und die atemarbeit [Interactions of chemosensitive and vagal afferents in respiratory motor activity and work of breathing]. *Pneumologie*. 2006;60(10):632-641.
9. Yang P, Frier BC, Goodman L, Duffin J. Respiratory muscle training and the performance of a simulated anti-G straining maneuver. *Aviat Space Environ Med.* 2007;78(11):1035-1041.
10. Borges JB, Hedenstierna G, Bergman JS, Amato MB, Avenel J, Montmerle-Borgdorff S. First-time imaging of effects of inspired oxygen concentration on regional lung volumes and breathing pattern during hypergravity. *Eur J Appl Physiol.* 2015;115(2):353-363.
11. Estenne M, Van Muylem A, Kinnear W, Gorini M, Ninane V, Engel LA, et al. Effects of increased +Gz on chest wall mechanics in humans. *J Appl Physiol (1985).* 1995;78(3):997-1003.
12. Turkish Armed Forces, The gendarmerie general command and coast guard command health aptitude regulation. Official Gazette No: 29885; 2016. p. 6625-6635. [cited 2025 September 05]. Turkish. Available from: https://www.msb.gov.tr/content/upload/docs/basin/saglik_2017.pdf
13. Hammond D. Smoking behaviour among young adults: beyond youth prevention. *Tob Control.* 2005;14(3):181-185.
14. Graham BL, Steenbruggen I, Miller MR, Barjaktarevic IZ, Cooper BG, Hall GL, et al. Standardization of spirometry 2019 update. An Official American Thoracic Society and European Respiratory Society Technical Statement. *Am J Respir Crit Care Med.* 2019;200(8):e70-e88.
15. Lutfi MF. The physiological basis and clinical significance of lung volume measurements. *Multidiscip Respir Med*. 2017;12:3.
16. Ntima NO, Lumb AB. Pulmonary function tests in anaesthetic practice. *BJA Educ.* 2019;19(7):206-211.
17. Bonjour J, Bringard A, Antonutto G, Capelli C, Linnarsson D, Pendergast DR, et al. Effects of acceleration in the Gz axis on human cardiopulmonary responses to exercise. *Eur J Appl Physiol.* 2011;111(12):2907-2917.
18. Miyamoto Y, Shimazu H, Nakamura A. Plasma catecholamine and cortisol concentrations during acceleration stress. *Eur J Appl Physiol Occup Physiol.* 1995;70(5):407-412.
19. Cheng YJ, Macera CA, Addy CL, Sy FS, Wieland D, Blair SN. Effects of physical activity on exercise tests and respiratory function. *Br J Sports Med*. 2003;37(6):521-528.
20. Chen HH, Wu YC, Kuo MD. An electromyographic assessment of the anti-G straining maneuver. *Aviat Space Environ Med.* 2004;75(2):162-167.
21. Raghunandan V. Can baroreceptors be trained by repeated exposure to +Gz acceleration? [dissertation]. Bangalore (India): Rajiv Gandhi University of Health Sciences; 2011 [cited 2025 Sep 02]. Available from: https://www.proquest.com/docview/2848394542
22. Cornelissen SJWM, Frijters E, Gray G. Lung function changes with acute +Gz exposure as assessed by impulse oscillometry. *Aerosp Med Hum Perform.* 2025;96(1):62-66.
23. Slungaard E, McLeod J, Green NDC, Kiran A, Newham DJ, Harridge SDR. Incidence of G-induced loss of Consciousness and Almost Loss of Consciousness in the Royal air force. *Aerosp Med Hum Perform.* 2017;88(6):550-555.
24. Tsigos C, Kyrou I, Kassi E, Chrousos GP. Stress: endocrine physiology and pathophysiology. 2020 Oct 17. In: Feingold KR, Adler RA, editors. Endotext [Internet]. South Dartmouth (MA): MDText.com, Inc.; 2000.
25. Viru A. Plasma hormones and physical exercise. *Int J Sports Med.* 1992;13:201-209.
26. Mills FJ. The endocrinology of stress. *Aviat Space Environ Med*. 1985;56:642-650.
27. Kraemer WJ, Häkkinen K, Newton RU, McCormick M, Nindl BC, Volek JS, et al. Acute hormonal responses to heavy resistance exercise in younger and older men. *Eur J Appl Physiol Occup Physiol.* 1998;77(3):206-211.
28. Jacks DE, Sowash J, Anning J, McGloughlin T, Andres F. Effect of exercise at three exercise intensities on salivary cortisol. *J Strength Cond Res*. 2002;16(2):286-289.
29. Tarui H, Nakamura A. Saliva cortisol: a good indicator for acceleration stress. *Aviat Space Environ Med.* 1987;58(6):573-575.
30. Obmiński Z, Wojtkowiak M, Stupnicki R, Golec L, Hackney AC. Effect of acceleration stress on salivary cortisol and plasma cortisol and testosterone levels in cadet pilots. *J Physiol Pharmacol*. 1997;48(2):193-200.
31. Enright RL, Connett JE, Bailey WC. The FEV1/FEV6 predicts lung function decline in adult smokers. *Respir Med.* 2002;96(6):444-449.
32. Kumar N, Chawla G, Kansal AP, Deokar K, Niwas R, Abrol N, et al. Air flow limitation in smokers - a cause of concern. *J Family Med Prim Care*. 2022;11(11):6807-6811.
33. Pişkin NE, Kutlu Z, Yavuz G, Aktuğ ZB, İbiş S, Aka H. The Effect of deviced respiratory muscle exercises applied to smokers and non-smokers on respiratory functions. *J Educ Recreat Patterns.* 2023;4(1):87-98.
34. Roh H, Lee D, Lee S, Park J. Respiratory muscle training of pulmonary function for smokers and non-smokers. *J Phys Ther Sci.* 2012;24(8):691-693.
35. Kotlyarov S. The role of smoking in the mechanisms of development of chronic obstructive pulmonary disease and atherosclerosis. *Int J Mol Sci.* 2023;24(10):8725.
36. Dillard TA, Hnatiuk OW, McCumber TR. Maximum voluntary ventilation: spirometric determinants in chronic obstructive pulmonary disease patients and normal subjects. *Am Rev Respir Dis.* 1993;147(4):870-875.
37. Araújo PRS, Fonseca JDMD, Marcelino AA, Moreno MA, Dornelas de Andrade AF, Yañez MO, et al. Reference values for respiratory muscle strength and maximal voluntary ventilation

in the Brazilian adult population: a multicentric study. *PLoS One.* 2024;19(11):e0313209.

38. Newman DG, Callister R. Cardiovascular training effects in fighter pilots induced by occupational high G exposure. *Aviat Space Environ Med.* 2008;79(8):774-778.

39. Convertino VA. High sustained +Gz acceleration: physiological adaptation to high-G tolerance. *J Gravit Physiol*. 1998;5(1):P51-P54.

40. Johnson BD, Aaron EA, Babcock MA, Dempsey JA. Respiratory muscle fatigue during exercise: implications for performance. *Med Sci Sports Exerc.* 1996;28(9):1129-1137.

41. Smith JR, Ade CJ, Broxterman RM, Skutnik BC, Barstow TJ, Wong BJ, et al. Influence of exercise intensity on respiratory muscle fatigue and brachial artery blood flow during cycling exercise. *Eur J Appl Physiol*. 2014;114(8):1767-1777.

42. Dempsey JA, Romer L, Rodman J, Miller J, Smith C. Consequences of exercise-induced respiratory muscle work. *Respir Physiol Neurobiol.* 2006;151(2-3):242-250.

43. Pollock RD, Jolley CJ, Abid N, Couper JH, Estrada-Petrocelli L, Hodkinson PD, et al. Pulmonary effects of sustained periods of high-G acceleration relevant to suborbital spaceflight. *Aerosp Med Hum Perform.* 2021;92(8):633-641.

44. Chang YK, Ren FF, Li RH, Ai JY, Kao SC, Etnier JL. Effects of acute exercise on cognitive function: a meta-review of 30 systematic reviews with meta-analyses. *Psychol Bull.* 2025;151(2):240-259.

45. Dhabhar FS. The short-term stress response - Mother nature's mechanism for enhancing protection and performance under conditions of threat, challenge, and opportunity. *Front Neuroendocrinol.* 2018;49:175-192.

DOI: 10.4274/gulhane.galenos.2026.99997
Gulhane Med J 2026;68(2):127-131

Evaluation of the incidence and clinical outcomes of permanent pacemaker implantation after the Ozaki procedure: a retrospective cohort study

Salim Yaşar[1], Özkan Eravcı[1], Serdar Fırtına[1], Mehmet Sadık Karpat[1], Erkan Yıldırım[1], Tayfun Özdem[2], Emre Kubat[3], Kubilay Karabacak[2], Hasan Kutsi Kabul[1]

[1]University of Health Sciences Türkiye, Gülhane Training and Research Hospital, Clinic of Cardiology, Ankara, Türkiye
[2]University of Health Sciences Türkiye, Gülhane Training and Research Hospital, Clinic of Cardiovascular Surgery, Ankara, Türkiye
[3]Ufuk University Faculty of Medicine, Dr. Rıdvan Ege Hospital, Department of Cardiovascular Surgery, Ankara, Türkiye

Cite this article as: Yaşar S, Eravcı Ö, Fırtına S, Karpat MS, Yıldırım E, Özdem T, et al. Evaluation of the incidence and clinical outcomes of permanent pacemaker implantation after the Ozaki procedure: a retrospective cohort study. *Gulhane Med J.* 2026;68(2):127-131.

Date submitted:
07.08.2025
Date accepted:
03.03.2026
Epub:
10.06.2026
Publication Date:
16.06.2026

Corresponding Author:
Salim Yaşar, M.D., University of Health Sciences Türkiye, Gülhane Training and Research Hospital, Clinic of Cardiology, Ankara, Türkiye
dr.salimyasar@hotmail.com

ORCID:
orcid.org/0000-0003-2290-0184

Keywords: Ozaki procedure, aortic valve reconstruction, autologous pericardium, permanent pacemaker, echocardiography

ABSTRACT

Aims: Data on permanent pacemaker implantation (PPI) after the Ozaki procedure are limited. This study evaluates the incidence of PPI and compares echocardiographic and clinical outcomes between patients with PPI and without PPI.

Methods: We conducted a retrospective study to evaluate patients who underwent the Ozaki procedure between January 1, 2019, and September 1, 2022. Patients were divided into PPI and non-PPI groups after the procedure. Preoperative and postoperative echocardiographic parameters, surgical details, and clinical outcomes were compared.

Results: The study included 89 patients: two patients in the PPI group, aged 69 and 71 years, and 87 patients in the non-PPI group, with a mean age of 62.3±13.6 years. PPI was required in 2.2% of patients. While the numbers of men and women in the pacemaker group were equal, the number of men in the non-pacemaker group was higher (male/female: 49/38). The PPI group had cardiopulmonary bypass times of 135 and 100 minutes, respectively, compared with 100±30 minutes in the non-PPI group, and aortic cross-clamp times of 75 and 88 minutes, respectively, compared with 70±20 minutes in the non-PPI group. At discharge, peak gradients decreased from 78 and 74 mmHg to 22 and 29 mmHg in the PPI patients (non-PPI: 78±30 to 25±12 mmHg), and mean gradients decreased from 44 and 45 mmHg to 10 and 14 mmHg (non-PPI: 45±15 to 12±6 mmHg). No in-hospital mortality or paravalvular leak was observed.

Conclusions: In our experience, PPI after the Ozaki procedure was uncommon, while early echocardiographic and clinical outcomes remained favorable. Our findings are consistent with the available literature and highlight the need for vigilant postoperative conduction monitoring, especially in patients with baseline conduction disease or prolonged operative times.

Introduction

Aortic valve diseases remain a significant cause of morbidity and mortality worldwide, often necessitating surgical intervention (1,2). The Ozaki procedure, which involves aortic valve reconstruction using autologous pericardium, offers an alternative to prosthetic valve replacement, providing favorable hemodynamic profiles and potentially reducing the need for lifelong anticoagulation (3). Since its introduction, the procedure has been increasingly adopted, demonstrating promising early and mid-term outcomes (2,3). However, as with other valve surgeries, the Ozaki procedure carries a risk of conduction disturbances, particularly atrioventricular (AV) block, which may necessitate permanent pacemaker implantation (PPI) (4,5). While PPI after conventional aortic valve replacement has been well studied, limited data exist regarding the incidence, clinical predictors, and echocardiographic consequences of PPI following the Ozaki procedure (6). This study aims to assess the incidence of PPI after the Ozaki operation at our center and to compare echocardiographic parameters and clinical outcomes between patients requiring PPI and those who did not require PPI. Our goal is to provide insights that improve perioperative management and patient selection for this innovative surgical technique.

Methods

Study design, participants and ethics

We conducted a retrospective cohort study that included 89 consecutive patients who underwent the Ozaki procedure at University of Health Sciences Türkiye, Gülhane Training and Research Hospital between 2019 and 2022. Patients with incomplete data or concomitant procedures (for example, coronary artery bypass grafting, mitral valve surgery, or ascending aortic surgery) were excluded. The study was approved by the Ethics Committee of the University of Health Sciences Türkiye, Gülhane Training and Research Hospital (approval no: 2022/272, date: 12.09.2022). The study protocol conforms to the Declaration of Helsinki and good clinical practice guidelines.

Data collection and clinical variables

Demographic variables collected included age, sex, height, weight, and calculated body mass index. Preoperative risk was assessed using the EuroSCORE II. Comorbidities such as smoking status, chronic obstructive pulmonary disease, diabetes mellitus, renal insufficiency, peripheral vascular disease, and coronary artery disease were documented.

Echocardiographic evaluation

Comprehensive transthoracic echocardiograms were performed preoperatively and before discharge. Recorded parameters were left ventricular ejection fraction (LVEF), aortic valve area (AVA), peak and mean aortic valve gradients (pressure gradient and mean gradient), and the presence of paravalvular leaks.

Surgical details

Cardiopulmonary bypass (CPB) and aortic cross-clamp (ACC) times were noted separately.

Postoperative outcomes

Recorded postoperative complications included acute renal failure, myocardial infarction, cerebrovascular events, new-onset arrhythmias (including atrial fibrillation), AV block, and PPI. Length of stay in the intensive care unit, total hospital stay, and hospital mortality were documented.

Statistical Analysis

Patients were categorized into two groups according to whether PPI was required postoperatively. Continuous variables were summarized as mean ± standard deviation or median with interquartile range, as appropriate. Categorical variables were summarized as counts and percentages. Given the very small number of PPI events (n=2), the analyses were restricted to descriptive statistics and no inferential statistical testing was performed.

Results

Among 89 patients undergoing the Ozaki procedure, two (2.2%; 1 male, 1 female) required PPI due to AV block. In the non-PPI group (n=87), 49 patients (56.3%) were male and 38 (43.7%) were female.

The PPI group consisted of two patients with EuroSCORE II values of 6.22% and 9.1%, whereas the non-PPI group had a mean EuroSCORE II of 7.2±3.5%. Cardiopulmonary bypass time was 135 and 100 minutes in the PPI group and 100±30 minutes in the non-PPI group. Similarly, aortic cross-clamp times were 75 and 88 minutes in the PPI group, compared with 70±20 minutes in the non-PPI group (Table 1). Preoperative LVEF was 60% and 65% in the PPI group, with a mean of 56±10% in the non-PPI group. The mean AVA preoperatively was 0.85 cm^2 and 1.2 cm^2 in the PPI group, and 0.75±0.2 cm^2 in the non-PPI group. Peak and mean aortic valve gradients were elevated preoperatively in both groups. At discharge, the PPI group showed sustained LVEF values (60% and 65%) and significant reductions in peak gradients (22 and 29 mmHg) and mean gradients (10 and 14 mmHg), consistent with the average reductions observed in the non-PPI group (Figures 1 and 2, Table 2). Mortality was not observed in either group. No paravalvular leaks were observed.

Discussion

In our cohort of 89 patients who underwent the Ozaki procedure, PPI was required in 2 (2.2%) patients. The first

patient requiring PPI was a 71-year-old man with preoperative sinus rhythm, incomplete right bundle branch block (iRBBB), QRS 118 ms, and severe periaortic tissue calcification. Postoperatively, he developed complete AV block. He received temporary epicardial pacing; because of persistent complete AV block, a dual-chamber permanent pacemaker was implanted on postoperative day 5 (DDD mode; lower rate limit of 55 bpm). The second patient requiring PPI was a 69-year-old woman with first-degree AV block (PR 232 ms) and non-specific intraventricular conduction delay (nsIVCD), QRS 112 ms, on baseline ECG, along with periaortic tissue calcification. Postoperatively, she exhibited persistent 2:1 AV block with intermittent episodes of complete AV block. A dual-chamber permanent pacemaker was implanted on postoperative day 7 (DDD mode; lower rate limit 50 bpm). At the 1 month device interrogation, the first patient was fully pacemaker-dependent (ventricular pacing 100% with no intrinsic rhythm during VVI 30 bpm testing), whereas the second patient had a ventricular pacing burden of 52%. PPI after the Ozaki procedure is infrequent and comparable to rates after conventional valve replacement. When the literature is reviewed, in the Ozaki procedure, the need for a permanent pacemaker is very low (0.25-2.9%), significantly less than the rates in traditional AVR or TAVR (4-6).

In a multicenter study conducted by Chernov et al. (7), the incidence of PPI following the Ozaki procedure was 1.8%. Conversely, in a study by Ozaki et al. (8), complete heart block necessitating a pacemaker was reported at 1.5% overall, with reduced rates observed after isolated Ozaki procedures compared to concomitant operations. Notably, our patients who required PPI had preoperative conduction abnormalities (iRBBB and prolonged PR/nsIVCD) and marked periaortic calcification; these features that have been repeatedly associated with postoperative high-grade AV block in the aortic valve literature. Extensive annular/periaortic calcification may necessitate deeper or more extensive suture placement and increased traction during leaflet fixation, thereby increasing mechanical stress and edema near the membranous septum and His bundle. Technical factors (stitch depth and proximity to the right-non-coronary commissure) and postoperative inflammation/ischemia represent plausible mechanisms for conduction system injury in this setting. Consistent with this concept, our

Table 1. Baseline and surgical characteristics by permanent pacemaker implantation status

Characteristic	PPI group (n=2)	Non-PPI group (n=87)
Continuous variables		
Age (years)	69; 71	62.3±13.6
Height (cm)	165; 171	165.0±9.8
Weight (kg)	75; 85	77.5±12.9
BMI (kg/m²)	27.5; 29.1	28.7±4.9
EuroSCORE II (%)	6.22; 9.1	7.2±3.5
Categorical variables		
Sex (male)	1 (50.0)	49 (56.3)
Sex (female)	1 (50.0)	38 (43.7)
Smoking	1 (50.0)	19 (21.8)
COPD	1 (50.0)	13 (14.9)
Diabetes mellitus	0 (0.0)	18 (20.7)
Renal insufficiency	1 (50.0)	16 (18.4)
Peripheral vascular disease	1 (50.0)	3 (3.4)
Coronary artery disease	1 (50.0)	37 (42.5)
Operative Times		
Cardiopulmonary bypass time (min)	135; 100	100±30
Aortic cross-clamp time (min)	75; 88	70±20

Data presentation: For the PPI group (n=2), continuous variables are presented as individual values for patient 1 and patient 2. For the non-PPI group (n=87), continuous variables are presented as mean ± SD; categorical variables are presented as n (%)
COPD: Chronic obstructive pulmonary disease, SD: Standard deviation, PPI: Permanent pacemaker implantation, min: Minute, BMI: Body mass index

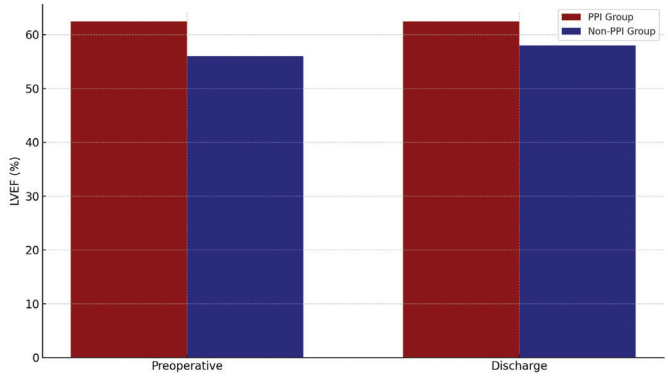

Figure 1. Preoperative and postoperative LVEF in patients with and without permanent pacemaker implantation after the Ozaki procedure

LVEF: Left ventricular ejection fraction, PPI: Permanent pacemaker implantation

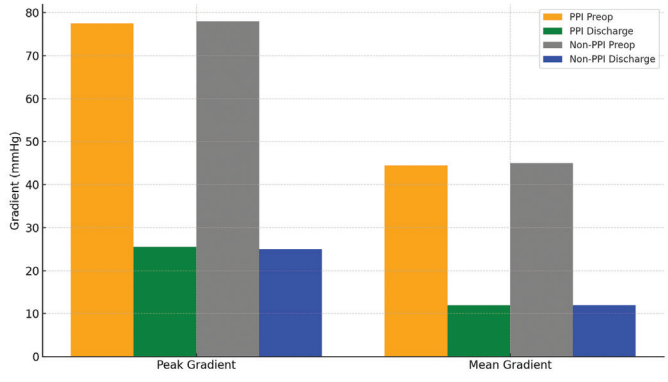

Figure 2. Changes in peak and mean aortic valve gradients preoperatively and at discharge between PPI and non-PPI groups

PPI: Permanent pacemaker implantation

Table 2. Echocardiographic parameters by permanent pacemaker implantation status

Parameter	Timepoint	PPI group (n=2)	Non-PPI group (n=87)
LVEF (%)	Preoperative	60; 65	56±10
	Discharge	60; 65	58±9
Aortic valve area (cm^2)	Preoperative	0.85; 1.2	0.75±0.2
Peak gradient (mmHg)	Preoperative	78; 74	78±30
	Discharge	22; 29	25±12
Mean gradient (mmHg)	Preoperative	44.5	45±15
	Discharge	10; 14	12±6

Data presentation: PPI group values are reported as individual values, whereas non-PPI values are presented as mean ± SD
PPI: Permanent pacemaker implantation, LVEF: Left ventricular ejection fraction, SD: Standard deviation

PPI patients also had longer CPB/ACC times, which may reflect more complex anatomy and prolonged manipulation-both linked to higher pacing rates in prior surgical series (4).

Similarly to previous studies, in our studuy echocardiographic parameters improved significantly in all patients, indicating effective restoration of valve function (9,10). As previous studies, longer operative times in the PPI group may contribute to conduction disturbances, though clinical outcomes remained similar (11). In this retrospective cohort of 89 patients undergoing the Ozaki procedure, PPI was required in 2.2% of cases, indicating a relatively low incidence of conduction disturbances requiring pacing. This rate is comparable to or slightly lower than those reported after conventional aortic valve replacement procedures, suggesting that the Ozaki procedure may not increase the risk of AV conduction system injury despite its technical nuances (12). Our findings demonstrate significant improvements in echocardiographic parameters postoperatively in both groups. Patients requiring PPI exhibited stable LVEF and substantial reductions in peak and mean aortic valve gradients, similar to those who did not require pacing (9,10,13). These results confirm the efficacy of the Ozaki procedure in restoring favorable hemodynamics and preserving ventricular function, even in patients who develop conduction abnormalities (14). The PPI group had longer CPB and ACC times compared to the non-PPI group, which may reflect more complex intraoperative courses or anatomical challenges potentially contributing to conduction system injury (6,11). However, given the small number of PPI cases, definitive conclusions about procedural risk factors are limited (15). No significant differences in early clinical outcomes, including mortality were observed between groups, suggesting that pacing does not adversely affect short-term recovery after the Ozaki procedure (16).

Our study supports the relative safety of the Ozaki procedure in terms of conduction system preservation, with a low rate of permanent pacing comparable to that observed after traditional valve replacement. Surgeons should remain vigilant for conduction disturbances, especially in cases with prolonged CPB or ACC times. Postoperative echocardiographic monitoring is essential for evaluating valve function and detecting potential complications early. Echocardiographic outcomes demonstrate significant and sustained improvement in valve function, regardless of pacing status. Overall, this series demonstrates that the Ozaki procedure can be performed successfully with favorable early echocardiographic and clinical outcomes at our center.

Study Limitations

The primary limitation of this study is the very small number of patients requiring PPI (n=2). This sample size precludes formal comparative statistical inference between PPI and non-PPI groups and precludes reliable identification of predictors; therefore, the findings should be interpreted as exploratory and descriptive. Consistent with this limitation, post hoc power analysis (G*Power) demonstrated low statistical power for between-group comparisons, with an achieved power of approximately 0.12 for cardiopulmonary bypass and cross-clamp time differences, primarily driven by the extremely small PPI group. Although patients requiring PPI were older than those without PPI, and age could confound associations with operative times, robust age-adjusted multivariable modeling (e.g., logistic regression/ANCOVA) was not feasible because of the high risk of overfitting with only two events. The retrospective design may introduce selection bias, and the single-center nature of the cohort may limit generalizability. Longer-term follow-up and larger, multicenter cohorts are needed to evaluate durability and validate potential predictors using appropriately powered and adjusted analyses.

Conclusion

The Ozaki procedure provides excellent echocardiographic and clinical outcomes with a low incidence of PPI. Although patients requiring pacing had longer operative times, short-term clinical outcomes were comparable to those without pacing. These findings support the safety and effectiveness of the Ozaki procedure in aortic valve reconstruction, with minimal risk of conduction disturbances.

Ethics

Ethics Committee Approval: The study was approved by the Ethics Committee of the University of Health Sciences Türkiye, Gülhane Training and Research Hospital (approval no: 2022/272, date: 12.09.2022).

Informed Consent: Retrospective study.

Declaration on the Use of Artificial Intelligence (AI): For transparency, the authors note that an artificial intelligence-assisted language model (ChatGPT, OpenAI) was utilized to support text editing and language correction. This assistance was limited to linguistic refinement; all scientific content, critical analysis, and final editorial decisions were made exclusively by the authors.

Footnotes

Authorship Contributions

Surgical and Medical Practices: T.Ö., E.K., K.K., Concept: S.Y., Ö.E., H.K.K., Design: S.Y., Ö.E., K.K., H.K.K., Data Collection or Processing: S.Y., Ö.E., S.F., Analysis or Interpretation: S.Y., Ö.E., M.S.K., T.Ö., H.K.K., Literature Search: Ö.E., S.F., M.S.K., E.K., K.K., Writing: S.Y., Ö.E., E.Y., H.K.K.

Conflict of Interest: The authors declare that they have no conflict of interest regarding this study.

Financial Disclosure: The authors declared that this study received no financial support.

References

1. Ozaki S, Kawase I, Yamashita H, Uchida S, Takatoh M, Hagiwara S, et al. Aortic valve reconstruction using autologous pericardium for aortic stenosis. *Circ J.* 2015;79(7):1504-1510.
2. Karabacak K, Kadan M, Demirkıran T, Yaşar AS, İnce ME, Bolcal C. Unrecognized indication for aortic valve neocuspidization: patient with warfarin-induced Stevens-Johnson syndrome and toxic epidermal necrolysis. *J Card Surg.* 2022;37(6):1733-1735.
3. Karabacak K. A new alternative to the Bentall procedure: aortic valve neocuspidization (Ozaki procedure) with the Florida sleeve aortic root reconstruction. *Multimed Man Cardiothorac Surg.* 2023;2023.
4. Dawkins S, Hobson AR, Kalra PR, Tang AT, Monro JL, Dawkins KD. Permanent pacemaker implantation after isolated aortic valve replacement: incidence, indications, and predictors. *Ann Thorac Surg.* 2008;85(1):108-112.
5. Leon MB, Smith CR, Mack M, Miller DC, Moses JW, Svensson LG, et al. Transcatheter aortic-valve implantation for aortic stenosis in patients who cannot undergo surgery. *N Engl J Med.* 2010;363(17):1597-1607.
6. Koechlin L, Eckstein FS. Aortic valve neocuspidization using autologous pericardium (Ozaki procedure): an alternative to aortic valve replacement in adult cardiac surgery? *Curr Anesthesiol Rep.* 2021;11(3):318-325.
7. Chernov II, Enginoev ST, Komarov RN, Bazylev VV, Tarasov DG, Kadyraliev BK, et al. Short-term outcomes of Ozaki procedure: a multicenter study. *Russian Journal of Cardiology*. 2020;25(S4):4157.
8. Ozaki S, Hoshino Y, Unai S, Harb SC, Frankel WC, Hayama H, et al. Mid-term experience with 1,196 Ozaki Procedures. *JACC Adv.* 2025;4(11 Pt 1):102156.
9. Toeg H, Chan V, Rao RV, Chan KL, Ruel M, Mesana T, et al. Contemporary midterm echocardiographic outcomes of Bentall procedure and aortic valve sparing root replacement. *Ann Thorac Surg.* 2014;98(2):590-596.
10. Arnold Z, Elnekheli A, Geisler D, Aschacher T, Lenz V, Winkler B, et al. Left ventricular reverse remodeling after surgical aortic valve replacement for aortic regurgitation-an explorative study. *Diseases*. 2024;12(8):191.
11. Kvidal P, Bergström R, Hörte LG, Ståhle E. Observed and relative survival after aortic valve replacement. *J Am Coll Cardiol.* 2000;35(3):747-756.
12. Arutyunyan V, Chernov I, Komarov R, Sinelnikov Y, Kadyraliev B, Enginoev S, et al. Immediate outcomes of aortic valve neocuspidization with glutaraldehyde-treated autologous pericardium: a multicenter study. *Braz J Cardiovasc Surg.* 2020;35(3):241-248.
13. Ozaki S, Kawase I, Yamashita H, Uchida S, Takatoh M, Kiyohara N. Midterm outcomes after aortic valve neocuspidization with glutaraldehyde-treated autologous pericardium. *J Thorac Cardiovasc Surg*. 2018;155(6):2379-2387.
14. Nkomo VT, Gardin JM, Skelton TN, Gottdiener JS, Scott CG, Enriquez-Sarano M. Burden of valvular heart diseases: a population-based study. *Lancet*. 2006;368(9540):1005-1011.
15. O'Brien SM, Shahian DM, Filardo G, Ferraris VA, Haan CK, Rich JB, et al. The Society of Thoracic Surgeons 2008 cardiac surgery risk models: part 2--isolated valve surgery. *Ann Thorac Surg.* 2009;88(1 Suppl):S23-S42.
16. Patel V, Unai S, Moore R, Layoun H, Harb S, Tong MZY, et al. The Ozaki procedure: standardized protocol adoption of a complex innovative procedure. *Struct Heart.* 2023;8(1):100217.

DOI: 10.4274/gulhane.galenos.2026.74419
Gulhane Med J 2026;68(2):132-137

Assessment of stress level, sleep quality and heart rate variability among the individuals with symptoms of depression

Monisha Ravi[1], Dhamodhini K S[2], Maheshkumar Kuppusamy[3], Suvarna Kantipudi[4], Santhi Silambanan[5], Padmavathi Ramaswamy[6]

[1]ACS Medical College and Hospital, Dr.M.G.R. Educational and Research Institute, Department of Physiology, Chennai, India
[2]Sri Ramachandra Medical College and Research Institute, Chennai, India
[3]Government Yoga and Naturopathy Medical College and Hospital, Department of Physiology, Chennai, India
[4]Sri Ramachandra Medical College and Research Institute, Department of Psychiatry, Chennai, India
[5]Sri Ramachandra Medical College and Research Institute, Department of Biochemistry, Chennai, India
[6]Sri Ramachandra Medical College and Research Institute, Department of Physiology, Chennai, India

Cite this article as: Ravi M, K S D, Kuppusamy M, Kantipudi S, Ramaswamy P. Assessment of stress level, sleep quality and heart rate variability among the individuals with symptoms of depression. *Gulhane Med J.* 2026;68(2):132-137.

Date submitted:
09.10.2023
Date accepted:
06.04.2026
Epub:
11.06.2026
Publication Date:
16.06.2026

Corresponding Author:
Prof. Padmavathi Ramaswamy, Sri Ramachandra Medical College and Research Institute, Department of Physiology, Chennai, India
rpadmavathi@sriramachandra.edu.in

ORCID:
orcid.org/0009-0007-4169-1257

Keywords: Depression, sleep quality, stress, autonomic function, heart rate variability

ABSTRACT

Aims: Long-term stress is a contributing factor to the development of major depressive disorder. Persistent stress can lead to sleep disturbances, which in turn, sustain sympathetic nervous system activation and elevate cortisol levels. Stress, poor sleep quality, and depression adversely affect mental and physical health, leading to increased morbidity and mortality. This study aims to assess stress levels, sleep quality, and heart rate variability (HRV) among individuals with depressive symptoms.

Methods: This cross-sectional study enrolled 80 participants (mean age of 23.4±5.57 years) comprising 40 individiuals diagnosed with the symptoms of depression by a psychiatrist and 40 healthy controls. Stress levels, sleep quality, depression levels, and cardiac autonomic function were measured using the Perceived Stress Scale (PSS), the Pittsburgh Quality of Sleep Index (PSQI), the Patient Health Questionnaire-9 (PHQ-9) and the Hamilton Depression Rating Scale (HAM-D) for depression, and HRV analysis for cardiac autonomic function.

Results: Participants with depressive symptoms demonstrated significantly poorer HRV parameters compared to healthy controls ($p<0.05$), as indicated by lower root mean square of successive differences (31.74±18.74 vs. 44.57±23.79), higher low frequency (LF) power in normalized units (LF nu: 70.57±12.45 vs. 42.69±11.96), and lower high frequency (HF) power in normalized units (HF nu: 29.48±11.57 vs. 55.39±11.45). Depression severity was significantly higher in patients with depression compared to healthy participants including PHQ-9 scores (9.90±3.84 vs. 1.98±1.33) and HAM-D scores (12.05±2.83 vs. 4.10±1.68) ($p<0.001$). Additionally, patients with depression exhibited significantly elevated PSS scores (27.42±3.21 vs. 13.35±2.68) and PSQI scores (8.62±2.12 vs. 3.67±1.67), indicating higher stress levels and poorer sleep quality ($p<0.001$).

Conclusions: Individuals with depressive symptoms exhibited significantly lower HRV parameters, higher perceived stress levels, and poorer sleep quality compared to healthy controls. The findings suggest that depression is associated with altered autonomic function and increased stress perception. These results highlight the importance of monitoring HRV, stress, and sleep quality as potential biomarkers for depression severity and treatment response.

Introduction

Depression represents a paramount global health challenge, emerging as a leading cause of disability worldwide. According to the Global Burden of Disease study, the prevalence of depressive episodes exhibits a marked gender disparity, affecting 1.9% of men and 3.2% of women (1). The impact of major depressive disorder transcends socioeconomic boundaries, establishing itself as the primary cause of years lived with disability in 56 countries, the secondary cause in another 56, and the tertiary cause in 34 nations (2). Regional studies from South India have revealed particularly concerning statistics, with depression prevalence reaching 15.1% (3). Projections indicate that depression's burden on global health systems may soon surpass that of any other disease (1).

Contemporary societal transformations, characterized by rapid changes in work patterns and lifestyle dynamics, have precipitated an escalation in stress levels among the general population (15.1%) (3). These changes have heightened vulnerability to psychosomatic disorders (4). The manifestations of stress extend beyond psychological domains, potentially triggering a cascade of physical symptoms including headaches, gastritis, dermatological conditions, and insomnia, while also increasing risk for serious conditions such as ulcers, hypertension, cardiovascular disease, and cerebrovascular events (5). The chronic stress response involves complex metabolic alterations, potentially manifesting as autonomic dysfunction and disruptions in hormonal homeostasis, cytokine profiles, and cellular growth factor expression (6).

The relationship between depression and cardiovascular health has garnered significant attention, with studies consistently demonstrating reduced heart rate variability (HRV) in depressed individuals. The increased incidence of cardiovascular conditions among patients with depression suggests autonomic dysfunction as a potential pathophysiological mechanism (7). Regulation of heart rate and rhythm occurs through the intricate interplay between components of the sympathetic and parasympathetic nervous systems. While sympathetic activation accelerates heart rate, parasympathetic influence, primarily mediated through vagal pathways, provides counterbalancing deceleration. HRV, defined as the temporal variation between consecutive heartbeats measured via standard electrocardiogram, serves as a non-invasive tool for assessing cardiac autonomic status.

Research utilizing HRV as an objective measure of psychological stress has consistently revealed stress-induced alterations in HRV parameters, predominantly characterized by attenuated parasympathetic activity. Neuroimaging studies have strengthened this association by demonstrating connections between HRV and cortical regions involved in stress processing (8). This evidence base supports the validity of HRV as an objective tool for assessing psychological stress and overall health status.

The triad of mental stress, poor sleep quality, and depression presents significant risks to health and well-being. While these conditions can be effectively managed through medical and complementary therapeutic approaches, their early identification and monitoring remain crucial for preventing adverse outcomes. Despite the clear importance of objective stress assessment in depression, studies using physiological measures such as HRV in this population remain limited (9,10). This cross-sectional comparative study addresses this research gap by examining stress levels, sleep quality, and HRV in patients with depressive symptoms and in healthy controls.

Methods

Study Design and Participants

This cross-sectional study was conducted at Sri Ramachandra Medical College and Research Institute in Chennai from 2021 to 2023. The study enrolled 80 participants aged 18-35 years, aligning with the required sample size to detect a medium effect size (f^2=0.15) in regression analysis using 2-3 predictors with 80% power at α=0.05, and minimizing age-related physiological variations that could affect HRV measurements. Participants were divided into two groups: 40 individuals with depressive symptoms and 40 healthy controls.

The depression group comprised recently diagnosed patients (within the last month) who scored above 5 on the Patient Health Questionnaire-9 (PHQ-9) (11). These participants had not initiated antidepressant treatment and had no history of depression treatment. The control group consisted of apparently healthy individuals with PHQ-9 scores below 5. Exclusion criteria included signs of other organic mental disorders, the current use of medications known to affect HRV, and a history of cardiovascular disease or other conditions affecting HRV. All participants remained medication-free for at least two weeks prior to the study to minimize potential impacts on HRV measurements. Written informed consent was obtained from the patient prior to participation in the study. The study received ethical approval from the Sri Ramachandra Institute of Higher Education and Research Institutional Ethics Committee (approval no: CSP/22/MAR/108/248, date: 14.07.2022).

Outcome measurements

Perceived Stress Scale (PSS)

The PSS, developed by Cohen et al. (12), was used to assess stress levels. This 10-item instrument measures global perceived stress over the past 30 days on a 5-point scale ranging from 0 (never) to 4 (very often). Total scores range from 0-40, with higher scores indicating greater perceived stress. Score interpretation: 0-13: Low stress; 14-26: Moderate stress; 27-40: High perceived stress. The scale demonstrates robust internal consistency, with Cronbach's alpha ranging from 0.78 to 0.91 across studies (13).

Pittsburgh Quality of Sleep Index (PSQI)

Sleep quality was assessed using the PSQI (14), which comprises 19 self-rated questions and 5 bed partner/roommate-rated questions (only self-rated items contribute to scoring). Seven component scores are derived, each ranging from 0 (no difficulty) to 3 (severe difficulty). These components sum to a global score (range 0-21), with higher scores indicating poorer sleep quality. The PSQI has demonstrated good internal consistency, with a Cronbach's alpha of approximately 0.83.

HRV

HRV, which represents cardiac beat-to-beat variation (15), was measured using the AD instrument-Equivital device. Each participant underwent a standardized protocol that began with a 10-minute seated rest period, followed by the placement of Equivital device leads and the securing of the measurement belt. HRV recording was then conducted for 15 minutes. The analysis incorporated both time-domain and frequency-domain parameters. Time-domain analysis included the measurement of the average R-R interval (RR) and the standard deviation of normal-to-normal intervals intervals, which provide insights into overall HRV. For frequency-domain analysis, the fast Fourier transform was employed to calculate the power spectral density, with a specific focus on low frequency (LF) and high frequency (HF) power components, measured both in milliseconds and in normalized units. The LF/HF ratio was calculated to assess autonomic nervous system balance (16).

Depression assessment

Depression severity was evaluated through two complementary instruments. The PHQ-9 served as a self-administered assessment tool, consisting of 9 items based on DSM-IV criteria for major depressive disorder (17). This instrument provides scores ranging from 0 to 27, with higher scores indicating greater depression severity. Additionally, the Hamilton Depression Rating Scale (HAM-D) was administered by clinicians to provide a comprehensive assessment of depression symptoms (18,19). This scale consists of 17 to 21 items, depending on the version used, with scores ranging from 0 to 52 on the 17-item version. Higher scores on the HAM-D indicate greater depression severity, and the scale is particularly valued for its sensitivity to change over time. The PHQ-9 has demonstrated good internal consistency, with a Cronbach's alpha typically ranging from 0.86 to 0.89.

Study procedure

The study followed a systematic assessment sequence for all participants. Initially, both groups underwent depression screening using the PHQ-9 and HAM-D scales, administered by qualified psychiatrists. Following this, participants completed the PSS to assess their stress levels and the PSQI to evaluate sleep quality. The final component of the assessment involved HRV measurement, which was consistently performed between 9 and 11 A.M. for all participants to minimize diurnal variation in autonomic function.

Statistical Analysis

Results are expressed as mean ± standard deviation. Data analysis was performed using R statistical software version 3.1.1. The Kolmogorov-Smirnov test assessed data normality. Between-group comparisons utilized Student's t-test for parametric data. Statistical significance was set at $p<0.05$.

Results

The study included 40 healthy participants who served as controls, and 40 patients with depressive symptoms. The demographic comparison (Table 1) revealed no significant differences in age (mean age: 23.4±5.57 years; p=0.14) or gender distribution (49% female, 51% male; p=0.3) between the groups, indicating balanced baseline characteristics for age and sex. Table 2 presents a comparison of HRV parameters between the control and depression groups. Notably, root mean square of successive differences (RMSSD) values were significantly higher in healthy controls (44.57±23.79 ms.) compared to the depression group (31.74±18.43 ms.) (p=0.012), indicating enhanced parasympathetic activity in controls. LF power (n.u.) was significantly lower in healthy controls (42.69±11.96 n.u.) compared to the depression group (70.57±12.45 n.u.) (p<0.001), signifying imbalanced autonomic activity. HF power (n.u.) was significantly higher in healthy controls (55.39±11.45 n.u.) compared to the depression group (29.48±11.57 n.u.) (p<0.001), indicative of altered autonomic balance. The LF/HF ratio was significantly lower in healthy controls (0.85±0.39) compared to the depression group (2.99±1.88) (p<0.001), reflecting an imbalanced sympathetic-vagal ratio in depression. The depression group demonstrated markedly higher scores on PHQ-9 (9.90±3.84 vs. 1.98±1.33, p<0.001) and HAM-D (12.05±2.83 vs. 4.10±1.68, p<0.001), indicating greater depression severity (Table 3). Additionally, the depression group reported significantly higher perceived stress levels as measured by the PSS scale (27.42±3.21 vs. 13.35±2.68, p<0.001) and poorer sleep quality on the PSQI (8.62±2.12 vs. 3.67±1.67, p<0.001).

Table 1. Description of the study participants

Variable	Overall (n=80)	Healthy controls (n=40)	Patients with depression (n=40)	p-value
	Mean ± SD	Mean ± SD	Mean ± SD	
Age (years)	23.4±5.57	22.4±4.32	24.8±6.42	0.14
Gender	n (%)	n (%)	n (%)	
Female	39 (49)	17 (42)	22 (55)	0.3
Males	41 (51)	23 (57)	18 (45)	

SD: Standard deviation

Table 2. Comparison of short term HRV parameters between healthy control group and depression group

Characteristic	Overall (n=80)	Control (n=40)	Depression (n=40)	t-value/p-value
Mean R-R interval (ms)	753.21±90.84	765.52±92.18	740.91±8.92)	1.24/0.3
Average HR (bpm)	81.14±9.51	79.82±9.18	82.45±9.77	-1.24/0.3
RMSSD (ms)	38.15±22.11	44.57±23.79	31.74±18.43	**2.57/0.012**
Total power (ms^2)	3,280.61±3,637.95	3,686.86±4,148.27	2,874.35±3,043.36	1.02/0.3
LF power (ms^2)	1,143.22±1,327.13	1,061.27±1,385.21	1,225.18±1,278.71	-0.57/0.7
LF power (n.u)	56.63±18.55	42.69±11.96	70.57±12.45	**-10.46/<0.001**
HF power (ms^2)	1,160.71±1,982.54	1,589.15±2,192.62	732.28±1,666.62	**1.96/<0.001**
HF power (n.u)	42.44±17.34	55.39±11.45	29.48±11.57	**10.06/<0.001**
LF/HF ratio	1.92±1.73	0.85±0.39	2.99±1.88	**-7.07/<0.001**

R-R, R R interval, bpm: Beats per minute, RMSSD: Root mean square of successive differences, LF: Low frequency, HF: High frequency, ms: Milliseconds, nu: Normalized units

Table 3. Comparison the PHQ-9 scores, HAM- D scores, PSS scores and PSQI scores between healthy control group and depression group

Characteristic	Overall (n=80)	Control (n=40)	Depression (n=40)	t-value/p-value
PHQ 9	5.94±4.91	1.98±1.33	9.90±3.84	**12.40/<0.001**
HAM D	8.07±4.62	4.10±1.68	12.05±2.83	**15.36/<0.001**
PSS	20.39±7.67	13.35±2.68	27.42±3.21	**21.45/<0.001**
PSQI	6.15±3.13	3.67±1.67	8.62±2.12	**11.83/<0.001**

Data is represented as mean ± SD. Independent t test used
PHQ-9: Patient health questionnaire-9, HAM-D: Hamilton Depression Rating Scale, PSS: Perceived stress scale, PSQI: Pittsburgh Sleep Quality Index

Discussion

This study demonstrates significant autonomic dysfunction in depression, characterized by sympathetic predominance and reduced parasympathetic activity, as evidenced by increased LF power and LF/HF ratio alongside reduced RMSSD and HF power compared to healthy controls. These findings align with previous research by Wang et al. (20) and Kumar et al. (21), who reported similar autonomic imbalances in depression.

The observed autonomic dysfunction correlates with clinical severity, as evidenced by significantly higher scores on validated depression scales (PHQ-9 and HAM-D) in the affected group. The concurrent elevation in perceived stress levels and deterioration in sleep quality suggest a complex interplay between mood, stress, and autonomic regulation. These findings support the growing body of evidence linking depression with dysregulation of the autonomic nervous system.

Our study reveals a robust association between depression and elevated stress levels, with the depression group showing significantly higher PSS scores. This finding aligns with a previous study demonstrating that each unit increase in perceived stress corresponds to a 1.40-fold increase in the odds of depression (95% confidence interval: 1.35-1.44). The bidirectional nature of this relationship suggests that stress and depression may create a self-reinforcing cycle that exacerbates autonomic dysfunction (22).

Sleep disturbances emerged as another significant factor, with patients with depression showing markedly elevated PSQI scores. This finding corresponds with regional research indicating that individuals with depression face a 4.3-fold higher risk of poor sleep quality (23). The concurrent presence of sleep disruption, autonomic dysfunction, and depression likely reflects shared underlying neurobiological mechanisms, including alterations in neurotransmitter systems (serotonin, norepinephrine, and dopamine), hypothalamic-pituitary-adrenal axis dysregulation, and elevated inflammatory markers (24). This biological overlap may explain the observed clustering of symptoms and physiological changes.

Our results have important clinical implications. The distinct HRV profile associated with depression could serve as a biomarker for the early detection and monitoring of the condition. The marked reduction in parasympathetic activity (as indicated by decreased RMSSD and HF power) suggests that interventions aimed at enhancing vagal tone, such as HRV biofeedback or vagal nerve stimulation, may be beneficial. Furthermore, the strong associations between depression, stress, and sleep disturbances indicate that comprehensive treatment approaches addressing all these domains may be more effective than targeting depression alone.

Study Limitations

Several limitations should be considered when interpreting these findings. First, the cross-sectional design precludes determination of causality between autonomic dysfunction and depression. Second, the moderate sample size may limit the generalizability of the findings. Third, while we controlled for major confounders, other factors affecting HRV, such as physical activity levels and dietary habits, were not assessed. Fourth, the complex interactions between stress, sleep, and autonomic function make it challenging to isolate the primary drivers of the observed changes.

Conclusion

This study provides compelling evidence of the profound impact of depression on both physiological and psychological parameters. The observed alterations in cardiac autonomic function, characterized by sympathetic predominance and parasympathetic withdrawal, suggest a potential mechanism linking depression to increased cardiovascular risk. The significant associations with stress levels and sleep quality underscore the multifaceted nature of depression and highlight the importance of comprehensive treatment approaches. These findings contribute to our understanding of depression's biological underpinnings and may inform the development of more effective therapeutic strategies.

Ethics

Ethics Committee Approval: The study received ethical approval from the Sri Ramachandra Institute of Higher Education and Research Institutional Ethics Committee (approval no: CSP/22/MAR/108/248, date: 14.07.2022).

Informed Consent: Informed consent was obtained from the participants after explaining the detailed procedure of the study.

Acknowledgement

The authors would like to express their sincere gratitude to the Management of SRMC&RI, Chennai.

Footnotes

Authorship Contributions

Concept: S.S, P.R., Design: S.J., P.R., Data Collection or Processing: M.R., D.K.S., Analysis or Interpretation: M.R., M.K., S.J., Literature Search: M.R., D.K.S., S.J., S.S., Writing: M.R., D.K.S., M.K., S.S., P.R.

Conflict of Interest: The authors declared no conflict of interest.

Financial Disclosure: The authors declared that this study received no financial support.

References

1. Tripathi P, Sharma B, Kadam N, Biswas MD, Tiwari D, Vyawahare A, et al. Prevalence and predictors of anxiety and depression in Indian patients with type 2 diabetes. *Ann Neurosci.* 2024;33(1):21-28.
2. Global Burden of Disease Study 2013 Collaborators. Global, regional, and national incidence, prevalence, and years lived with disability for 301 acute and chronic diseases and injuries in 188 countries, 1990-2013: a systematic analysis for the Global Burden of Disease Study 2013. *Lancet*. 2015;386(9995):743-800.
3. R P, Kumar AP, Dhamodhini K S, Venugopal V, Silambanan S, K M, Shah P. Role of yoga in stress management and implications in major depression disorder. *J Ayurveda Integr Med.* 2023;14(5):100767.
4. Nandakumar H, Kuppusamy M, Sekhar L, Ramaswamy P. Prevalence of premenstrual syndrome among students–stress a potential risk factor. *Clinical Epidemiology and Global Health.* 2023;23:101368.
5. Sureshkumar PN. Epidemiological findings on the prevalence of mental disorder in India. *Indian Journal of Psychiatry.* 2000;42(4):444.
6. Behere SP, Yadav R, Behere PB. A comparative study of stress among students of medicine, engineering, and nursing. *Indian J Psychol Med.* 2011;33(2):145-148.
7. Asberg M, Nygren A, Leopardi R, Rylander G, Peterson U, Wilczek L, et al. Novel biochemical markers of psychosocial stress in women. *PLoS One.* 2009;4(1):e3590.
8. Kim HG, Cheon EJ, Bai DS, Lee YH, Koo BH. Stress and heart rate variability: a meta-analysis and review of the literature. *Psychiatry Investig.* 2018;15(3):235-245.
9. Pizzoli SFM, Marzorati C, Gatti D, Monzani D, Mazzocco K, Pravettoni G. A meta-analysis on heart rate variability biofeedback and depressive symptoms. *Sci Rep.* 2021;11(1):6650.
10. Carneiro ER, Azoubel LA, Dias RC, Dias CJ, Sá ES, Brito DA, et al. Correlation of sleep quality and cardiac autonomic modulation in hemodialysis patients. *Sleep Sci.* 2022;15(Spec 1):59-64.
11. Ganguly S, Samanta M, Roy P, Chatterjee S, Kaplan DW, Basu B. Patient health questionnaire-9 as an effective tool for screening of depression among Indian adolescents. *J Adolesc Health*. 2013;52(5):546-551.
12. Cohen S, Kamarck T, Mermelstein R. Perceived stress scale. *Meas Stress A Guid Heal Soc Sci*. 1994;10(2):1-2.
13. Pangtey R, Basu S, Meena GS, Banerjee B. Perceived stress and its epidemiological and behavioral correlates in an urban area of Delhi, India: a community-based cross-sectional study. *Indian J Psychol Med.* 2020;42(1):80-86.
14. Smyth C. The Pittsburgh Sleep Quality Index (PSQI). *J Gerontol Nurs*. 1999;25(12):10-11.
15. Arvind S, Maheshkumar K, Vaishali S, Lavanya S, Padmavathi R. Development and validation of an integrated portable heart rate variability (HRV) analysis system - STREME. *Med Hypotheses.* 2020;143:109887.

16. Maheshkumar K, Dilara K, Maruthy KN, Sundareswaren L. Validation of PC-based sound card with biopac for digitalization of ECG recording in short-term HRV analysis. *N Am J Med Sci.* 2016;8(7):307-311.

17. Levis B, Benedetti A, Thombs BD; DEPRESSion Screening Data (DEPRESSD) Collaboration. Accuracy of Patient Health Questionnaire-9 (PHQ-9) for screening to detect major depression: individual participant data meta-analysis. *BMJ*. 2019;365:l1476.

18. Bagby RM, Ryder AG, Schuller DR, Marshall MB. The Hamilton Depression Rating Scale: has the gold standard become a lead weight? *Am J Psychiatry.* 2004;161(12):2163-2177.

19. Carrozzino D, Patierno C, Fava GA, Guidi J. The Hamilton Rating Scales for depression: a critical review of clinimetric properties of different versions. *Psychother Psychosom.* 2020;89(3):133-150.

20. Wang Y, Zhao X, O'Neil A, Turner A, Liu X, Berk M. Altered cardiac autonomic nervous function in depression. *BMC Psychiatry*. 2013;13:187.

21. Kumar C, Sakshi P, Sinha N, Sunita, Kumar T. HRV changes in young adults with depression. *J Family Med Prim Care.* 2024;13(7):2585-2588.

22. Cristóbal-Narváez P, Haro JM, Koyanagi A. Perceived stress and depression in 45 low- and middle-income countries. *J Affect Disord.* 2020;274:799-805.

23. Majumdar A, Ramya S, Ramakrishnan J. Depression, anxiety, and bodily pain independently predict poor sleep quality among adult women attending a primary health center of Puducherry, India. *J Family Med Prim Care.* 2019;8(3):1182-1188.

24. Wang M, Wei J, Yang X, Ni P, Wang Y, Zhao L, et al. The level of IL-6 was associated with sleep disturbances in patients with major depressive disorder. *Neuropsychiatr Dis Treat*. 2019;15:1695-1700.

DOI: 10.4274/gulhane.galenos.2026.48243
Gulhane Med J 2026;68(2):138-146

Influence of age and cerebrospinal fluid diversion techniques on infection risk in pediatric hydrocephalus: a 10-year single-center experience

Sait Kayhan[1], Adem Doğan[2], Şahin Kırmızıgöz[3], Mehmet Can Ezgü[1], Mehmet Ozan Durmaz[1], Demet Evleksiz Karımzada[4], Ecma Yılmaz[1], Cafer Ak[5], Sezen Yılmaz Sarıaltın[6], Yusuf İzci[1]

[1]*University of Health Sciences Türkiye, Gülhane Training and Research Hospital, Clinic of Neurosurgery, Ankara, Türkiye*
[2]*Şehitkamil State Hospital, Clinic of Neurosurgery, Gaziantep, Türkiye*
[3]*Dr. Ersin Arslan Training and Research Hospital, Clinic of Neurosurgery, Gaziantep, Türkiye*
[4]*Hitit University, Çorum Erol Olçok Training and Research Hospital, Department of Neurosurgery, Çorum, Türkiye*
[5]*Deva Hospital, Clinic of Neurosurgery, Gaziantep, Türkiye*
[6]*Ankara University Faculty of Pharmacy, Department of Pharmaceutical Toxicology, Ankara, Türkiye*

Cite this article as: Kayhan S, Doğan A, Kırmızıgöz Ş, Ezgu MC, Durmaz MO, Evleksiz Karımzada D, et al. Influence of age and cerebrospinal fluid diversion techniques on infection risk in pediatric hydrocephalus: a 10-year single-center experience. *Gulhane Med J.* 2026;68(2):138-146.

Date submitted:
04.11.2025
Date accepted:
06.04.2026
Epub:
11.06.2026
Publication Date:
16.06.2026

Corresponding Author:
Sait Kayhan, M.D., University of Health Sciences, Türkiye, Gülhane Training and Research Hospital, Clinic of Neurosurgery, Ankara, Türkiye
dr.saitkayhan@icloud.com

ORCID:
orcid.org/0000-0002-6777-7864

Keywords: Hydrocephalus, infection, shunt, endoscopic third ventriculostomy, Ommaya reservoir

ABSTRACT

Aims: Hydrocephalus in children can be treated using various surgical techniques, each associated with distinct risks of infection and revision. This study aimed to evaluate and compare these risks associated with different surgical approaches in pediatric patients.

Methods: This retrospective study included pediatric patients aged 0-60 months who underwent surgical treatment of hydrocephalus between January 2010 and October 2020 at a tertiary neurosurgical centre. Demographic, clinical, and laboratory data were analysed, including cerebrospinal fluid (CSF) protein levels and microbiological culture results. The primary endpoint was the occurrence of postoperative infection, which was compared across surgical techniques and age groups.

Results: Eighty-seven children (mean age 11±3 months; 56.3% male) were included. Five surgical techniques were performed: ventriculoperitoneal shunting (VPS), external ventricular drainage, Ommaya reservoir insertion, endoscopic third ventriculostomy (ETV), and combined ETV+VPS. Infection occurred in 12 patients (13.8%), with significantly higher rates in neonates than in older children (25.9% vs. 8.3%, p=0.042). Among procedures, infections were more frequent in patients who underwent Ommaya reservoir implantation than in patients treated with other methods (28% vs. 8%, p=0.034). CSF protein levels showed no significant correlation with age or sex.

Conclusions: Neonatal age and Ommaya reservoir use were associated with an increased risk of infection in pediatric hydrocephalus. Careful patient selection and early conversion to definitive shunt procedures may help reduce infection-related complications.

Introduction

Hydrocephalus is a common condition in the pediatric population and is associated with significant morbidity and mortality. As the surgical diversion of cerebrospinal fluid (CSF) is the treatment option of choice in hydrocephalus, various surgical techniques can be applied for successful clinical outcomes (1,2). Shunting is the most frequent and effective treatment for pediatric hydrocephalus worldwide. Endoscopic techniques are also in use for the definitive treatment of hydrocephalus (3). Meanwhile, external ventricular drainage (EVD) systems are used especially in premature newborns and low birth-weight infants before the permanent treatment methods are applied (4). Temporary procedures for CSF diversion are percutaneous lumbar or ventricular CSF aspiration and external drainage using a ventriculosubgaleal shunt, EVD system with a catheter and a bag, or a ventricular catheter with a subcutaneous reservoir (Ommaya reservoir) (5). The Ommaya reservoir is one of the temporary drainage systems, especially for children with post-hemorrhagic hydrocephalus (6). Ventriculoperitoneal (VP) shunt insertion is the preferred method, but it frequently fails in premature infants and low birth-weight newborns (7).

Infection is the primary risk associated with temporary CSF diversion procedures. Prolonged drainage may cause serious CSF infections, such as meningitis or ventriculitis (8). To avoid this severe complication, antibacterial catheters are introduced for surgical procedures (9,10). The most straightforward approach to overcome this serious complication is to shorten the drainage period and perform definitive treatment for hydrocephalus.

Despite the widespread use of multiple CSF diversion techniques in pediatric hydrocephalus, comparative data regarding procedure-specific infection risks remain limited. Moreover, the impact of patient age, especially the neonatal period, on infection rates across different surgical strategies has not been sufficiently clarified. Accordingly, this study aimed to assess postoperative infection rates following different CSF diversion procedures in pediatric hydrocephalus and to identify age-related differences in infection risk.

Methods

Patients and study design

Data from 87 pediatric patients treated for hydrocephalus in our department between January 2010 and October 2020 were retrospectively reviewed (Figure 1). The study population comprised children aged 0-60 months with radiologically and clinically confirmed hydrocephalus who underwent surgical intervention during this period. The sample size was determined by the number of eligible patients treated during the study period; no a priori power analysis was performed.

Patient histories and physical examination findings were recorded, and their etiological, clinical, and laboratory

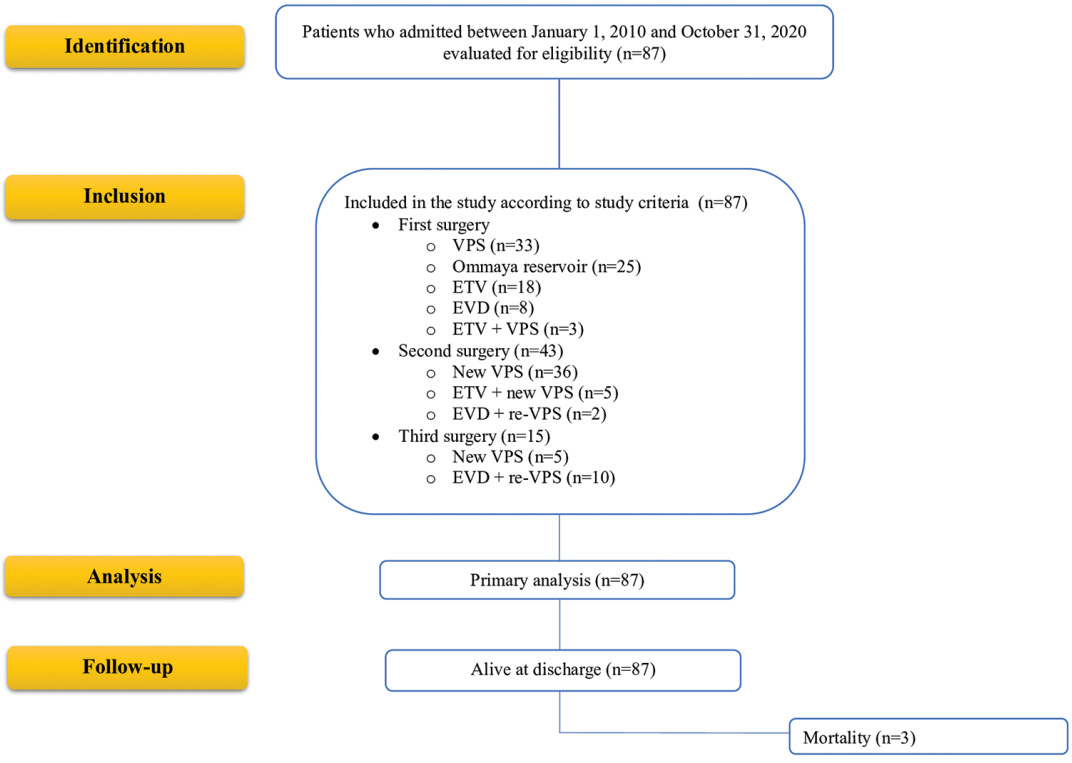

Figure 1. Flow diagram

ETV: Endoscopic third ventriculostomy, EVD: External ventricular drainage, VPS: Ventriculoperitoneal shunt

characteristics were analysed. Eligible patients underwent one of the primary CSF diversion procedures: VP shunting (VPS), EVD, Ommaya reservoir insertion, endoscopic third ventriculostomy (ETV), or combined ETV+VPS. All patients had complete documentation at the time of surgery, including demographic data, operative notes, and postoperative follow-up sufficient to evaluate outcomes. Intraoperative CSF protein measurements and postoperative microbiological assessments were available for infection-related analyses.

The indication for surgery was established based on the development of clinical symptoms and signs of increased intracranial pressure. Cranial computed tomography (CT) was performed preoperatively and postoperatively in all patients to confirm ventricular dilatation and assess the effectiveness of the surgical intervention. Surgical risks were explained to the parents, and informed consent was obtained before each procedure.

The indication for surgery and the type of surgery were always determined based on the patient's clinical and radiological characteristics, in close cooperation with the neonatologist. CSF samples were obtained intraoperatively in all patients for microbiological culture and biochemical analysis. The rate of infection was compared statistically across patient gender and age groups. In addition, CSF protein levels were compared for each group and each surgical technique.

Management of postoperative shunt infection

Postoperative infection was diagnosed in patients who developed clinical signs suggestive of infection during follow-up, including fever, neurological deterioration, or shunt dysfunction, and whose diagnoses were supported by laboratory findings such as elevated inflammatory markers. CSF for microbiological analysis was obtained only in cases with clinical suspicion of infection. Infection was confirmed by a positive CSF culture; only culture-proven cases were classified as infections for statistical analysis. Accordingly, in patients diagnosed with postoperative shunt infection, the infected shunt system was completely removed, and an EVD was placed to maintain CSF diversion. This decision was based on clinical improvement (reduction of fever, disappearance of restlessness and signs of systemic infection), normalization of CSF findings (cell count, glucose, and protein), and two consecutive sterile CSF cultures taken at least 48 hours apart after completion of a full course of intravenous antibiotic treatment. In all cases, the new shunt was placed through a different entry site.

Ethical Approval

The Non-Interventional Scientific Research Ethics Committee of the University of Health Sciences, Türkiye, Gülhane Training and Research Hospital approved the study (approval no: 2020-419, date: 17.12.2020). This study was conducted in accordance with the STROBE guidelines and the Helsinki Declaration (11).

Study groups

Five surgical protocols were applied to the patients: VPS, ETV, simultaneous VPS+ETV, EVD, and Ommaya reservoir insertion. Endoscopic irrigation was also performed during ETV and ETV+VPS surgeries (Figure 1).

Surgical techniques

All procedures were performed under general anesthesia in the supine position, using a standardized sterile technique. The choice of surgical approach was based on patient age, etiology of hydrocephalus, clinical condition, and radiological findings. The ventricular catheter was inserted into the lateral ventricle through a frontal burr hole, preferentially targeting the most dilated ventricle.

VPS implantation was performed using a frontal burr hole, and the ventricular catheter was placed into the lateral ventricle. A valve-regulated shunt system was used, and the distal catheter was tunneled subcutaneously and inserted into the peritoneal cavity. We used position-sensitive Christoph Miethke® paediGAV valves (Aesculap, Tuttlingen, Germany) with opening pressures of 4 or 9 cm H_2O in a horizontal position and 24 cm H_2O in a vertical position. ETV was performed via a frontal approach using a rigid neuroendoscope (Karl Storz GmbH & Co. KG, Tuttlingen, Germany). After entering the lateral ventricle, the endoscope was advanced into the third ventricle. The floor of the third ventricle was identified, and fenestration was performed at the tuber cinereum. Intraventricular irrigation was carried out using warmed Ringer's lactate solution.

EVD was established by inserting a ventricular catheter into the lateral ventricle through a frontal burr hole. The catheter was connected to a closed external drainage system (DESU, Ankara, Türkiye), allowing continuous CSF drainage. Ommaya reservoir implantation was performed; a ventricular catheter connected to a subcutaneous reservoir was inserted into the lateral ventricle through a frontal burr hole. The reservoir was positioned in a subgaleal pocket. CSF drainage was performed intermittently via reservoir puncture. We used either right-angled or straight CSF reservoir systems (Medtronic Inc., Goleta, CA, USA).

In selected cases, ETV and VPS were performed during the same surgical session to provide combined CSF diversion. CSF samples were obtained intraoperatively for biochemical analysis and culture when clinically indicated.

All patients underwent cranial CT to confirm catheter position and the presence of ventricular decompression.

Statistical Analysis

Numerical variables of patient data were expressed as mean ± standard error of the mean and minimum (lowest) - maximum (highest values). Categorical variables were presented as the number of patients (n) and the percentage (%) using descriptive statistics. The distributional properties

of numerical variables were evaluated using the Shapiro-Wilk test. The homogeneity of the variances was analysed by Levene's test. The Student's t-test was used to compare two independent groups when the data showed a normal distribution and parametric test assumptions were satisfied; one-way ANOVA followed by Fisher's least significant difference post-hoc test was used to compare more than two independent groups. If parametric test assumptions were not met, the Mann-Whitney U test was used for comparisons between two independent groups, and the Kruskal-Wallis H test was used for comparisons among more than two independent groups. The relationship between categorical data in independent groups was evaluated with the chi-square (χ^2) test. If the assumptions of the chi-square test were not met, Fisher's exact test or the Fisher-Freeman-Halton exact test was used, depending on group characteristics.

Due to the relatively small number of patients within individual surgical subgroups, an additional dichotomised analysis was performed, comparing patients who underwent Ommaya reservoir implantation with those who underwent all other procedures combined. This approach was adopted to improve statistical interpretability and to explore potential differences in infection risk that might not be detectable in multi-group comparisons with limited sample sizes. Differences at the $p<0.05$ level were considered statistically significant. Data were analyzed using IBM SPSS version 25.0 (Armonk, NY, USA).

Results

Baseline demographic and clinical data

A total of 87 children underwent surgical treatment for hydrocephalus over 10 years; 49 (56.3%) were male. The mean age at first surgery was 11.0 months (range, 0-60 months), with a mean body weight of 7,250 g and a mean follow-up of 25.2 months (Table 1). Post-hemorrhagic hydrocephalus was the most common etiology (n=32, 36.8%), followed by spina bifida, aqueductal stenosis, tumors, post-traumatic hydrocephalus, and other causes. During follow-up, three patients (3.4%) died.

Results of the first surgical interventions

VPS insertion was the most common first procedure (n=33), followed by Ommaya reservoir (n=25), ETV (n=18), EVD (n=8), and VPS+ETV (n=3). Mean CSF glucose was 46.2±3.0 mg/dL, with no findings suggestive of acute bacterial infection. CSF protein levels were ≤60 mg/dL in 17 patients (19.5%) and >60 mg/dL in 70 (80.5%); all intraoperative CSF cultures were negative (Table 2). VPS removal due to infection was required in two patients, in whom *Staphylococcus epidermidis* and *Staphylococcus aureus* were identified. VPS was reinserted after cultures were negative. The median duration of antibiotic therapy was 12 days, and the median hospital stay was 25 days.

Results of the second surgical intervention

A second surgical intervention was required in 43 patients (49.4%), primarily due to catheter obstruction. The mean interval between the first and second surgeries was 26.5 days. In five patients with ETV failure secondary to stoma closure, simultaneous VPS+ETV was performed. The majority of CSF cultures obtained during follow-up were negative (Table 2).

Following the second surgery, infections necessitating shunt removal and EVD placement occurred in 10 patients. Identified pathogens included *Staphylococcus epidermidis* (n=4), *Staphylococcus aureus* (n=2), *Klebsiella pneumoniae* (n=2), *Staphylococcus haemolyticus* (n=1), and *Enterococcus faecium* (n=1). The median duration of intravenous antibiotic therapy was 14 days, and the median hospital stay was 28 days.

Results of the third surgical intervention

Fifteen patients (17.2%) underwent a third surgical intervention, with a mean interval of 42.33 days following the second procedure. VPS reinsertion for shunt dysfunction was performed in 5 patients. All CSF cultures were negative, and no postoperative infections were observed after the third surgery.

Table 1. Demographic data and subgorups of the patients (n=87)

Variable	Mean ± SD	Range[a]
Age (month)	11.01±1.69	0.10-56
Birth weight (g)	7.250.00±513.32	1.950-17.900
Follow-up (month)	25.21±1.11	13-59
Age range (months)	**Groups**	**Number of patients n (%)**
Newborns	0-1	27 (31)
	2-60	60 (69)
	2-12	37 (42.5)
	13-60	23 (26.5)
	Total	87 (100)
Sex	Female	38 (43.7)
	Male	49 (56.3)
	Total	87 (100)
Etiology	Post-hemorrhagic	32 (36.8)
	Spina bifida	19 (21.8)
	Tumor	11 (12.6)
	Aquaductal stenosis	18 (20.7)
	Post-traumatic	5 (5.7)
	Others	2 (2.3)
	Total	87 (100)
Survey	Death	3 (3.4)
	Alive	84 (96.6)
	Total	87 (100)

SD: Standard deviation, [a]: Minimum-maximum value, n=Number

Table 2. The comprehensive data of all surgical procedures

Variable	
First surgical procedure	**Number of patients n (%)**
VPS	33 (37.9)
Ommaya reservoir	25 (28.7)
ETV	18 (20.7)
EVD	8 (9.2)
ETV+VPS	3 (3.4)
Infection based on the CSF protein level at the first surgery (mg/dL)	
CSF protein ≤60	17 (19.5)
CSF protein >60	70 (80.5)
CSF culture at the first surgery	
Negative	87 (100)
	Mean ± SD
CSF glucose level at the first surgery (mg/dL)	46.21±2.97
CSF protein level at the first surgery(mg/dL)	228.67±28.57
Time period between the first and second surgical procedure (days)	26.51±4.91
Cause of the second surgical procedure	**Number of patients n (%)**
Permanent CSF diversio n	33 (37.9)
Recurrence	5 (5.7)
Shunt dysfunction	3 (3.4)
Infection	2 (2.3)
Second surgical procedure	
VPS	36 (41.4)
ETV+VPS	5 (5.7)
Removal of VPS followed by EVD insertion and re-VPS, after antibiotherapy	2 (2.3)
Infection based on the CSF protein level at the second surgery (mg/dL)	
CSF protein ≤60	8 (9.2)
CSF protein >60	35 (40.2)
CSF culture at the second surgery[a]	
Negative	41 (47.1)
S. epidermidis	1 (1.1)
S. aureus	1 (1.1)
	Mean ± SD
CSF Glucose level at the second surgery (mg/dL)	42.84±2.63
CSF Protein level at the second surgery (mg/dL)	215.47±22.52
Time period between the second and third surgical procedure	42.33±5.01
	Number of patients n (%)
Cause of the third surgical procedure	
Shunt dysfunction	5 (5.7)
Infection	10 (11.5)
Third surgical procedure	
New VPS	5 (5.7)
Removal of VPS, EVD insertion and re-VPS insertion after the antibiotherapy	10 (11.5)
Infection based on the CSF protein level at the third surgery (mg/dL)	
None (Not third surgical procedure)	72 (82.8)
CSF protein >60	15 (17.2)
CSF culture at the third surgery[a]	
Negative	5 (5.7)
S. epidermidis	4 (4.6)
S. aureus	2 (2.3)
Klebsiella pneumoniae	2 (2.3)
S. haemolyticus	1 (1.1)
Enterococcus faceum	1 (1.1)
	Mean ± SD
CSF Glucose level at the third surgery (mg/dL)	39.53±3.34
CSF Protein level at the third surgery (mg/dL)	275.40±37.76

[a]: CSF culture results obtained at the time of shunt removal in patients who developed infection after the relevant surgery, n=number
SD: Standard deviation, ETV: Endoscopic third ventriculostomy, EVD: External ventricular drainage, VPS: Ventriculoperitoneal shunt, CSF: Cerebrospinal fluid

Comparing infection rates according to gender and age

Infection occurred in 7 of 38 female patients (18.4%) and in 5 of 49 male patients (10.2%); there was no statistically significant difference between the groups (p=0.270). When the data were stratified by age, infection was observed in 7 of 27 neonates (25.9%) and in 5 of 60 patients aged 2-60 months (8.3%). The infection rate was significantly higher in neonates (p=0.042).

Comparing infection rates of surgical procedures

No statistically significant difference in infection rates was observed among surgical procedures. Although the Ommaya reservoir group demonstrated a higher infection rate (28%) compared with other procedures (6-12%), this difference

did not reach statistical significance. However, following dichotomization, infection rates were significantly higher in the Ommaya group than in all other procedures combined (28% vs. 8%, p=0.034).

Comparison of CSF protein levels

CSF protein levels did not differ significantly by sex or between neonates (0-1 month) and older children (2-60 months) across the first three surgeries. However, when patients were stratified into detailed age groups, CSF protein levels were significantly higher in patients aged 2-12 months than in other age groups during the first and second surgeries ($p<0.05$), and no significant difference was observed at the third surgery.

Discussion

Hydrocephalus remains a significant health problem, particularly in premature and low birth-weight infants, and is associated with considerable morbidity and mortality in the pediatric population (4,6,12). Its prevalence is approximately 6 per 10,000 live births, yet it continues to represent an under-recognized condition despite its substantial clinical and economic burden (13,14).

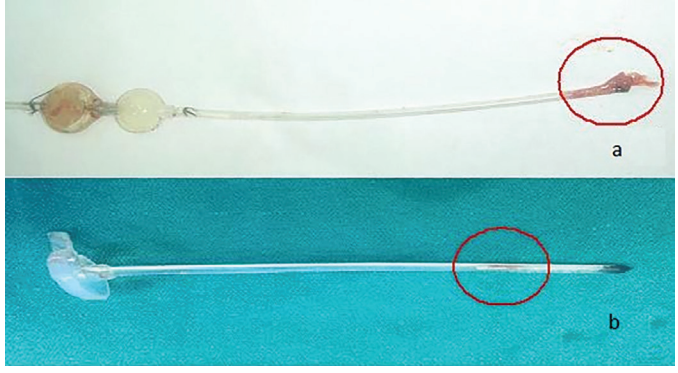

Figure 2. (a) Ventricular catheter tip of VP shunt occluded as a result of infection. (b) Ventricular tip of Ommaya reservoir occluded with particles

VP: Ventriculoperitoneal

A wide spectrum of etiologies contributes to pediatric hydrocephalus. In line with previous reports, post-hemorrhagic hydrocephalus was the most common cause in our series (36.8%), followed by spina bifida (21.8%) (15). Nearly half of the patients (49.4%) required a second surgical intervention, and 17.2% underwent a third procedure, supporting the notion that repeated surgeries are a frequent and often unavoidable aspect of disease management, particularly in post-hemorrhagic cases.

Gender differences are an important factor in the development of hydrocephalus. Enger et al. (16) showed that hydrocephalus is more frequent in male patients among 407 pediatric patients with hydrocephalus, which is consistent with our findings. There is no precise information on the cause of the male predominance in pediatric hydrocephalus.

Accurate and effective treatment is the first aim of pediatric neurosurgeons for hydrocephalus. Etiological factors affecting the development of hydrocephalus are elucidated day-by-day (17). Although neuroendoscopic techniques have increasingly been adopted in neurosurgical practice for the treatment of hydrocephalus, VPS is still most widely used and effective treatment modality (9,18). ETV is an established option for obstructive hydrocephalus, particularly in aqueductal stenosis. It has gradually spread, especially over the last three decades. In the literature, several studies have reported that simultaneous application of ETV and VPS in the same session is a reasonable approach (19,20). The rapid closure of the ventriculostomy is a frequently reported complication, especially in infants under one year of age and in cases of post-hemorrhagic hydrocephalus; it is attributed to immaturity of CSF circulation pathways, intraventricular inflammation, and clot formation, and it plays an important role in the selection of this combined procedure (21,22). Implementation of ETV in combination with VPS provides a potential dual route for CSF diversion, whereby in the event of early VPS failure, a functional ETV may help prevent acute intracranial hypertension and reduce the need for urgent shunt revision. Additionally, endoscopic lavage performed during ETV may facilitate clearance of intraventricular debris

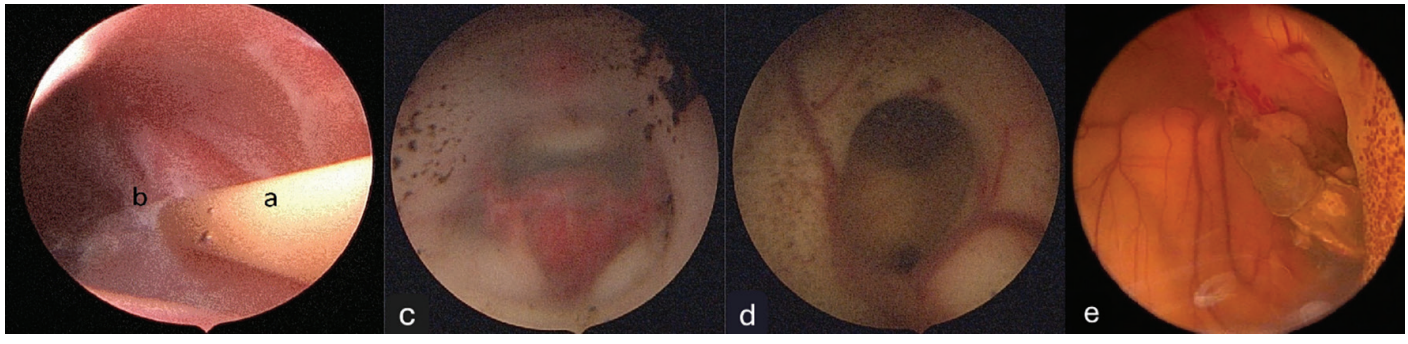

Figure 3. Dysfunctional VPS catheter (a) adhered to lateral ventricle wall (b). (c) Post-hemorrhagic particles around the tuber cinereum at the base of the third ventricle. (d) Particles on lateral ventricle walls and near the foramen of Monro, cleared by endoscopic irrigation. (e) Coagulum around the choroid plexus

VPS: Ventriculoperitoneal shunt

and potentially reduce infection risk (22,23). Although not a conventional approach, this strategy was adopted to optimise safety and long-term outcomes, particularly in high-risk patients with post-hemorrhagic hydrocephalus.

Temporary CSF diversion techniques, including EVD and Ommaya reservoirs, are valuable in patients with prematurity, poor general condition, or infection risk precluding immediate permanent shunting (5). These procedures allow enough time for the newborns to gain weight and transition to permanent shunt systems for the treatment of hydrocephalus. However, these approaches are not without complications (24). In our series, ventriculosubgaleal shunting was not utilized due to concerns regarding infection risk and limited long-term efficacy.

Infections are among the primary complications associated with the use of drainage systems. The incidence of infection after the surgical management of pediatric hydrocephalus is about 11% (14), while most of the infections occur within the 3 months after surgery (25). In our study, the overall infection rate was 13.7%. Coagulase-negative staphylococci were the cause of infection in 6 (50%) patients and *Staphylococcus aureus* in 3 (25%) patients, consistent with the literature. Coagulase-negative staphylococci (*Staphylococcus epidermidis*) and *Staphylococcus aureus* were the most frequently identified pathogens, reflecting the role of skin flora in shunt-related infections (8,16,26). Notably, infection rates increased following successive surgical interventions, rising from 2.3% after the first procedure to 11.5% after the second, highlighting the cumulative risk associated with multiple revisions.

Patient age is a well-established determinant of infection risk. Previous studies have demonstrated a markedly higher infection rate in younger infants (16,27,28). Consistent with these findings, neonates in our cohort had a significantly higher infection rate compared with older children (25.9% vs. 8.3%, $p<0.05$). This increased susceptibility is likely related to immunological immaturity, impaired skin barrier function, delayed wound healing, and prolonged hospitalization (29). Although infection rates were numerically higher in female patients, no statistically significant sex-related difference was observed.

The relationship between CSF protein levels and infection risk remains controversial. Yakut et al. (29) reviewed 290 patients with shunt infection and suggested that elevated protein levels may be associated with reinfection. We did not observe a significant association with either age or sex. However, higher protein levels were noted in the 2-12-month age group during early surgical stages, which may reflect disease severity or inflammatory burden.

Neuroendoscopic lavage has been proposed by Gaderer et al. (30) as a strategy to reduce infection and revision rates by clearing inflammatory debris from the ventricular system. In our limited cohort, no infections were observed in patients undergoing combined ETV and VPS with endoscopic lavage; however, the small sample size precludes definitive conclusions.

Procedure-specific infection rates remain a subject of debate. Lu et al. (31) reported significantly lower postoperative infection rates in the ETV group compared to VPS. In our series, infection occurred in 2 of 18 patients (11.1%) who underwent ETV and in 2 of 33 patients (6.1%) who underwent VPS as the initial procedure; no clear difference was observed, likely due to the limited sample size. In contrast, Palpan Flores et al. (32) reported an infection rate of 10.9% following Ommaya reservoir implantation and a 76.1% conversion rate to permanent shunting. Similarly, in our cohort, infection occurred in 28% of patients with Ommaya reservoirs, and all patients ultimately required permanent CSF diversion, consistent with previous findings (33). Notably, infection rates were significantly higher in the Ommaya group compared with rates for other procedures (28% vs. 8%, $p=0.034$), likely related to repeated reservoir access and the introduction of skin flora, despite antiseptic precautions. Therefore, the Ommaya reservoir should be used only for a short period and be converted to a permanent shunt as early as possible.

Mortality remains an important outcome in pediatric hydrocephalus. While previous studies have reported rates as high as 16.5% (22), the mortality rate in our series was 3.4%, with no deaths attributable to infection. The relatively short follow-up duration in our study may account for this lower rate.

Study Limitations

This study has several limitations that should be acknowledged. First, its retrospective, single-centre design inherently limits causal inference. However, potential selection bias was minimised because the surgical technique was chosen collaboratively by the neonatology and neurosurgery teams according to each patient's clinical and radiological findings, rather than by individual surgeon preference. Second, the relatively small overall sample size, particularly that of some subgroups such as ETV and combined ETV+VPS, reduces statistical power and may obscure subtle associations. Third, potential confounding factors, including gestational age, nutritional status, and antibiotic prophylaxis protocols, were not uniformly recorded and therefore could not be fully controlled. Fourth, surgical techniques and postoperative management may have evolved during the ten-year study period, potentially introducing variability in outcomes. Finally, the lack of long-term neurodevelopmental follow-up limits the assessment of functional outcomes beyond infection and revision rates.

Conclusion

Neonates demonstrated a nearly threefold higher risk of infection compared with older children, likely due to immunological immaturity and an impaired skin barrier. Use of an Ommaya reservoir was also associated with a significantly

increased infection rate, underscoring the vulnerability of patients requiring temporary CSF diversion.

These findings identify patient age and diversion strategy as key, modifiable determinants of infection risk in pediatric hydrocephalus. Early transition from temporary to permanent CSF diversion, together with meticulous aseptic technique, appears essential to minimize complications. Given the substantial impact of infection on morbidity, reoperation rates, and healthcare costs, targeted preventive strategies are critical.

Further large-scale, multicenter studies are needed to refine patient selection and optimize treatment protocols.

Ethics

Ethics Committee Approval: The Non-Interventional Scientific Research Ethics Committee of the University of Health Sciences, Türkiye, Gülhane Training and Research Hospital approved the study (approval no: 2020-419, date: 17.12.2020).

Informed Consent: Surgical risks were explained to the parents, and informed consent was obtained before each procedure.

Acknowledgments

This study is derived from the corresponding author's master's thesis, titled "Evaluation of Surgical Techniques and Outcomes in Pediatric Patients with Hydrocephalus", which was completed in 2021 at the University of Health Sciences, Gülhane Faculty of Medicine, Department of Neurosurgery.

Footnotes

Authorship Contributions

Surgical and Medical Practices: S.K., A.D., Ş.K., M.C.E., M.O.D., Concept: S.K., Y.İ., Design: S.K., M.C.E., Y.İ., Data Collection or Processing: S.K., D.E., E.Y., Analysis or Interpretation: S.K., D.E., C.A., S.Y.S., Literature Search: S.K., Writing: S.K., Y.İ.

Conflict of Interest: The authors declared no conflict of interest.

Financial Disclosure: The authors declared that this study received no financial support.

References

1. Evleksiz Karimzada D, Can Ezgu M, Karimzada G, Izci Y. Ventricular anatomical differences-a different perspective on endoscopic treatment of pediatric hydrocephalus: anomalies, variations, and deformations. *World Neurosurg.* 2024;191:e80-e91.
2. Tully HM, Dobyns WB. Infantile hydrocephalus: a review of epidemiology, classification and causes. *Eur J Med Genet*. 2014;57(8):359-368.
3. Kamikawa S, Inui A, Kobayashi N, Kuwamura K, Kasuga M, Yamadori T, et al. Endoscopic treatment of hydrocephalus in children: a controlled study using newly developed Yamadori-type ventriculoscopes. *Minim Invasive Neurosurg.* 2001;44(1):25-30.
4. Cornips E, Van Calenbergh F, Plets C, Devlieger H, Casaer P. Use of external drainage for posthemorrhagic hydrocephalus in very low birth weight premature infants. *Childs Nerv Syst.* 1997;13(7):369-374.
5. Nee LS, Harun R, Sellamuthu P, Idris Z. Comparison between ventriculosubgaleal shunt and extraventricular drainage to treat acute hydrocephalus in adults. *Asian J Neurosurg.* 2017;12(4):659-663.
6. Tröbs RB, Sander V. Posthemorrhagic hydrocephalus in extremely low birth weight infants: Ommaya reservoir vs. ventriculoperitoneal shunt. *Childs Nerv Syst.* 2015;31(8):1261-1266.
7. Kuo MF. Surgical management of intraventricular hemorrhage and posthemorrhagic hydrocephalus in premature infants. *Biomed J.* 2020;43(3):268-276.
8. Jiménez-Mejías ME, Márquez-Rivas FJ. CNS infections in patients with temporary CSF shunts: diagnostic, preventive and therapeutic approach. *Enferm Infecc Microbiol Clin (Engl Ed*). 2020;38(2):49-53.
9. Izci Y, Secer H, Akay C, Gonul E. Initial experience with silver-impregnated polyurethane ventricular catheter for shunting of cerebrospinal fluid in patients with infected hydrocephalus. *Neurol Res.* 2009;31(3):234-237.
10. Secer HI, Kural C, Kaplan M, Kilic A, Duz B, Gonul E, et al. Comparison of the efficacies of antibiotic-impregnated and silver-impregnated ventricular catheters on the prevention of infections. An in vitro laboratory study. *Pediatr Neurosurg.* 2008;44(6):444-447.
11. von Elm E, Altman DG, Egger M, Pocock SJ, Gøtzsche PC, Vandenbroucke JP, et al. Strengthening the reporting of observational studies in epidemiology (STROBE) statement: guidelines for reporting observational studies. *BMJ*. 2007;335(7624):806-808.
12. Paulsen AH, Lundar T, Lindegaard KF. Pediatric hydrocephalus: 40-year outcomes in 128 hydrocephalic patients treated with shunts during childhood. Assessment of surgical outcome, work participation, and health-related quality of life. *J Neurosurg Pediatr.* 2015;16(6):633-641.
13. Kahle KT, Kulkarni AV, Limbrick DD Jr, Warf BC. Hydrocephalus in children. *Lancet*. 2016;387(10020):788-799.
14. Wright Z, Larrew TW, Eskandari R. Pediatric hydrocephalus: current state of diagnosis and treatment. *Pediatr Rev*. 2016;37(11):478-490.
15. Holwerda JC, van Lindert EJ, Buis DR, Hoving EW; Dutch Pediatric Neurosurgery Study Group. Surgical intervention for hydrocephalus in infancy; etiology, age and treatment data in a Dutch cohort. *Childs Nerv Syst.* 2020;36(3):577-582.
16. Enger PØ, Svendsen F, Wester K. CSF shunt infections in children: experiences from a population-based study. *Acta Neurochir (Wien).* 2003;145(4):243-248; discussion 248.
17. Beuriat PA, Puget S, Cinalli G, Blauwblomme T, Beccaria K, Zerah M, et al. Hydrocephalus treatment in children: long-term outcome in 975 consecutive patients. *J Neurosurg Pediatr.* 2017;20(1):10-18.

18. Drake JM, Kestle JR, Milner R, Cinalli G, Boop F, Piatt J, et al. Randomized trial of cerebrospinal fluid shunt valve design in pediatric hydrocephalus. *Neurosurgery*. 1998;43(2):294-303; discussion 303-305.

19. Geyik M, Geyik S, Dogan A. Comparison of different endoscopic techniques for the treatment of hydrocephalus in children. *Turk Neurosurg.* 2022;32(2):271-276.

20. Shim KW, Kim DS, Choi JU. Simultaneous endoscopic third ventriculostomy and ventriculoperitoneal shunt for infantile hydrocephalus. *Childs Nerv Syst.* 2008;24(4):443-451.

21. Deopujari CE, Karmarkar VS, Shaikh ST. Endoscopic third ventriculostomy: success and failure. *J Korean Neurosurg Soc*. 2017;60(3):306-314.

22. Karımzada G, Kaya MB, Karımzada DE, Ezgü MC, Karımzada G, Kaya MB, et al. Postnatal management and outcomes of hydrocephalus in patients with myelomeningocele: a retrospective study from a single institution. *Hamidiye Med J.* 2025;6(1):43-49.

23. Koch D, Wagner W. Endoscopic third ventriculostomy in infants of less than 1 year of age: which factors influence the outcome? *Childs Nerv Syst.* 2004;20(6):405-411.

24. Willis B, Javalkar V, Vannemreddy P, Caldito G, Matsuyama J, Guthikonda B, et al. Ventricular reservoirs and ventriculoperitoneal shunts for premature infants with posthemorrhagic hydrocephalus: an institutional experience. *J Neurosurg Pediatr.* 2009;3(2):94-100.

25. Dinçer A, Kohan S, Özek MM. Is all “communicating” hydrocephalus really communicating? prospective study on the value of 3D-constructive ınterference in steady state sequence at 3T. *AJNR Am J Neuroradiol*. 2009;30(10):1898-1906.

26. Lee JK, Seok JY, Lee JH, Choi EH, Phi JH, Kim SK, et al. Incidence and risk factors of ventriculoperitoneal shunt ınfections in children: a study of 333 consecutive shunts in 6 years. *J Korean Med Sci.* 2012;27(12):1563-1568.

27. Pople IK, Bayston R, Hayward RD. Infection of cerebrospinal fluid shunts in infants: a study of etiological factors. *J Neurosurg.* 1992;77(1):29-36.

28. Renier D, Lacombe J, Pierre-Kahn A, Sainte-Rose C, Hirsch JF. Factors causing acute shunt infection. Computer analysis of 1174 operations. *J Neurosurg.* 1984;61(6):1072-1078.

29. Yakut N, Soysal A, Kepenekli Kadayifci E, Dalgic N, Yılmaz Ciftdogan D, Karaaslan A, et al. Ventriculoperitoneal shunt infections and re-infections in children: a multicentre retrospective study. *Br J Neurosurg*. 2018;32(2):196-200.

30. Gaderer C, Schaumann A, Schulz M, Thomale UW. Neuroendoscopic lavage for the treatment of CSF infection with hydrocephalus in children. *Childs Nerv Syst.* 2018;34(10):1893-1903.

31. Lu L, Chen H, Weng S, Xu Y. Endoscopic third ventriculostomy versus ventriculoperitoneal shunt in patients with obstructive hydrocephalus: meta-analysis of randomized controlled trials. *World Neurosurg.* 2019;129:334-340.

32. Palpan Flores A, Saceda Gutiérrez J, Brin Reyes JR, Sierra Tamayo J, Carceller Benito F. Risk factors associated with conversion of an Ommaya reservoir to a permanent cerebrospinal fluid shunt in preterm posthemorrhagic hydrocephalus. *J Neurosurg Pediatr.* 2020;25(4):417-424.

33. Mazzola CA, Choudhri AF, Auguste KI, Limbrick DD, Rogido M, Mitchell L, et al. Pediatric hydrocephalus: systematic literature review and evidence-based guidelines. Part 2: management of posthemorrhagic hydrocephalus in premature infants. *J Neurosurg Pediatr.* 2014;14(Suppl 1):8-23.

DOI: 10.4274/gulhane.galenos.2026.26086
Gulhane Med J 2026;68(2):147-150

Alström syndrome presenting with life-threatening variceal bleeding in an adolescent: the youngest reported case in Türkiye

Birce İzgi Akçay[1], Selçuk Teke[1], Yasin Maruf Ergen[1], İsmihan Merve Tekin[2], Necati Balamtekin[1]

[1]University of Health Sciences Türkiye, Gülhane Training and Research Hospital, Clinic of Pediatric Gastroenterology, Ankara, Türkiye

[2]GENOKS Genetic Diseases Diagnostic Center, Ankara, Türkiye

Cite this article as: Akçay Bİ, Teke S, Ergen YM, Tekin İM, Balamtekin N. Alström syndrome presenting with life-threatening variceal bleeding in an adolescent: the youngest reported case in Türkiye. *Gulhane Med J.* 2026;68(2):147-150.

Date submitted:
29.09.2025
Date accepted:
08.01.2026
Epub:
21.05.2026
Publication Date:
16.06.2026

Corresponding Author:
Birce İzgi Akçay, M.D., University of Health Sciences Türkiye, Gülhane Training and Research Hospital, Clinic of Pediatric Gastroenterology, Ankara, Türkiye
izgiakcay@gmail.com

ORCID:
orcid.org/0000-0002-1325-0899

Keywords: Alström syndrome, esophageal varices, liver cirrhosis, case report

ABSTRACT

Alström syndrome (AS) is a rare autosomal recessive ciliopathy caused by pathogenic variants in the *ALMS1* gene on chromosome 2p13, with multisystem involvement including the retina, cochlea, heart, liver, and kidneys. It is characterized by progressive cone-rod dystrophy, sensorineural hearing loss, truncal obesity, insulin resistance, type 2 diabetes mellitus and cardiomyopathy. Although hepatic involvement is frequent, advanced complications such as portal hypertension and variceal bleeding are extremely rare in childhood. We report the case of a 16-year-old girl with AS who presented with hematemesis and altered mental status. Laboratory evaluation revealed chronic liver disease and diabetic ketoacidosis. Upper gastrointestinal endoscopy demonstrated grade 2-3 esophageal varices that were treated with band ligation. Genetic testing identified a homozygous pathogenic frameshift mutation (NM_001378454.1:c.10218del, p.Ser3407Valfs*12) in exon 15 of the *ALMS1* gene. This patient is the youngest reported pediatric AS case in Türkiye presenting with life-threatening variceal hemorrhage secondary to portal hypertension. The case underscores the importance of early genetic confirmation and proactive hepatic monitoring in pediatric patients with AS.

Introduction

Alström syndrome (AS) is a rare autosomal recessive ciliopathy caused by biallelic *ALMS1* mutations on chromosome 2p13, with an estimated prevalence of 1 in 1,000,000 (1,2).

It leads to progressive multiorgan dysfunction, affecting the ocular, auditory, metabolic, cardiac, renal, pulmonary, and hepatic systems. Infantile-onset cone-rod dystrophy causes early blindness with nystagmus and photophobia, while sensorineural hearing loss develops later. Metabolic features include truncal obesity, severe insulin resistance, dyslipidemia, and type 2 diabetes mellitus (T2DM). Cardiomyopathy may present in infancy or recur later, and renal or pulmonary disease manifests as chronic kidney disease, restrictive lung disease, or recurrent infections (3,4). Hepatic involvement affects up to 80% of patients, typically starting with mild steatosis or transaminase elevation in childhood and progressing to fibrosis, cirrhosis, and portal hypertension in adolescence. Insulin resistance, ciliary dysfunction, and stellate-cell activation drive fibrogenesis, which often remains subclinical until advanced stages (2,4).

Diagnosis is challenging because of gradual, overlapping features with other ciliopathies such as Bardet-Biedl syndrome. While early retinal dystrophy, hearing loss, obesity, and insulin resistance raise suspicion, confirmation requires molecular identification of biallelic *ALMS1* variants (3,4).

We report a case of a 16-year-old girl with genetically confirmed AS who developed life-threatening variceal bleeding due to portal hypertension, the youngest reported case in Türkiye. According to the literature, this is the second pediatric patient with AS requiring liver transplantation. This case underscores the importance of early genetic diagnosis and vigilant hepatic surveillance to prevent irreversible complications.

Case Presentation

A 16-year-old girl was admitted with hematemesis, melena, and altered mental status. She was the second child of healthy, non-consanguineous parents and was born at term with normal growth. In infancy, cone-rod dystrophy caused photophobia and nystagmus. During the school-age period, truncal obesity and dyslipidemia developed. At 13 years of age, she was diagnosed with T2DM and subsequently had multiple intensive care admissions for recurrent diabetic ketoacidosis (DKA). Two years before presentation, an upper endoscopy revealed esophageal varices and portal hypertensive gastropathy; however, she was subsequently lost to follow-up.

On admission, her Z-scores for weight, height, and body mass index were 0.44, -1.35, and 1.32, respectively. She was confused and disoriented, with involuntary eye movements. Abdominal examination revealed hepatomegaly and splenomegaly, each 1 cm below the costal margin, and ascites; a grade 2/6 systolic murmur was audible. Laboratory studies revealed a white blood cell (WBC) count 19.8x10^3 µL, platelets (PLT) 115x10^3 µL; PLT of 115×10^9; alanine aminotransferase 47 U/L; aspartate aminotransferase 46 U/L; gamma-glutamyl transferase 123 U/L; albumin of 3.1 g/dL; international normalized ratio (INR) 1.3; C-reactive protein (CRP) 16.4 mg/L; glucose 530 mg/dL, and marked hyperammonemia (539 µmol/L). There was no history of exposure to hepatotoxic medications, supplements, or environmental agents.

Abdominal ultrasound showed granular liver parenchyma. Differential diagnoses, including autoimmune and viral diseases, Wilson disease, α1-antitrypsin deficiency, Budd-Chiari syndrome, and extrahepatic portal vein thrombosis, were excluded. Doppler ultrasonography (USG) revealed a 12.5 mm portal vein with preserved hepatopetal flow and no thrombosis, confirming intrahepatic portal hypertension.

Echocardiography showed mild pericardial effusion, and ophthalmologic assessment confirmed retinitis pigmentosa. After stabilization with fluids, diuretics, insulin, and supportive care, urgent endoscopy revealed grade 2-3 esophageal varices with red wale signs; band ligation was performed successfully (Figure 1). No further bleeding occurred; DKA resolved by day 2; mental status normalized by day 4.

Genetic testing confirmed a NM_001378454.1: c.10218del, p.Ser3407Valfs*12 homozygous mutation in exon 15 of the *ALMS1* gene confirming AS (Figure 2).

Eight months later, the patient was readmitted with hematemesis. Laboratory evaluation revealed findings consistent with acute hemorrhagic and metabolic decompensation [WBC 16.9×10^3/µL, hemoglobin (Hb) 4.4 g/dL, PLT 101×10^3/µL, absolute neutrophil count 13.32×10^3/µL, absolute lymphocyte count 2.53×10^3/µL, glucose 472 mg/dL, albumin 2.8 g/dL, CRP 19 mg/L, INR 1.2]. Transaminase and bilirubin levels were normal. Arterial blood gas analysis revealed mild acidosis.

Abdominal USG showed coarse hepatic echotexture with irregular contours and left-lobe blunting. The main portal vein measured 12 mm, and up to 6 cm of pelvic free fluid was detected. Echocardiography was normal.

Supportive therapy with octreotide was initiated, but the Hb level continued to decline, necessitating urgent band ligation of grade 2-3 esophageal varices. After stabilization, she was transferred to a liver transplant center for recurrent life-threatening bleeding.

Written informed consent was obtained from the parents; ethics approval was not required under institutional policy.

Discussion

The unusually early hepatic decompensation in our patient may reflect the combined effects of severe insulin resistance, recurrent DKA, and a homozygous truncating ALMS1 mutation in exon 15. Although this specific

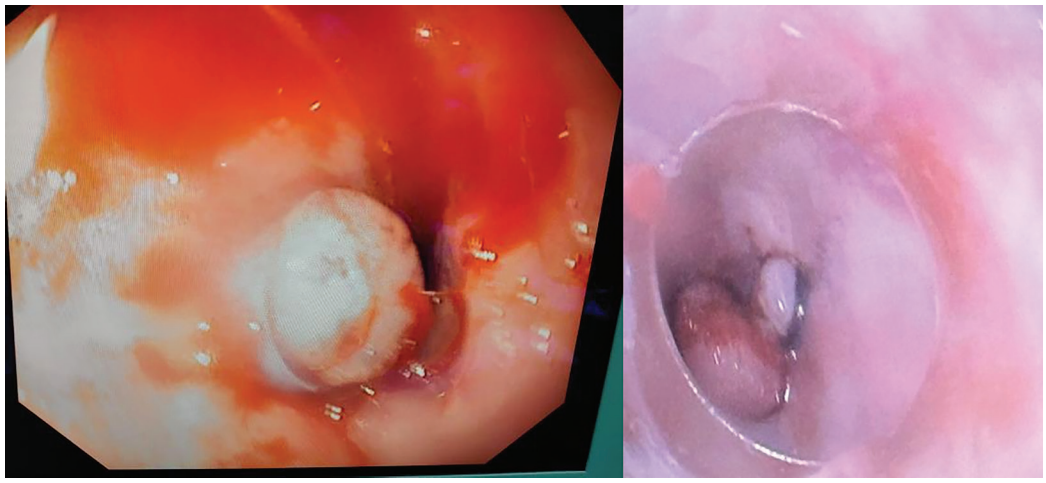

Figure 1. Endoscopic image of successful obliteration of varices following band ligation in a 16-year-old girl with Alström syndrome

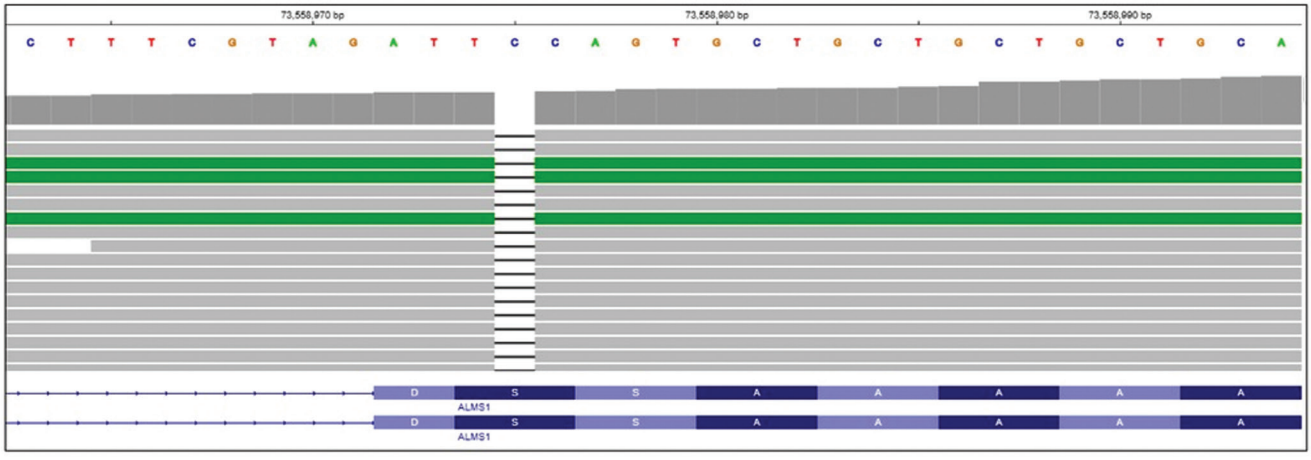

Figure 2. Genetic testing confirmed a NM_001378454.1: c.10218del, p.Ser3407Valfs*12 homozygous mutation in exon 15 of the *ALMS1* gene

variant has been rarely reported, truncating ALMS1 mutations have been associated with progressive multisystem disease and may predispose patients to earlier hepatic fibrosis and portal hypertension (5,6). Therefore, these factors could have contributed to the rapid evolution of hepatic disease in our patient. Our patient had poorly controlled T2DM from age 13, experiencing three DKA episodes over two years. Although uncommon in T2DM, DKA can occur when severe insulin resistance coexists with β-cell failure, as in AS. Recurrent metabolic and hemodynamic stress from dehydration, acidosis, and hypoperfusion may have exacerbated ongoing hepatic injury and accelerated fibrosis progression beyond what is typically expected in the steatosis-to-cirrhosis trajectory, while the concurrent marked hyperammonemia was likely due to transient perfusion-related dysfunction rather than intrinsic hepatic failure, as it resolved rapidly after correction of acidosis and fluids. Collectively, these genetic and metabolic factors could help explain the unusually young age at which our patient developed clinically significant portal hypertension and variceal bleeding.

In comparison to our findings, reported pediatric AS cases generally present with mild hepatic manifestations, such as steatosis or moderate transaminase elevation, progressing to fibrosis or cirrhosis later in life (7,8). However, exceptions similar to our case have been reported in the literature. Connolly et al. (9) reported an 8-year-old with chronic hepatitis-like changes and preserved function; Awazu et al. (10) described siblings with childhood steatohepatitis progressing to cirrhosis; and Quiros-Tejeira et al. (11) presented an 8-year-old with portal hypertension and acute liver failure, possibly triggered by metabolic or mitochondrial stress. While severe early decompensation is rare, progressive hepatic disease is a significant complication in AS, with specific truncating ALMS1 variants associated with higher prevalence and worse clinical progression (6,12).

Clinical features evolve with age, often delaying diagnosis. An average diagnostic delay of 8-10 years has been reported (4). A probable pediatric diagnosis of AS requires at least two major (e.g., visual loss, hearing deficit, metabolic abnormality) and two minor features (e.g., hepatic, renal, or endocrine involvement), while confirmation relies on identifying biallelic ALMS1 pathogenic variants. No biochemical, histologic, or imaging test can confirm the disease; thus, molecular analysis remains essential despite phenotypic overlap with other ciliopathies (3).

Lessons from this case highlight the need for structured hepatic surveillance in metabolically unstable AS patients. The following recommendations derive from pediatric portal hypertension guidelines and previously published reports, rather than from the actual follow-up course of this patient, who was lost to follow-up for extended periods. According to these guidelines, monitoring every 3-6 months with Doppler USG (± elastography) may facilitate early detection of portal hypertension. Endoscopic evaluation is generally advised when splenomegaly or thrombocytopenia develops, typically at 6-12-month intervals, depending on severity. For patients with high-risk varices, recommended schedules include re-endoscopy 1 month after band ligation and then every 1-3 months until eradication, followed by examinations every 3-6 months for two years and annually thereafter, ideally in coordination with a transplant center (13). Preventing DKA is also critical, as recurrent metabolic decompensation may aggravate hepatic injury. Early referral for transplant evaluation is recommended when signs of decompensation emerge.

The main limitation is the single-patient nature of this report, which limits generalizability. However, it provides valuable insight into the scarce pediatric data on hepatic involvement in AS.

Ethics

Informed Consent: Written informed consent was obtained from the parents.

Footnotes

Authorship Contributions

Concept: B.İ.A., S.T., N.B., Design: B.İ.A., S.T., N.B., Data Collection or Processing: B.İ.A., S.T., Y.M.E., İ.M.T., Analysis or Interpretation: B.İ.A., S.T., Y.M.E., İ.M.T., N.B., Literature Search: B.İ.A., S.T., Y.M.E., N.B., Writing: B.İ.A., S.T., Y.M.E., İ.M.T., N.B.

Conflict of Interest: The authors declared no conflict of interest.

Financial Disclosure: The authors declared that this study received no financial support.

References

1. Alstrom CH, Hallgren B, Nılsson LB, Asander H. Retinal degeneration combined with obesity, diabetes mellitus and neurogenous deafness: a specific syndrome (not hitherto described) distinct from the Laurence-Moon-Bardet-Biedl syndrome: a clinical, endocrinological and genetic examination based on a large pedigree. *Acta Psychiatr Neurol Scand Suppl.* 1959;129:1-35.
2. Marshall JD, Bronson RT, Collin GB, Nordstrom AD, Maffei P, Paisey RB, et al. New Alström syndrome phenotypes based on the evaluation of 182 cases. *Arch Intern Med*. 2005;165(6):675-683.
3. Marshall JD, Beck S, Maffei P, Naggert JK. Alström syndrome. *Eur J Hum Genet.* 2007;15(12):1193-1202.
4. Sinha A, Leeson-Beevers K, Lewis C, Loughery E, Geberhiwot T. Alström syndrome: the journey to diagnosis. *Orphanet J Rare Dis*. 2025;20(1):5.
5. Tahani N, Maffei P, Dollfus H, Paisey R, Valverde D, Milan G, et al. Consensus clinical management guidelines for Alström syndrome. *Orphanet J Rare Dis*. 2020;15(1):253.
6. Bea-Mascato B, Valverde D. Genotype-phenotype associations in Alström syndrome: a systematic review and meta-analysis. *J Med Genet.* 2023;61(1):18-26.
7. Ozantürk A, Marshall JD, Collin GB, Düzenli S, Marshall RP, Candan Ş, et al. The phenotypic and molecular genetic spectrum of Alström syndrome in 44 Turkish kindreds and a literature review of Alström syndrome in Turkey. *J Hum Genet*. 2015;60(1):1-9. Erratum in: J Hum Genet. 2015;60(1):51.
8. Aksoy F, Özgür T, Dundar HZ, Kaya E. Liver transplantation in alstrom syndrome: a case report. *Exp Clin Transplant*. 2024;22(3):244-245.
9. Connolly MB, Jan JE, Couch RM, Wong LT, Dimmick JE, Rigg JM. Hepatic dysfunction in Alström disease. *Am J Med Genet.* 1991;40(4):421-424.
10. Awazu M, Tanaka T, Sato S, Anzo M, Higuchi M, Yamazaki K, et al. Hepatic dysfunction in two sibs with Alström syndrome: case report and review of the literature. *Am J Med Genet.* 1997;69(1):13-16.
11. Quiros-Tejeira RE, Vargas J, Ament ME. Early-onset liver disease complicated with acute liver failure in Alstrom syndrome. *Am J Med Genet.* 2001;101(1):9-11.
12. Marshall JD, Maffei P, Collin GB, Naggert JK. Alström syndrome: genetics and clinical overview. *Curr Genomics*. 2011;12(3):225-235.
13. BSPGHAN. Assessment and management of oesophageal varices in children. Version 2. 2021. Available from: https://bspghan.org.uk/wp-content/uploads/2021/12/Varices-guideline_BSPGHAN_v2.pdf